# BIOGEOCHEMICAL COUPLINGS AMONG EARTH'S ECOSYSTEMS: A FOCUS ON OLD-GROWTH TROPICAL RAINFORESTS

*By*

*Philip Graham Taylor*
*B.S., Eastern University, 2004*
*M.S., Virginia Tech, 2008*

*A thesis submitted to the*
*Faculty of the Graduate School of the*
*University of Colorado in partial fulfillment*
*of the requirement for the degree of*
*Doctor of Philosophy*
*Department of Ecology and Evolutionary Biology*
*2012*

*This thesis entitled:*
***Biogeochemical couplings among Earth's ecosystems: a focus on old-growth tropical rainforests***
*written by Philip Graham Taylor has been approved for the Department of Ecology and Evolutionary Biology*

_____
*(Alan R. Townsend)*

_____
*(Cory C. Cleveland)*

_____
*(William D. Bowman)*

_____
*(Noah Fierer)*

_____
*(Jason C. Neff)*

*The final copy of this thesis has been examined by the signatories, and we find that both the content and the form meet acceptable presentation standards of scholarly work in the above mentioned discipline.*

Taylor, Philip Graham (Ph.D., Ecology and Evolutionary Biology)
***Biogeochemical couplings among Earth's ecosystems: a focus on old-growth tropical rainforests***
Thesis directed by Professor Alan R, Townsend

## ABSTRACT

This dissertation explores how physical and biological processes organize the interaction of carbon and nutrient cycles, which underpin life on Earth. In **Chapter 2**, I establish that ecosystem nitrate accrual exhibits consistent and negative nonlinear correlations with organic carbon availability along a hydrologic continuum from soils, through fresh- water systems and coastal margins, to the open ocean. Across this diversity of environments, we find evidence that resource stoichiometry strongly influences nitrate accumulation by regulating a suite of microbial processes that couple dissolved organic carbon and nitrate cycling.

In **Chapter 3**, I address the climate sensitivity of carbon cycling in old-growth tropical rainforests, which are among Earth's most carbon-rich and productive ecosystems. Collectively they exchange more $CO_2$ with the atmosphere than any other terrestrial biome – annually, about 16 times more C than the change in atmospheric CO2 concentration resulting from fossil fuel use – thus small imbalances between rainforest carbon uptake and release can influence atmospheric $CO_2$ concentrations. Here, I use meta-analysis of field data to examine the long-term climate sensitivity of rainforest $CO_2$ exchange and storage. I found that net primary productivity and biomass carbon peaks in warm, lowland rainforests peaks at the highest rainfall levels, contrasting with a saturating response expected from previous studies in montanae forests. The pattern results from interactions between climatic, edaphic, geographic and biotic controls over

carbon accumulations.

In **Chapter 4**, I found that seasonal water availability plays an important role in structuring the tropical nitrogen cycle. Counter to current paradigms that expect tropical lowland rainforests to freely leach bioavailable N, I discovered very low export of bioavailable N from an old-growth tropical watershed. Nitrate loss was closely tied to organic carbon availability for heterotrophic microbes. PON export constituted the largest hydrologic loss pathway for N and was regulated by episodes of intense rainfall that caused surges of sediment yield from erosion. The magnitude of PON loss is larger than measured N inputs, and may constrain N accumulation within the ecosystem over long timescales.

## ACKNOWLEDGEMENTS

My personal and professional growth has fundamentally depended upon the wonderful network of friends and colleagues that surrounded me in graduate school. Words cannot express my gratitude to those I am thankful for, for their character is ineffable. Firstly, I thank Alan Townsend, advisor and comrade. His intellect, vision, enthusiasm, creativity, support (financial and intellectual) and leadership guided my scientific pursuit. Our mutual interest in outdoor adventure and academic excellence propelled me through graduate school with joy and fulfillment. Above all, our time together has been tremendously fun, which will continue well into the future.

My dissertation committee was comprised of remarkable scientists that provided many great conversations and guidance over the past four years. Cory Cleveland has been a constant inspiration and pushed me to be my best. Some of my best times where spent with Noah Fierer, a seeker on the frontier of knowledge. I also thoroughly enjoyed my time with Bill Bowman, with whom I shared engaging scientific dialogue and many fishing holes on Colorado rivers – alongside Alan.

My labmates were indelibly important to my success, most notable Will Wieder. Through many adventures, many epic and some difficult, we've become great friends, and share a passion for fatherhood. Teresa Legg, Hana Fancher, Sam Wientraub, John Mischler, Janet Prevey, Sasha Reed, Rebecca Cole, Diana Nemergut, and Tim Seastedt were the beating heart of north hall of the 'double wide', a.k.a. INSTAAR. This was my second home, and I enjoyed my stay thoroughly.

INSTAAR and EBIO were nurturing communities. The community orientation of both departments facilitated a playful and earnest dedication to science. The directors,

faculty and students all contributed to my growth; the names are too innumerable to list (you know who you are).

My Ph.D. would not have been possible without my mother and father, Deborah and John Taylor. At my birth they left me unbridled to pursue my highest dreams. They feed, cared, cultivated and guided my path with support and remarkable wisdom. Their disciplined life is a daily inspiration and constant reminder of the rewards of purpose-driven work with a higher cause. I dedicate my dissertation to my grandfather, Dr. Neil R. Taylor, who died shortly before I began my Ph.D. His love for people, nature and knowledge compelled me attend graduate school, and continues to inspire my pursuit of solving unanswered questions about how the Earth works. My grandmother, Judy Cox, who lives through the woods and across the creek from Goshen (where I grew up), kept me grounded. I always feel her love no matter the distance that separates us.

Above all I am forever grateful to my wife, Nicole Brinks. She has been my biggest support, and amazes me daily with her energy, perspective and undying commitment to doing what is right in this world. She has led the way in raising our children, Thatcher, Hudson and Ada, whom are intelligent, perceptive, wild, free and full of joy. My family brings me all the happiness I could ever desire.

Finally, this work was funded by the National Science Foundation, through a GK-12 fellowship and research grant awarded to Alan Townsend and Cory Cleveland. Thanks guys for bringing me aboard, our journey has just begun.

# TABLE OF CONTENTS

# TABLES

TABLE

# FIGURES

# CHAPTER 1: OVERVIEW

## 1.1. Coupled biogeochemical cycles

Since the Holocene, civilization has been very successful and rapidly expanded to nearly all areas of the globe. Unprecedented and dramatic changes to Earth's elemental cycles have left virtually no ecosystems untouched by human impact. Much of the modern economy relies on pervasive alterations to the carbon, nitrogen, and phosphorus cycles – elements that are at the foundation of life since primordial times. The uses of ancient hydrocarbons for energy, as well as the synthetic creation of nitrogen and mining of phosphorus for fertilizer, are salient examples of changes to these biogeochemical cycles, which have been key to our advance since the Industrial revolution. As we enter a new epoch – the *Anthropocene* – where human activities are the prime drivers of environmental change, there are growing concerns that we could exceed planetary boundaries that ensure a sustainable future. For example, fossil fuel combustion along with land use has driven an increase in atmospheric $CO_2$ and caused global warming, which may harm people and ecosystems, even in remote locations. Defining where these boundaries lie and how close we are to them requires a better understanding of the Earth system and how sensitive it is to environmental changes.

This task requires a multidisciplinary approach, including my field of biogeochemistry. A biogeochemical perspective is one that borrows from many different scientific fields to make sense of the interactions that characterize complex ecological systems. A leading principle in this field is that elemental cycles are strongly coupled through chemical reactions, which organisms often mediate. Organisms require specific elements for metabolic purposes, such that patterns of availability in a certain element are

frequently linked to the cycling of many others; that is, one elemental cycle cannot exist without many others. Physical factors, such as climate, also often regulate rates of biological processes, and as such provide additional constrains to coupled elemental cycling. These features of the world can make things complicated, but strategic examination of multiple elemental patterns in tandem is crucial for understanding how the Earth system works. This approach is what links seemingly disparate topics in my dissertation, which include, stoichiometric controls over the accretion of nitrate in Earth's ecosystem (**Chapter 2**), climate and plant – soil feedbacks regulate tropical forest $CO_2$ exchange (**Chapter 4**) and the responses of nitrogen loss from a watershed to hydrologic and biological seasonality (**Chapter 4**).

*1.2 Accrual of nitrate in Earth's ecosystems*

The availability of nitrogen is a key control over the productivity, diversity, composition and functioning of many ecosystems across the globe (Vitousek et al. 1997). Human alterations of the nitrogen cycle mainly occur through agricultural intensification (*i.e.* creation and use of synthetic fertilizers) and industrial development (*i.e.* fossil fuel combustion; Davidson *et al.* 2012). Though many regions of the world could use more nitrogen to boost crop yields (Vitousek et al. 2009), the effects of too much reactive N in circulation in the developed world are mostly detrimental to both human and ecosystem welfare. A major player is nitrate, a particularly bioavailable form of nitrogen, when in overabundance, causes economic and aesthetic deterioration via eutrophication, promoting invasive of alien species, reducing biodiversity, among other impacts (Vitousek *et al.* 1997).

Finding solutions requires an understanding of the control factors that regulate and remove reactive N from the environment. Before I started to pursue my Ph.D., I'd discovered a negative, nonlinear relationship between organic carbon and nitrate in Appalachian ecosystems, which aligned with patterns previously observed in the Northeast USA and Colorado's Front Range mountains. Curious about it's global distribution, I found the same relationship in all of Earth's major ecosystems early in my Ph.D. pursuit. In **Chapter 2** I applied principles of ecological stoichiometry to explain this global pattern. Notably, even in ecosystems substantially altered by inputs of fertilizer, stoichiometric controls over unwanted nitrate accumulation are robust, suggesting potential applications for reactive N solutions.

*1.3 Climatic and biogeochemical drivers of tropical carbon cycling*

Tropical rainforests are among Earth's most carbon (Malhi *et al.* 2004, 2006) and species rich (Gentry 1988) ecosystems. The twentieth century saw global fossil fuel use and land use change increase atmospheric $CO_2$ by 25% and ambient air temperatures by 0.6 $^{o}$C (IPCC 2001). Along with these atmospheric changes have come both sharp (*i.e.* droughts) and slower shifts in rainfall, with large regions in the Amazon showing declining trends (Phillips *et al.* 2009, 2010; Lewis *et al*. 2011). At large spatial scales, tropical rainforests affect climate and vice versa, however rainforest sensitivity to changes in climate is uncertain.

With the help of meta-analysis, in **Chapter 3** I examined how $CO_2$ exchange in old growth tropical rainforests changes along gradients of mean annual temperature and rainfall. In the past, limited data availability restricted empirical studies to only portions of the full climate spectrum present in the tropics. Fortunately, there has been an increase

in tropical C flux research in the past two decades, which has afforded new opportunities to reexamine current conceptions of climate controls on rainforest C cycling. In contrast with some syntheses, I found that the wettest of lowland tropical rainforests are the most productive and carbon rich terrestrial ecosystems. In chapter 3 I explore how this is driven by climate influences on plant – soil nutrient feedbacks that accelerate tropical $CO_2$ exchange.

*1.4 Nitrogen cycling in wet lowland tropical rainforests*

It is commonly thought that old-growth primary rainforests cycle nitrogen (N) in excess of biologically demand. N abundance is observed in a variety of old-growth tropical rainforests, as suggested by high foliar N to phosphorus ratios (Townsend *et al.* 2007), an abundance of N fixation (Cleveland *et al.* 1999), elevated isotopic signals of $^{15}N$ (Houlton *et al.* 2006), and large losses of bioavailable N to gaseous (Davidson *et al.* 2000) and hydrologic (Brookshire *et al.* 2012) pathways. However, in a rainforest on the Osa Peninsula, Costa Rica, such telltale signs of "loose" N cycling are largely not present (Townsend *et al.* 2007, Wieder *et al.* 2011, *In prep*). In fact, the plant – soil – microbial systems appear to very efficiently use and recycle N.

In **Chapter 4** I examine the magnitude and controls over hydrologic nitrogen loss from a wet lowland tropical rainforest. Unlikely predictions based on classical notions of tropical N cycling, I found ultra-low concentrations and export of bioavailable N and dominance of organic forms in dissolved N export. High rates of rainfall played a large role in driving the erosional export of sediment, which carried with it particulate organic N (PON). In this chapter I explore hydrology and biological controls over N cycling, and

postulate that erosional loss of PON might play a role in constraining ecosystem N balance over longer time scales.

## CHAPTER 2: STOICHIOMETRIC CONTROL OF ORGANIC CARBON – NITRATE RELATIONSHIPS FROM SOILS TO THE SEA

**Published:** Taylor P.G. & Townsend A.R. (2010) Stoichiometric control of organic carbon-nitrate relationships from soils to the sea. *Nature*, 464, 1178-1181

### 2.1 Abstract

Human creation of reactive nitrogen (Nr) has risen an order of magnitude since the dawn of the Industrial Revolution (Galloway *et al.* 2008). This dramatic reorganization of a global biogeochemical cycle has brought substantial benefits (Smil 1999), but increasingly causes detrimental outcomes for both people and ecosystems (Vitousek *et al.* 1997) . One such problem is the accumulation of nitrate ($NO_3^-$) in both freshwater and coastal marine ecosystems. Here we establish that ecosystem $NO_3^-$ accrual exhibits consistent and negative nonlinear correlations with organic carbon (C) availability along a hydrologic continuum from soils, through freshwaters and coastal margins, to the open ocean. The trend also prevails in ecosystems subject to substantial human alteration. Across this diversity of environments, we find evidence that resource stoichiometry (organic C:$NO_3^-$) strongly influences $NO_3^-$ accumulation by regulating a suite of microbial processes which couple DOC and $NO_3^-$cycling. Through meta-analysis, we show that heterotrophic microbes maintain low $NO_3^-$ concentrations when organic C:$NO_3^-$ ratios match the stoichiometric demands of microbial anabolism. However, when resource ratios drop below the minimum C:N ratio of microbial biomass, the onset of C limitation appears to drive rapid $NO_3^-$ accrual, which may then be further enhanced by nitrification. At low organic C:$NO_3^-$ ratios, denitrification appears to constrain the extent of $NO_3^-$accretion once organic C and $NO_3^-$ availability approach the 1:1 stoichiometry of this catabolic process. Collectively, these microbial processes express themselves on

local to global scales by restricting the threshold ratios underlying $NO_3^-$ accrual to a constrained stoichiometric window. Our findings indicate that ecological stoichiometry can help explain the fate of $NO_3^-$ across disparate environments and in the face of human disturbance, which has significant implications for the management of a rapidly changing N cycle.

**2.2. Introduction**

Nr refers to inorganic and organic forms of N that are biologically, photochemically and/or radiatively active, in contrast to the vast but inert atmospheric $N_2$ pool (Galloway *et al.* 2008). Absent human disturbance, relatively low Nr availability constrains both the structure and function of a wide variety of ecosystems (Richards 1965). However, the rapid expansion of the global economy from the Industrial Revolution onward, fueled by fossil fuel combustion, creation of synthetic fertilizer, widespread land conversion and accelerating global trade, has quickly increased Nr in the environment (Galloway *et al.* 2008). A litany of environmental threats, including air pollution, eutrophication, soil acidification, losses of biodiversity and climate change stem from the diverse fates of newly created Nr (Vitousek *et al.* 1997). Given the environmental and social importance of managing a changing N cycle, there is growing demand for conceptual and analytical models (Vitousek and Howarth 1991, Mulholland *et al.* 2008, Barnes and Raymond 2010, Arango and Tank 2008, Bohlke *et al.* 2009) that can help predict the fate of Nr across multiple environments.

Generally, efforts to understand the sources and sinks of $NO_3^-$ in ecosystems have focused on the roles of resource quantity and quality. As with any biogeochemical species, both kinetic and energetic controls will affect nitrate cycling, and models rooted

in the principles of Michaelis—Menten uptake kinetics have improved our predictive ability of $NO_3^-$ dynamics in streams Mulholland *et al.* 2008, Barnes and Raymond 2010, Arango and Tank 2008, Bohlke *et al.* 2009). However, one challenge to such efforts arises from the fact that N does not cycle independently of other elements. Instead, transformations of Nr in the environment are closely linked with several other major biogeochemical cycles, perhaps most notably that of carbon (Arango and Tank 2008, Bohlke *et al.* 2009, Hungate *et al.* 2003, Manzoni *et al.* 2010, Hill *et al.* 2000, Hedin *et al.* 1998, Goodale *et al.* 2005, Evans *et al.* 2006) Thus, understanding human disruptions to either the N or C cycle is often not possible without a multi-element perspective.

**2.3. Results and Discussion**

Here, we show that consistent and negative nonlinear relationships between $NO_3^-$ and dissolved or particulate organic carbon (DOC/POC, respectively) occur along a hydrologic continuum from soils, to streams and lakes, and on to estuaries and the open ocean (Fig. 2.1). Notably, the pattern remains robust even in human-disturbed streams and rivers (Fig. 2.1C). The consistency of the pattern across a wide range of environments and disturbance regimes suggests the potential for common underlying controls. Past studies in streams and groundwater have proposed several explanations for this pattern (Hill *et al.* 2000, Hedin *et al.* 1998, Goodale *et al.* 2005, Evans *et al.* 2006, Monteith *et al.* 2007) with some recent discussions focusing on increased DOC leaching from ecosystems recovering from acid deposition (Monteith *et al.* 2007). However, acid deposition cannot account for the widespread coherence shown in Figure 2.1, nor do kinetic models alone seem to offer a good explanation, given the frequently low nitrate values even in regions with high nitrogen loading to watersheds (Fig. 2.1C).

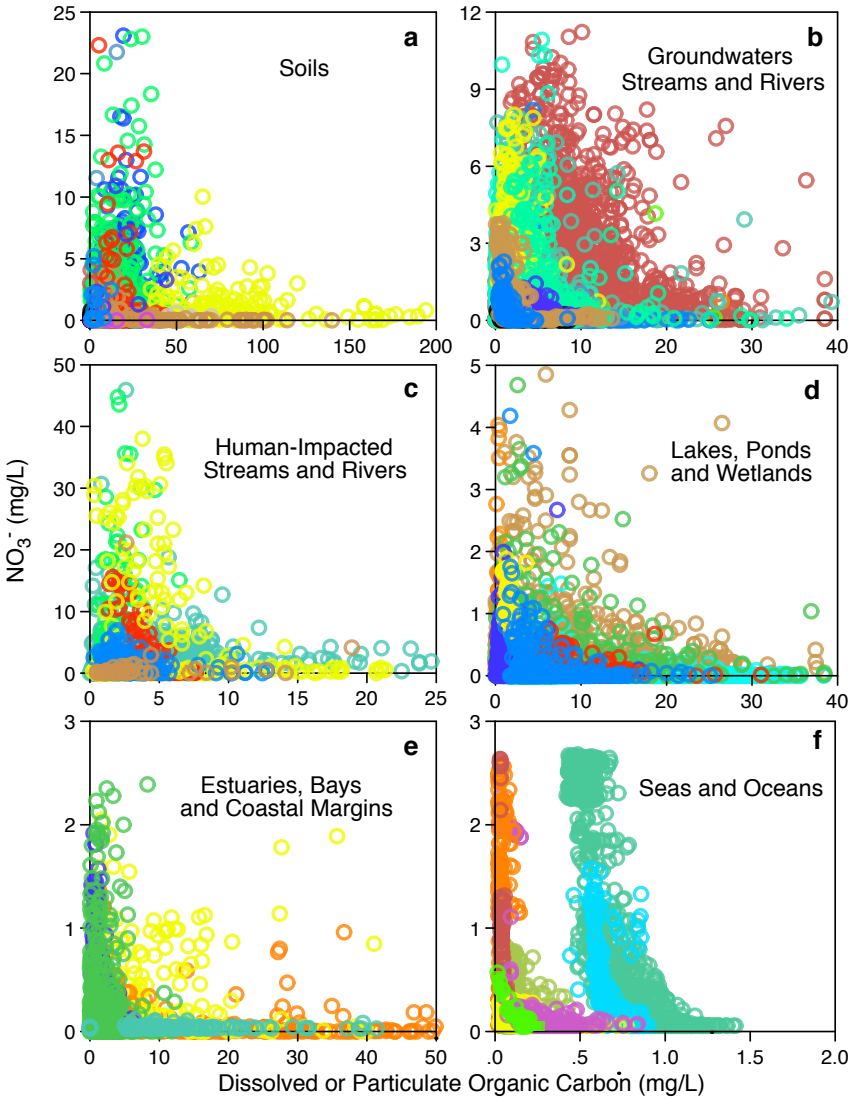


Figure 2.1 | $NO_3^-$ concentration as a function of DOC or POC concentration among earth's major ecosystems. Databases were gathered from ecosystems in tropical, temperate, boreal and arctic regions, and include data sets collected on local, watershed, regional, national and global scales. Human impacted streams and rivers are waterways within the USA, which are predominantly influenced by agricultural activities. The separation of the pattern in Seas and Oceans reflects biogeochemical differences in C richness among distinct ocean provinces. See Table 2.1 for statistical analyses. Axes are truncated for best observation of data. Appendix A lists specific data sources.

Table 2.1 | Analysis of global organic C – $NO_3^-$ trends

| Global System | DOC observations (%)** | Modeled Parameters ($y=a+b^{-k(x)}$)*** | | | Model Fit ($r^2$) | Molar C:N-$NO_3^-$ at Inflection Point (x,y)**** |
|---|---|---|---|---|---|---|
| | | a | b | *k* | | |
| Soils | 100 | 0.85 | 1.72 | 0.13 | 0.25 | 5.22 (7.03,1.56) |
| Streams/Rivers | 45 | 0.94 | 1.67 | 0.32 | 0.26 | 4.79 (10.12, 2.41) |
| | 100 | 1.20 | 1.51 | 0.40 | 0.28 | 3.12 (4.04,1.50) |
| Human Impacted Streams/Rivers* | 100 | 2.95 | 2.61 | 0.14 | 0.24 | 3.29 (10.42, 3.67) |
| Lakes/Wetlands | 26 | 0.05 | 1.25 | 1.39 | 0.35 | 15.7 (1.97, 0.13) |
| | 100 | 1.19 | 1.51 | 0.31 | 0.42 | 4.76 (0.76, 0.16) |
| Ocean Margins | 31 | 0.02 | 2.11 | 1.38 | 0.44 | 16.7 (2.02, 0.14) |
| | 100 | 0.12 | 0.43 | 3.55 | 0.39 | 2.19 (3.68, 1.68) |
| Oceans (high C) | 0 | 0.33 | 26.21 | 4.86 | 0.50 | 3.79 (0.20, 0.06) |
| Oceans (low C) | 0 | 0.19 | 0.78 | 8.15 | 0.47 | 2.67 (0.76, 0.33) |

*Human impacted streams and rivers include systems in agricultural and urban landscapes.
** Databases were assembled that contained paired NO3- and DOC or POC observations. For Lakes/Wetlands and Ocean Margins, exponential models were fit to data using POC and DOC observations together (i.e. Lakes/Wetlands and Ocean Margins) and DOC only. (We separated DOC and POC observations for reasons described in the text.
*** An exponential model with three estimated parameters was chosen based on root mean-squared error comparisons with one and two parameter exponential models. Parameters a, b and *k* were optimized using the root mea-squared error criterion (versus regression coefficient) with a least squares curve-fitting procedure. All exponential models significant at $p < 0.001$.
**** We used the second derivative of the exponential model to find the x,y coordinate at the inflection point of each exponential model to determine the molar C:N ratio for organic C:NO3- in each environment. The organic C:NO3- is reported molar whereas x,y coordinates are mass based (mg/L) for visual comparison with Fig. 2.1.

Here we develop and test a model (Figure 2.2) that describes how shifts in elemental limitation may drive organic C–$NO_3^-$ patterns by governing the relative rates of key microbial processes that couple dissolved C and N cycling. All organisms require energy and nutritional resources in characteristic stoichiometric ratios[3], which couples the global N cycle to other biogeochemical cycles in predictable ways (Smil 1999, Sarmiento and Gruber 2006, McGroddy *et al.* 2004, Cleveland *et al.* 2007). The point at which growth limitation shifts from one element to another due to inadequate supply of an energy or nutritional resource is known as the threshold elemental ratio (Sterner and Elser

2002, Anderson *et al.* 2005, Manzoni *et al.* 2010). Critical thresholds can underlie ecological processes when organisms that encounter nutritionally imbalanced resources maintain stoichiometric homeostasis by recycling or avoiding the element in excess (Sterner and Elser 2002, Anderson *et al.* 2005). For example, critical threshold ratios are known to prompt phosphorus and nitrogen accrual in aquatic and soil systems, respectively, when resource organic carbon:nutrient ratios fall below the requisite ratios of biomass construction.

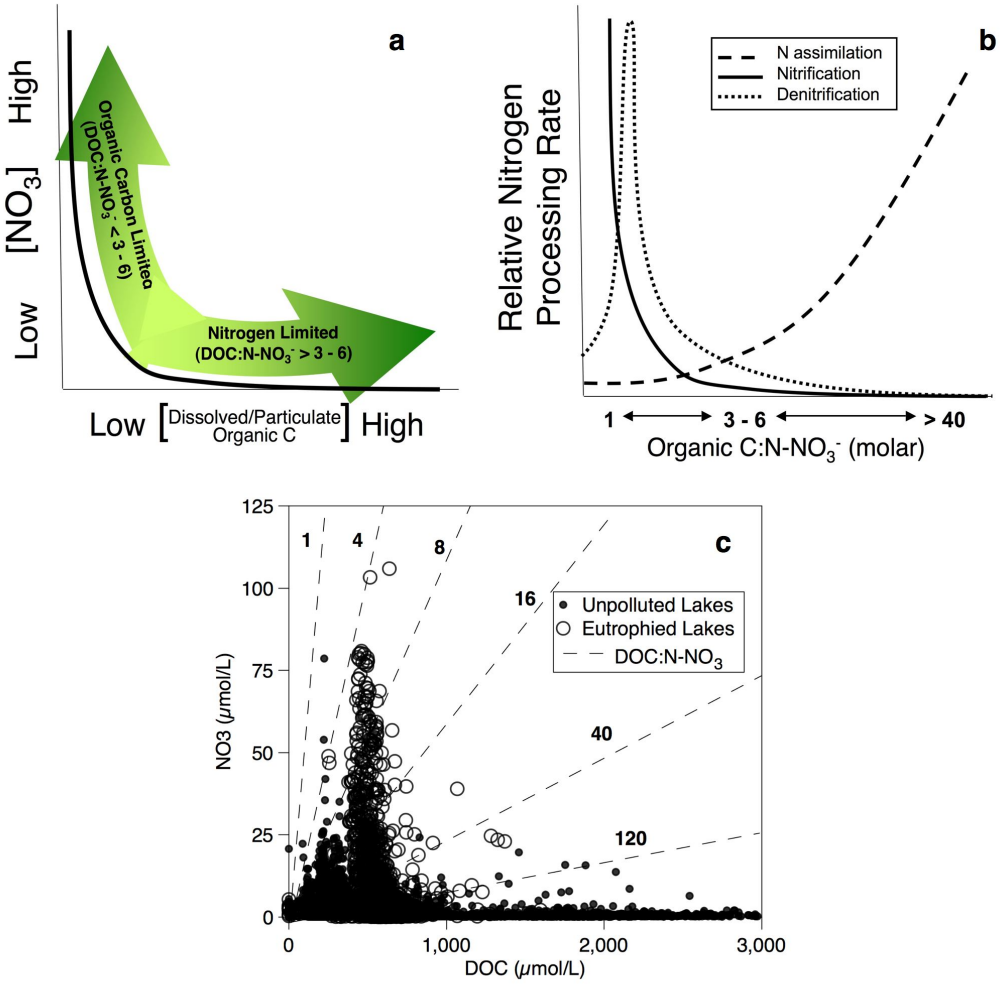

Figure 2.2 | Conceptual schematic summarizing the major findings of the paper, illustrating how changes in resource stoichiometry along inverse DOC-$NO_3^-$ patterns alter microbial processes that couple the C and N cycles. (a) Stoichiometric shifts in organic C:$NO_3^-$ ratios underlie inverse DOC—$NO_3^-$ patterns, in part, by organizing elemental limitation of microbial anabolism. A minimal threshold ratio of around 4 represents the transition from C to N limitation of microbial anabolism after microbial carbon use efficiency is accounted for (Supplementary Discussion). Reduced N assimilation when resource stoichiometry drives C limitation may allow $NO_3^-$ to accumulate. (b) A trio of microbial-driven nitrogen transformations governs inverse DOC—$NO_3^-$ relationships by responding to discrete changes in resource stoichiometry. Shifts in resource ratios alter the availability and fate of $NO_3^-$ by differentially affecting microbial N assimilation, nitrification and denitrification. Heterotrophic N assimilation strongly reduces $NO_3^-$ concentration when the C:N ratios of anabolic resources equal or exceed microbial requirements. Declines in heterotrophic $NO_3^-$ uptake at resource C:N ratios across the N to C limitation transition may indirectly promote nitrification if $NH_4^+$ availability is relatively higher when heterotrophs are C limited. Finally, the extent of $NO_3^-$ accrual may be constrained by denitrification of $NO_3^-$ to $N_2O$ or $N_2$ gas when DOC:$NO_3^-$ ratios approach the catabolic stoichiometry of denitrification. (c) Data ($n$ = 7,965) from the Northern Temperate Lakes LTER illustrate the imprint of heterotrophic N uptake, nitrification and denitrification on DOC—$NO_3^-$ relationships. Up to DOC:$NO_3^-$ ratios of 4, $NO_3^-$ concentrations remain very low because resource stoichiometry favors strong denitrification. When resource ratios rise above 4, nitrification and/or C limitation of heterotrophy generates a sharp accumulation of $NO_3^-$. However, as DOC:$NO_3^-$ ratios rise into the range of anabolic demand, $NO_3^-$ depletion occurs. These data were collected from 11 lakes that range dramatically in human-caused eutrophication, which exemplifies the robust dependence of the microbial processes described herein on discrete shifts in resource stoichiometry in the face of human disturbance to the C and N cycles.

C:N ratios of microbial biomass vary widely, from a low of ~3 to a high of ~20[3,18,20]. In addition, critical supply ratios are higher than microbial C:N tissue quotients because heterotrophic microbes use some of their organic carbon resource for energy production and building new cellular material. However, such bacterial growth efficiency (BGE) varies widely, often in response to the trophic state of the ecosystem (Apple *et al.* 2007, Jahnke *et al.* 1995, del Girogio *et al.* 1998). In oligotrophic conditions, with high resource C:N ratios and relatively low C lability, BGE tends to range between 5-20% (Apple *et al.* 2007, Jahnke *et al.* 1995, del Girogio *et al.* 1998). In contrast, BGE values in nutrient-rich systems are much higher and typically range

between 40-80% (Apple *et al.* 2007, Jahnke *et al.* 1995, del Girogio *et al.* 1998). Moreover, bacteria exhibit compositional plasticity can modify threshold ratios because biomass C:N can shift in concert with changes in resource C:N ratios (Tezuka *et al.* 1990). Such capability can shift the point at which N is in excess relative to heterotrophic demand. Notably for our analysis, microbial C:N ratios tend to decline as N supply increases relative to C (Tezuka *et al.* 1990). This fact, coupled with data showing that BGE values reach their peak in nutrient rich conditions, suggests that the critical ratio determining a switch from N to C limitation of microbial anabolism – and thus the point at which $NO_3^-$ concentrations may rise sharply – should approach the low end of the microbial C:N tissue quotient range. Hence, the flexibility inherent in both BGE and tissue stoichiometry likely underlies the variation in threshold ratios seen in Figure 2.3.

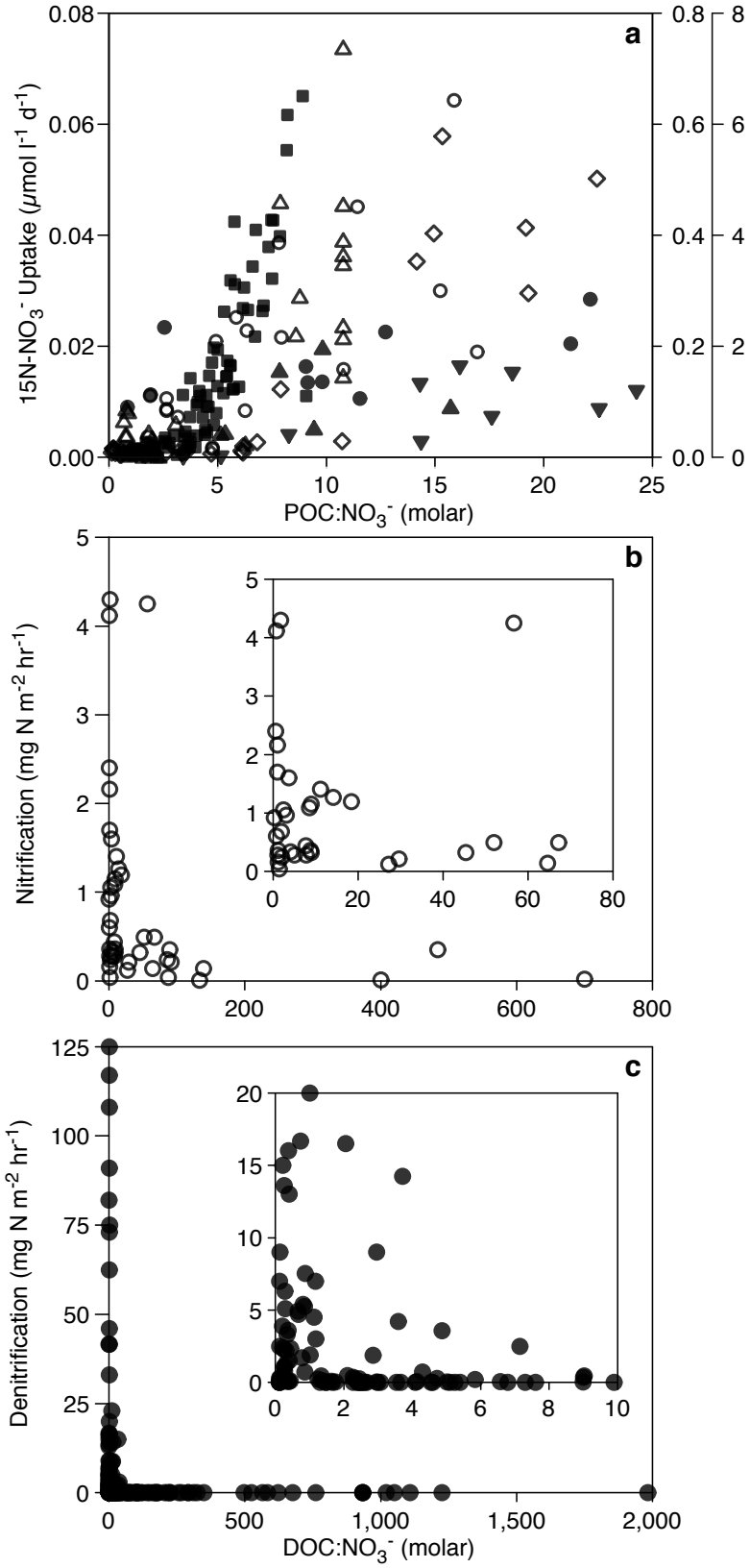
a
0.08
0.06
0.04
0.02
0.00
0.8
0.6
0.4
0.2
0.0
8
6
4
2
0
0
5
10
15
20
25
15N-NO3- Uptake (μmol l-1 d-1)
POC:NO3- (molar)
b
5
4
3
2
1
0
0
200
400
600
800
0
20
40
60
80
Nitrification (mg N m-2 hr-1)
c
125
100
75
50
25
0
0
500
1,000
1,500
2,000
0
2
4
6
8
10
20
15
10
5
0
Denitrification (mg N m-2 hr-1)
DOC:NO3- (molar)

Figure 2.3 | Resource stoichiometry controls on microbial NO3- processing. **(a)** Regression of planktonic nitrate uptake on oceanic POC:NO3- ratios in the Atlantic (open diamonds) and Lake Superior (inverted closed triangles) [low rates]; Equatorial Pacific (closed squares), Southern Ocean (open triangles), English Channel (closed triangles), Pacific Upwellings (closed diamonds) [medium rates]; Scheldt Estuary (open circles) and Rio de Ferrol (closed circles) [high rates]. See Supplementary Discussion for details on data assembly and Table 2.2 for statistical analysis. **(b)** Regression of in-stream nitrification and denitrification on DOC:NO3- ratios. Inset panel simply shows the low values more clearly.

Table 2.2 | Model results for data presented in Figure 2.1.

| Site | Reference (See SI Notes) | Model Parameters Best-fit Empirical Equation X = POC for oceans and DOC for streams and rivers Equation | *n* | $r^2$ |
|---|---|---|---|---|
| **N-$NO_3^-$ Uptake** | | | | |
| Lake Superior | 54 | $y = 0.0007^{1.578(x)}$ | 11 | .60* |
| Scheldt Estuary | 52 | $y = 0.24(x) + 0.21$ | 18 | .51 |
| Eastern Pacific | 41 | $y = 0.37^{0.024\,(x)}$ | 9 | .42 |
| Coastal Upwellings | | | | |
| Rio de Ferrol, Spain** | 53 | $y = 1.15^{0.018\,(x)}$ | 12 | .42 |
| English Channel** | 51 | $y = 0.0078(x)^{0.735}$ | 10 | .62 |
| Equatorial Pacific | 82 | $y = 0.0065^{0.22(x)}$ | 25 | .79 |
| Southern Ocean | 82 | $y = 0.004^{0.64(x)}$ | 100 | .83 |
| Northeastern Atlantic | 82 | $y = 0.0008^{0.24(x)}$ | 117 | .78 |
| **Nitrification** | | | | |
| Streams and Rivers | See 1 - 50 | $y = 0.23 + 1.27^{-0.11(x)}$ | 88 | .55 |
| **Denitrification** | | | | |
| Streams and Rivers | See 1 - 50 | $y = 0.13 + 3.24^{-0.03(x)}$ | 230 | .68 |

* All empirical models significant at $p < 0.001$
** POC values were not provided in publication text, so POC was estimated by multiplying PON by the C:N of the Redfield ratio.

We first tested this notion by comparing rates of microbial $NO_3^-$ assimilation to POC:$NO_3^-$ ratios in marine biomes, where data on gross rates $NO_3^-$ assimilation are most widely available. We use POC as the organic carbon resource because it reflects the bioavailable pool of marine organic carbon more so than DOC, which is typically comprised of older and more recalcitrant material (Sarmiento and Grubver 2006). We found POC:$NO_3^-$ breakpoint ratios between 4 and 14 across three distinct ocean biomes, as well as coastal, estuarine, riverine and lacustrine ecosystems. (Fig. 2.3A). Commonly

available $^{15}N–NO_3^-$ uptake data do not delineate between phytoplankton and bacterial N assimilation. However, using data from three marine systems, we found that strong increases in bacterial production track the rise in threshold ratios seen for N uptake across a gradient of eutrophic to oligotrophic conditions (Fig. 2.3A; Fig. 2.4,2.5; Table 2). In contrast, we found that autotrophy was largely unrelated to C:N breakpoints (Fig. 2.4C,D; Table 2.2; Supplementary Discussion).

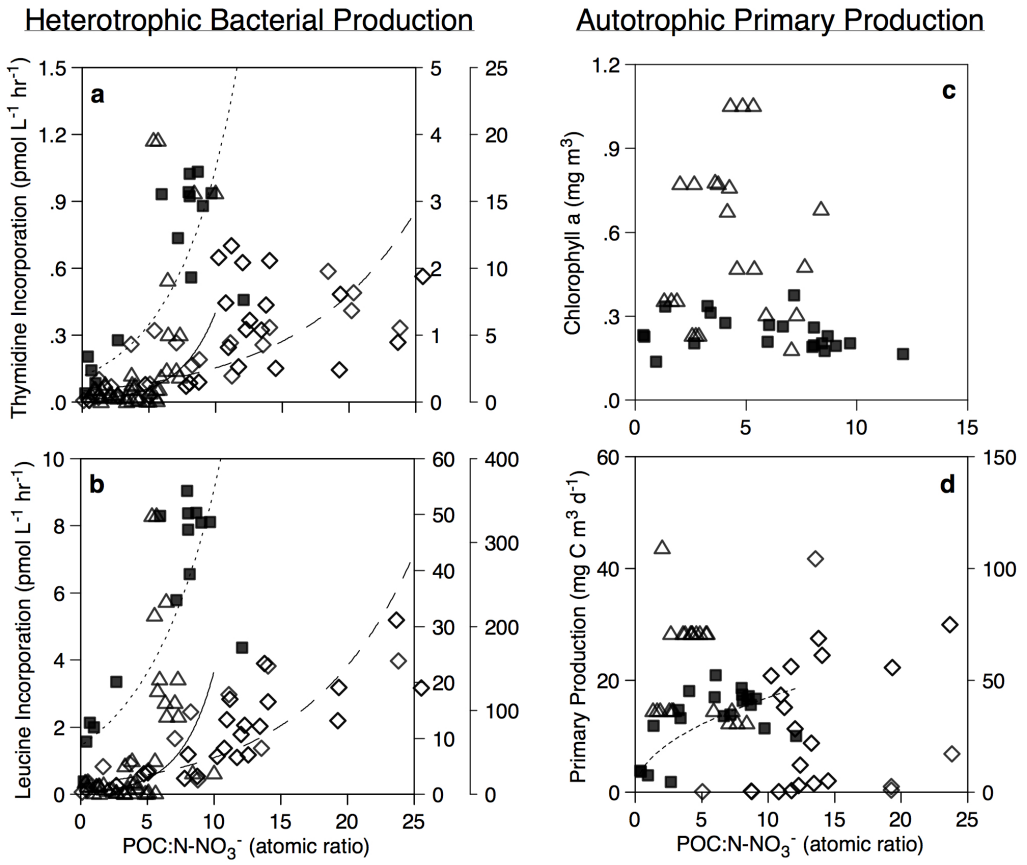


Figure 2.4 | Relationships between heterotrophic production and autotrophic activity on POC:N-$NO_3^-$ resource ratios. Heterotrophic bacterial production, measured as thymidine incorporation (a) and leucine incorporation (b), shows nonlinear increases at breakpoints that match $NO_3^-$ uptake thresholds observed in Figure 2.2. Autotrophic activity, measured as chlorophyll a concentration (c) and primary production (d) generally shows no relation with POC:N-$NO_3^-$ resource ratios, with the exception of the Equatorial Pacific (d). Markers are the same as found in Figure 2.3. See Table 2.3 for empirical model results for best-fit regression analysis.

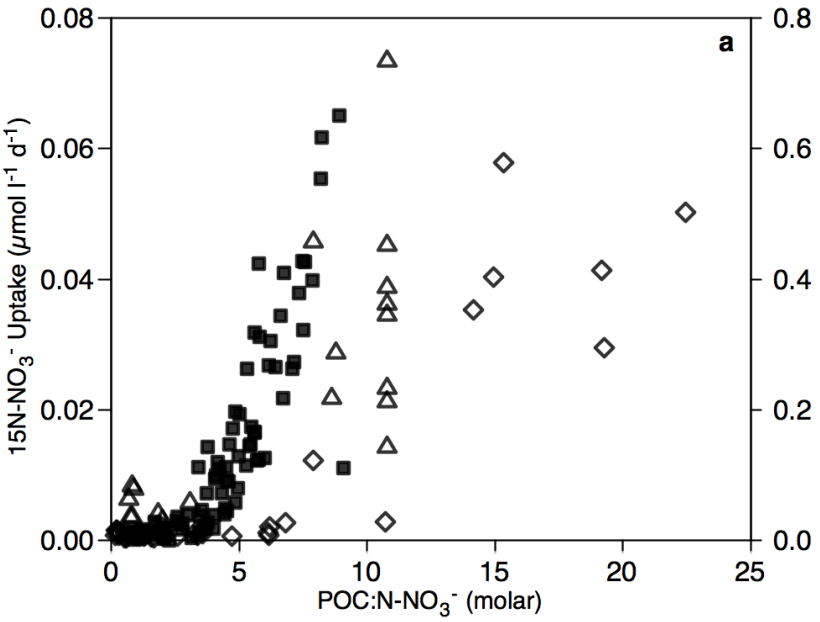


Figure 2.5 | Relationships between $^{15}N\text{-}NO_3^-$ uptake and POC:$N\text{-}NO_3^-$ resource ratios for three ocean provinces. This plot is duplicated from select data observed in Figure 4 for direct comparison of N uptake on resource ratios (shown here) and heterotrophic and autotrophic activity in resource ratios (Figure 2.4). A gradient of nutrient poor to nutrient rich conditions generally extends from the North Atlantic, Equatorial Pacific and Southern Ocean.

Table 2.3 | Model results for data presented in Figure 2.5.

| Process | Model Parameters<br>Best-fit Empirical Equation<br>Equation | *n* | $r^2$ |
|---|---|---|---|
| **Heterotrophic Production (thymidine incorporation)** | | | |
| Southern Ocean | $y = 0.007^{0.39(x)}$ | 29 | .41* |
| Equatorial Pacific | $y = 0.009^{0.38(x)}$ | 52 | .42 |
| North Atlantic | $y = 0.811^{0.11\,(x)}$ | 121 | .53 |
| **Heterotrophic Production (leucine incorporation)** | | | |
| Southern Ocean | $y = 0.037^{0.54\,(x)}$ | 29 | .42 |
| Equatorial Pacific | $y = 0.065^{0.41(x)}$ | 52 | .59 |
| North Atlantic | $y = 12.552^{0.13(x)}$ | 121 | .78 |
| **Autotrophy** | | | |
| Equatorial Pacific | $y = 5.606\,(x)^{0.48}$ | 34 | .38 |

* All empirical models significant at $p < 0.001$

Thus, we believe these patterns may reflect a contemporary view of marine N cycling, where bacterioplankton significantly contribute to $NO_3^-$ uptake, regeneration and nitrification (Mulholland and Lomas 2008). This pattern suggests that high N assimilation by heterotrophs activates only when resources and theoretical consumer stoichiometry come into balance. As POC:$NO_3^-$ ratios rise above minimal ratios near to 4, resource C:N composition becomes increasingly N-poor relative to the microbial N assimilation stoichiometry for anabolism, and $NO_3^-$ concentrations remain consistently low. Most notably, declines below a POC: $NO_3^-$ ratio of 4 likely reflects increasing C limitation of microbial anabolism, suggesting that stoichiometric controls over heterotrophic activity regulate $NO_3^-$ buildup.

Of course, nitrate is not the only potential N source for microbial activity in these environments. However, in both freshwater and marine ecosystems, inorganic N pools tend to be dominated by $NO_3^-$ (Barnes and Raymond 2010, Arango and Tank 2008, Bohlke *et al.* 2009, Perakis and Hedin 2002), and using a subset of representative sites from oceans and streams, we find that including ammonium ($NH_4^+$) does not alter inverse relationships (Figure 2.6A, C; Table 2.4; Supplementary Discussion). In contrast, organic forms of N (DON or PON) display positive correlations with their organic carbon counterparts (DOC and POC, respectively; Figure 2.6 B, D), but this is to be expected since the vast majority of organic matter in ecological environments contains both C and N in fairly constrained ratios[3,18-20].

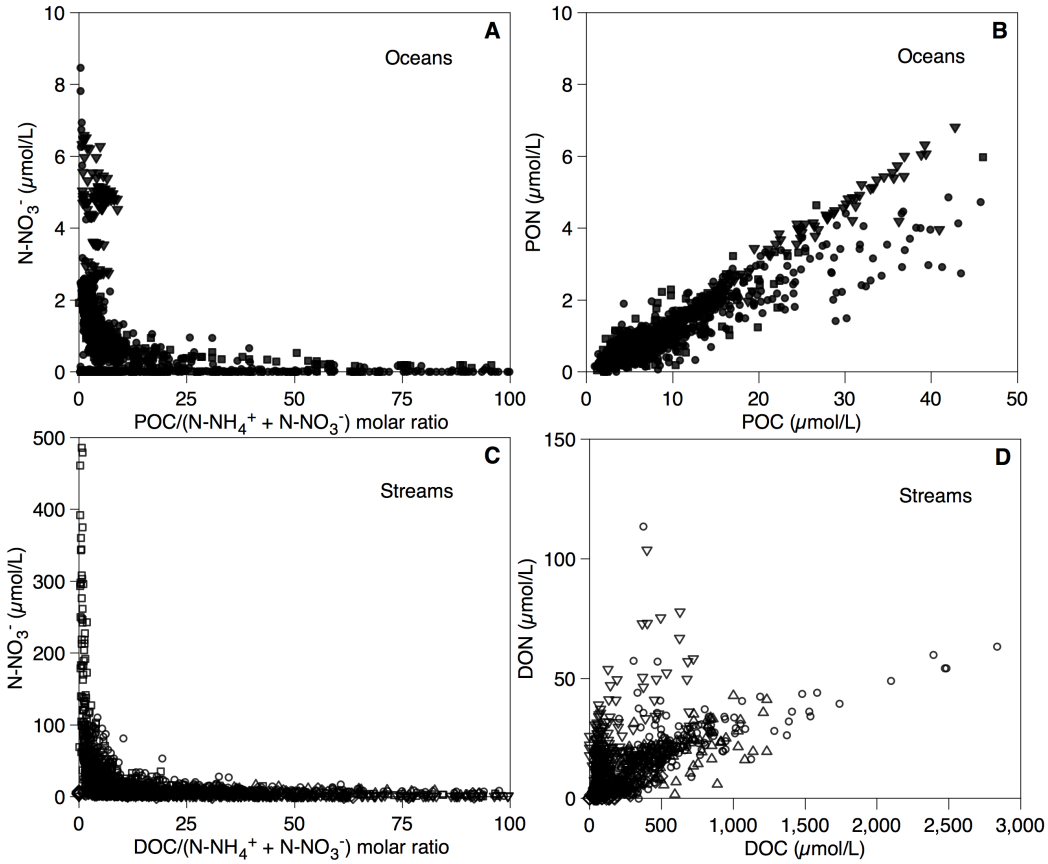


Figure 2.6 | Relationships between $NO_3^-$ concentration and resource ratios for select (A) ocean and (C) stream locations, where $NH_4^+$ is included in the supply quotient in addition to $NO_3^-$. Panels B and D show organically bound nitrogen abundance in oceans (B) and streams (D) as a function of organic carbon concentration. (A, C) Negative trends remain practically unaltered relative to patterns shown in Figure 2.1. Oceans: closed circles = CARIACO basin, closed triangles = Southern Ocean, closed diamonds = Equatorial Pacific, closed squares = North Atlantic. Streams: open triangles = Arctic (Partners), open squares = continental USA (EPA EMAP), open diamonds = Puerto Rico (Luquillo LTER), inverted triangles = Brazil (MBL Brazil), open circles = Northeast USA (Plum Island LTER). See Table 2.4 for system-specific correlation coefficient and statistical significance.

Table 2.4 | Correlation results for DON or PON as a function POC or DOC, respectively, for data presented in Figure 2.6.

| Site | Model Parameters * Empirical Equation: y = *a*(x) +/- *b* x = POC for oceans and DOC for streams and rivers | | |
|---|---|---|---|
| | *a* | *b* | *r* |
| **Oceans** | | | |
| Southern Ocean | .14 | -.09 | .98 |
| Equatorial Pacific | .16 | -.23 | .98 |
| Northeast Atlantic | .15 | .01 | .99 |
| CARIACO Basin | ,07 | .07 | .81 |
| **Streams** | | | |
| Arctic | .02 | 10.76 | .52 |
| Puerto Rico LTER | .01 | 1.95 | .48 |
| Brazil | .05 | 12.96 | .55 |
| Plum Island LTER | .02 | 9.6 | .61 |

***** All trends significant at $p < 0.001$.

$NO_3^-$ accumulation may also be driven by nitrification, which could be enhanced as a consequence of C limitation of heterotrophic N assimilation. Heterotrophic organisms often out-compete nitrifying organisms for $NH_4^+$, but that effect will be strongest when nitrogen supply limits metabolism. Consequently, when N assimilation is C limited at low DOC:$NO_3^-$ ratios, enhanced $NH_4^+$ availability may promote nitrification. Indeed, we find that across streams with wide variation in adjacent land-use and underlying biome-scale differences, resource controls on nitrification are more complex than basic concentration-dependent uptake kinetics (Figure 2.7E, F; Table 2.5; Supplementary Discussion). Instead, nitrification rapidly increases at resource ratios below the minimum supply C:N ratios for heterotrophic microbes (Fig. 2.3B).

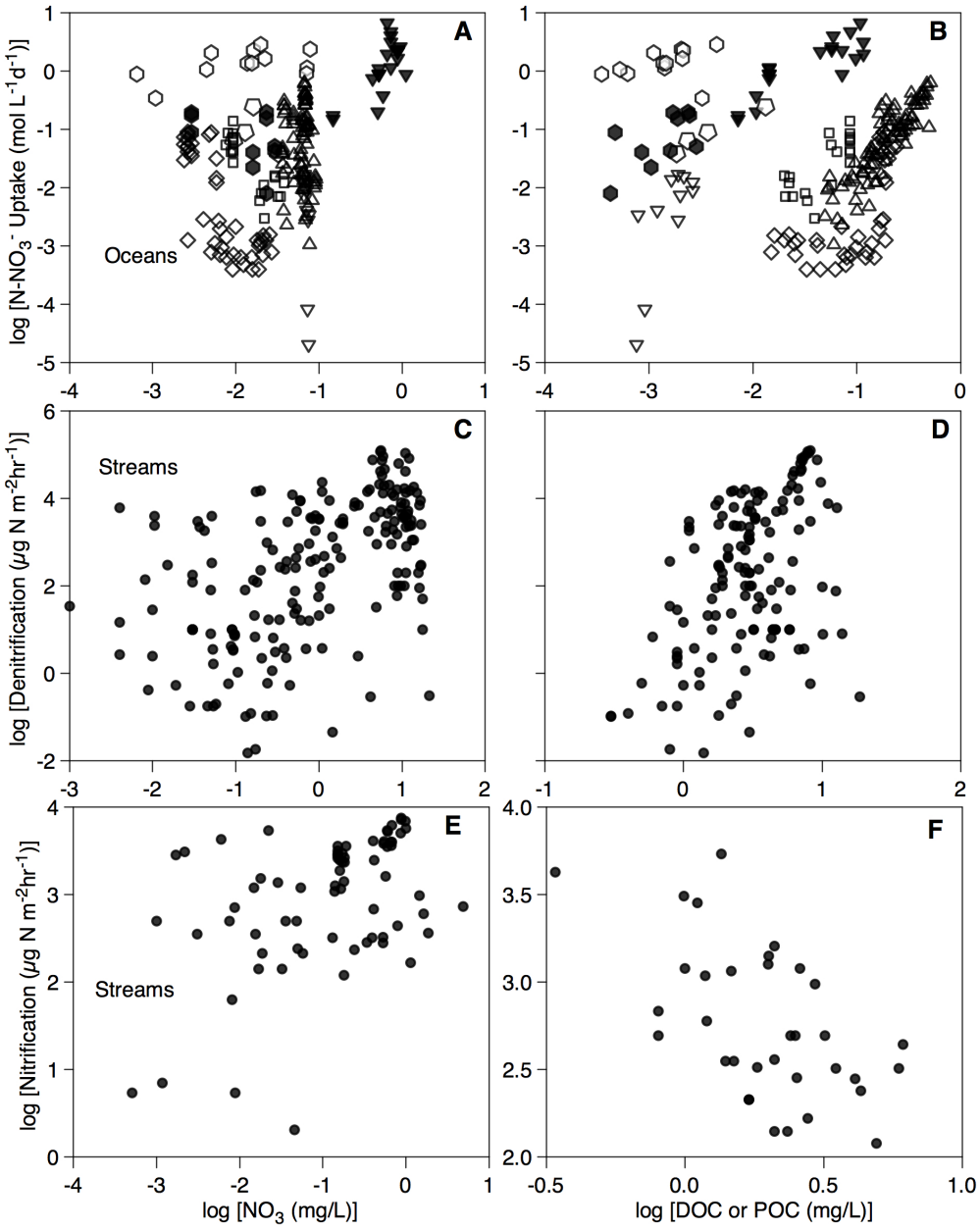


Figure 2.7 | Plots of oceanic $^{15}N\text{-}NO_3^-$ uptake (A, B), in-stream denitrification (C, D) and in-stream nitrification (E, F) as a function of $NO_3^-$ and DOC (streams) or POC (oceans) concentration. Site markers: Atlantic (open diamonds), Lake Superior (inverted closed triangles), Equatorial Pacific (closed squares), Southern Ocean (open triangles), English Channel (closed hexagons), Pacific Upwellings (pentagons), Scheldt Estuary (inverted closed triangles) and Rio de Ferrol (open hexagons). See Table 2.5 for regression analysis and statistical significance.

Table 2.5 | Regression model results for Figure 2.7 for direct comparison of concentration versus stoichiometric controls over $NO_3$- assimilation, nitrification and denitrification.

| Site | Model Parameters * Empirical Equation: log[y] = log[*a*(x)] +/- *b* | | | | | | | | |
|---|---|---|---|---|---|---|---|---|---|
| | x = $NO_3^-$ | | | x = organic C | | | x = organic C:N-$NO_3^-$ | | |
| | *a* | *b* | $r^2$ | *a* | *b* | $r^2$ | *a* | *b* | $r^2$ |
| **N-$NO_3^-$ Uptake** | | | | | | | | | |
| Lake Superior | -25.8 | -32.3 | .47 | 3.7 | 7.7 | .57 | **3.4** ** | **- 3.7** | **.61** |
| Scheldt Estuary | 1.5 | .39 | .53 | **.91** | **1.4** | **.72** | 1.0 | -.6 | .52 |
| Eastern Pacific Upwellings | -.5 | -1.9 | .10 (ns) | .9 | 1.1 | .89 | **.6** | **-2.0** | **.97** |
| Rio de Ferrol | -.1 | .1 | 0 (ns) | **.5** | **1.6** | **.60** | .2 | -.1 | .42 |
| English Channel | -.5 | -2.1 | .21 (ns) | 1.0 | 1.7 | .39 (ns) | **.7** | **-2.1** | **.62** |
| Equatorial Pacific | -1.6 | -4.5 | .68 | 1.4 | .3 | .56 | **.8** | **-2.1** | **.86** |
| Southern Ocean | -.3 | -1.6 | 0 (ns) | 2.1 | .3 | .69 | **2.0** | **-2.3** | **.79** |
| Northeastern Atlantic | -1.9 | -6.5 | .59 | 1.6 | -.8 | .44 | **.9** | **-3.4** | **.64** |
| **Nitrification** | | | | | | | | | |
| U.S. and Puerto Rico Streams and Rivers | .7 | 3.6 | .42 | -1.7 | 3.4 | .45 | **-.53** | **3.5** | **.47** |
| **Denitrification** | | | | | | | | | |
| U.S. and Puerto Rico Streams and Rivers | 4.5 | 0 | .42 | 1.5 | 2.3 | .47 | **-1.6** | **2.9** | **.53** |

* All trends significant at $p < 0.001$.
** Bold indicates empirical model with best goodness of fit.

As with heterotrophic assimilation and nitrification, the availability of both organic C and $NO_3^-$ regulates denitrification. Unlike the anabolic process of $NO_3^-$ uptake explored above, denitrification is a catabolic process that requires organic C and $NO_3^-$ in approximately a 1:1 ratio (when biomass synthesis is ignored). Our meta–analysis revealed that denitrification activity abruptly responds with increases up to 125-fold at DOC:$NO_3^-$ ratios that are in-line with the stoichiometric requirements (Fig. 2.3C). For systems where $NO_3^-$ accumulation continues at very low organic C:$NO_3^-$ ratios, other environmental factors (e.g. oxic conditions) may constrain denitrification activity.

Taken as a whole, the above analyses of marine and stream ecosystems suggest that N assimilation, nitrification and denitrification all likely contribute to the comparative uniformity of the patterns in Figure 1. Thus, we explored whether organic $C:NO_3^-$ ratios at the inflection point of each exponential model (Fig. 2.1) to see whether the threshold C:N ratios for each major environment align with the breakpoints found in Figure 2. We focused on $DOC:NO_3^-$ ratios in all systems except oceans because POC in non-pelagic systems may encompass a greater proportion of terrigenous, recalcitrant C (Raymond and Bauer 2001, Cebrian 1999), which would explain the higher $POC:NO_3^-$ ratios for those systems (Table 2.1). We find that despite wide variation in pools of organic carbon and $NO_3^-$ among earth's ecosystems (Fig. 1), the $DOC:NO_3^-$ ratio at the inflection point averages 3.5 across all systems and is constrained between 2.2 and 5.2 (Table 2.1). At the global scale, threshold ratios are greater for lakes and ocean margins when POC is used in the numerator (Table 2.1), as well as for several system-specific scenarios (Figure 2.8; Table 2.6). These higher ratios rest within the expected stoichiometric window for $NO_3^-$ accretion, and likely reflect the response of bacterial compositional plasticity and growth efficiency to organic C bioavailability accretion (Supplementary Discussion). When viewed across all systems and scales of observation, $NO_3^-$ tends to rise sharply at organic $C:NO_3^-$ requirements between those of heterotrophic assimilation and denitrification, a pattern which may arise from both an alleviation of N limitation to many heterotrophs and an increase in nitrification rates.

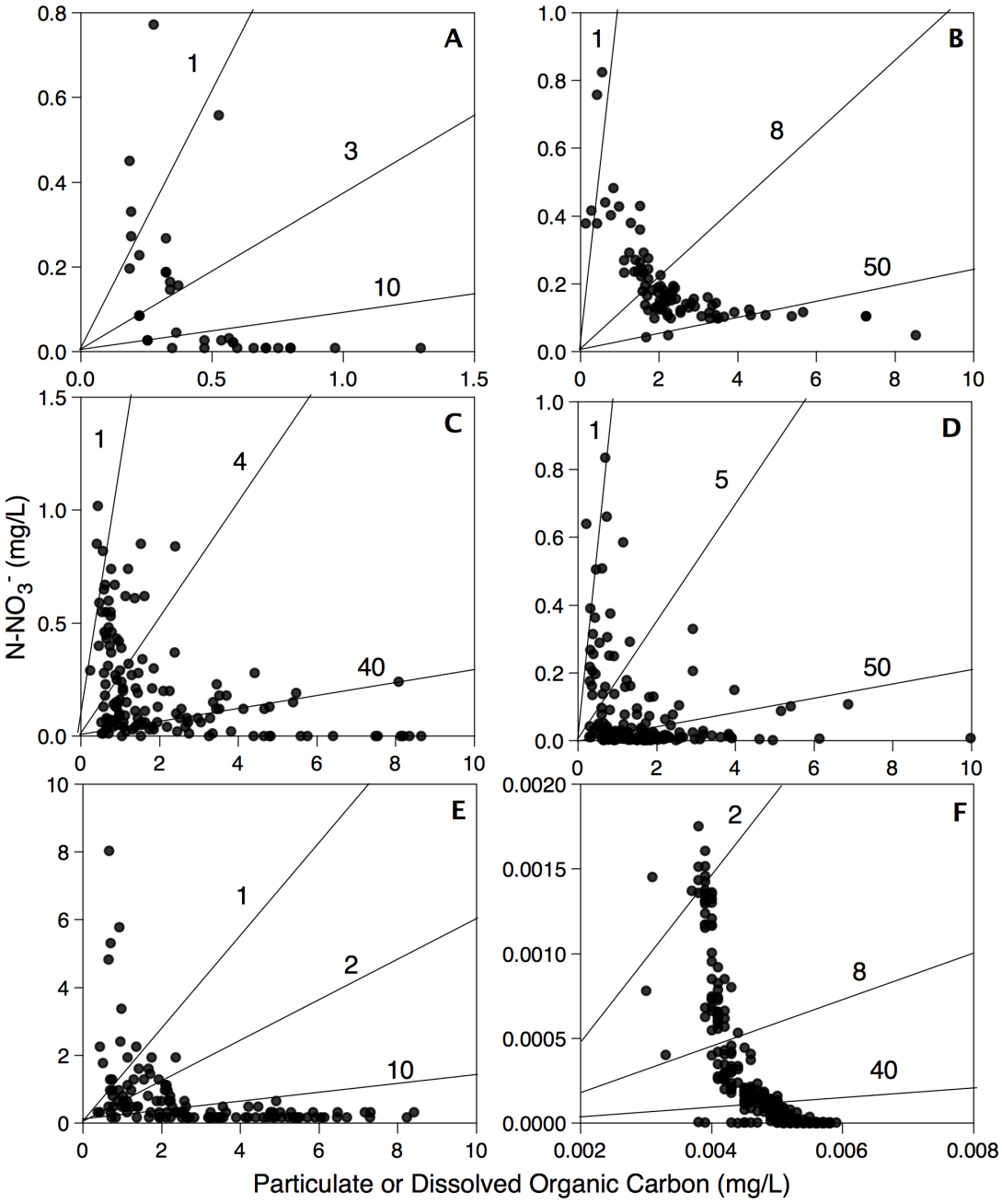


Figure 2.8 | Plots of N-$NO_3$ concentration as a function of DOC concentration for select system-specific scenarios for (A) soils[58], (B) streams[62], (C) human impacted streams[78], (D) lakes[81], (E) bays[81] and (F) oceans[82]. Lines represent the organic carbon:N-$NO_3$ atomic molar ratio. See Table 2.6 for regression analysis. See SI Discussion for details on data assembly and analysis.

Table 2.6 | Empirical assessment of select system-specific DOC-$NO_3^-$ relations in Figure 2.8.

| Global System | Modeled Parameters ($y=a+b^{-k(x)}$) | | | Model Fit ($r^2$) |
|---|---|---|---|---|
| | a | b | *k* | |
| Soils* | -0.04 | 0.47 | 2.63 | 0.58 |
| Streams* | 0.07 | 0.61 | 0.85 | 0.72 |
| Human Impacted Streams* | 0.09 | 0.55 | 1.21 | 0.62 |
| Lakes* | 0.03 | 0.37 | 2.07 | 0.56 |
| Bay* | 0.17 | 2.75 | 2.85 | 0.68 |
| Oceans* | -0.09 | 232.78 | 9.87 | 0.84 |

* Data taken from references numbers 58, 62, 78, 81, 81, 82 for soils, streams, human impacted streams, lakes, bays and oceans, respectively.

Finally, we believe the increase in the exponential decay constant (*k*) from soils to the sea reveals a systematic (Table 2.1) decline in energetic constraints over nitrate cycling along the hydrologic continuum. Where terrestrial plant derivatives dominate DOC pools, more chemically complex, decay-resistant compounds are more prevalent than in systems where aquatic sources prevail (Raymond and Bauer 2001, Cebrian 1999). In fact, the *k*-value for human impacted rivers and streams is more comparable to soils than to undisturbed rivers and streams (Table 2.1), which suggests increased terrestrial DOC inputs to freshwater systems in landscapes susceptible to anthropogenic runoff. Also, the concurrent decline in unexplained variation in DOC—$NO_3^-$ relationships as one moves from soils to the sea (Table 2.1) may support a weakening influence of C quality on the expression of resource-consumer imbalance as organic C supply shifts from terrestrial to aquatic sources. Taken together, these trends might signal a progressive shift towards increasingly pure stoichiometric control in marine environments versus freshwaters with substantial allochthonous sources of C (Cebrian 1999)

In this paper, we have attempted to link stoichiometric and metabolic theories of ecology (Allen and Gillooly 2009) to develop a new context in which to understand coupled organic C and $NO_3^-$ cycling from local to global scales. We believe the framework presented here may aid a variety of Nr-related management challenges. For instance, downscaling from our global analysis to a variety of system-specific scenarios shows that DOC—$NO_3^-$ relationships become stronger (Fig. 2.8, Table 2.6). Such analyses, when done at scales most relative to management, could allow managers to focus on a subset of conditions to direct the fate of $NO_3^-$. For example, resource ratios could be strategically regulated to optimize heterotrophic $NO_3^-$ assimilation, where high $NO_3^-$ accumulation rarely occurs.

That said, we do not advocate for a stoichiometric perspective to the exclusion of kinetic, thermodynamic and mass-balance approaches. Indeed, substantial variation in organic C—$NO_3^-$ relations suggests a role for environmental factors in addition to stoichiometric controls. Thus, we believe that better integration of established applications with the first-principles of ecological stoichiometry would improve a range of diagnostic and prognostic models of water quality. Achieving this goal will require continued evaluation of the mechanisms that underlie inverse organic C—$NO_3^-$ patterns. Furthermore, additional research should resolve key uncertainties in what determines C—$NO_3^-$ thresholds; we believe a focus on the controls over microbial compositional plasticity and growth efficiency is particularly important. Nonetheless, the results presented here provide a testable framework for further unraveling the controls over $NO_3^-$ accumulation in ecosystems worldwide.

**2.4. Supplementary Discussion**

*2.4.1. The influence of bacterial growth efficiency and compositional plasticity on critical threshold ratios for $NO_3^-$ accumulation*

Understanding the dynamics of rapid $NO_3^-$ depletion above critical threshold ratios requires consideration of both bacterial growth efficiency (BGE) and the stoichiometric plasticity of microbial biomass at the community scale. Each factor can contribute to variation in the system-specific C:$NO_3^-$ breakpoints at which nitrate begins to accumulate rapidly. First, we will address the role of BGE in influencing the POC:N-$NO_3^-$ thresholds observed in Figure 2.2. BGE represents the proportion of assimilated organic carbon allocated to production versus respiratory processes, like active nutrient transport and extracellular enzyme production. Different BGE among bacterial communities can shift the threshold ratio by changing the proportion of C allocated for different metabolic purposes. In many ecosystem models, BGE is commonly assumed to be somewhere between 40 - 60% , which reflects the average BGE of several meta-analyses (Jahnke *et al.*1995, Cole *et al.* 1988).

However, the true variability of BGE among taxa and environmental trophic conditions is much greater than the 40 – 60% typically assumed in models. In extremely oligotrophic open oceans, where BGE has been evaluated extensively in comparison to inland aquatic or terrestrial systems, BGE values are commonly found to be <15% (Jahnke *et al.*1995, Cole and Pace 1995, Kirchman *et al.*1991). In fact, most BGE studies have been conducted in oligotrophic, open ocean systems (Urrutia-Lopez and Moran 2007), which has potentially biased our understanding of BGE toward lower values. In contrast, strikingly high BGE values have been observed in nutrient-rich systems, such as nutrient-rich open oceans, upwelling regions, coastal margins and estuaries (Jahnke *et al.* 1995), where BGE values often greatly exceed 50%. Goldman et al. (2001) and del

Girogio et al. (1998) among others (Ram *et al.* 2003, Biddanda *et al.* 2001), provide empirical evidence that BGE shifts in concert with reduced resource C:N ratios. Thus, as bacterial and resource C:N stoichiometry come into balance, microbes appear to shift C allocation pathways proportionally away from maintenance processes toward intracellular compounds that facilitate higher production.

It is conceivable that the strong correlation between reduced C:N substrate ratio and greater BGE reflects an influence of decreased organic C recalcitrance on bacterial metabolism. As aquatic systems become more nutrient rich and autotrophic production increases, phytoplanktonic carbon derivatives, which are lower in C:N composition and highly bioavailable, become the prime energy and nutritional supply to heterotrophs. In a recent study, Apple and del Giorgio (2007) found that BGE was strongly and positively correlated with increases in labile C availability, which in turn, was highly related to both phytoplankton and bacterial production. There is also evidence from many studies (e.g. Kanda *et al.* 2009, Kirchman *et al.* 1994, Wheeler *et al.* 1986) that increases in phytoplankton production in nutrient-rich aquatic systems provide the predominant source of simple carbon compounds, like transparent exopolymers, that to serve as substrates for bacterial growth. In fact, del Giorgio et al. (1998) among many other studies (Cole *et al.* 1995, Murrell 2003, Goldman *et al.* 1987) show that bacterial and phytoplankton production are closely coupled and that phytoplankton-derived C compounds with lower C:N composition (Biddanda *et al.* 2001) yield the highest BGE, which results in strong positive correlations between phytoplankton productivity with nutrient richness and high BGE.

Yet, organic carbon bioavailability almost certainly does not regulate BGE independently of resource stoichiometry. Theoretically, when resource C:N ratios lower into the range of potential C:N biomass ratios, it should require less C investment into cellular maintenance operations, like building energy intensive enzymes to breakdown organic C is quest for N. Consequently, BGE should rapidly increase as energy allocation swings towards increasing relative biomass production. Experiments conducted by Goldman *et al.* (2001) and others (Manzoni *et al.* 2008) illustrate this mechanism, where BGE increases nonlinearly across declining substrate C:N ratios when organic C bioavailability is held virtually constant. More broadly, a recent meta-analysis provides further evidence showing that BGE ranges from 60 – 90% at low C:N substrate ratios (<10) for bacterial communities grown in controlled media inoculated with simple carbon compounds and nutrients (Jahnke *et al.* 1995). Additional support comes from modeling efforts aimed at exploring the influence of resource quantity (concentration) and quality (C:N) on bacterial growth, respiration and excretion. Touratier *et al.* (1999) found that nonlinear BGE increases from 40 to 80% across a range of resource C:N ratios declining from 14 to 3.

Analysis of BGE has been disproportionately conducted in aquatic systems, as the above studies highlight. Yet, recent meta-analyses in terrestrial systems (Manzoni *et al.* 2010, Lancelot 1985) illustrate the same mechanism for soil systems that range widely in biological and physical conditions from boreal to tropical regions. That is, in decomposing leaf litter, bacterial BGE increases with nutrient content and vice versa. Using a stoichiometrically explicit model, Manzoni *et al*. (2010) demonstrate the patterns of N immobilization and production are strongly governed by the metabolic activity of

microbes that grow according to constrained compositional requirements to achieve balanced growth. Compared to aquatic systems however, BGE in soils tends to be lower, averaging close to 25% BGE. Collectively, these experimental, observational and modeling results demonstrate that shifts in nutritional quality can strongly regulate BGE independently of energetic quality, potentially in all of earth's ecosystems.

Variability in BGE may affect the imprint of both denitrification and microbial N assimilation on observed stoichiometric C:$NO_3^-$ breakpoints because both of these processes require heterotrophic metabolism of organic matter for energy and carbon, and thus carbon use efficiency becomes an issue in calculating threshold ratios. In most biogeochemical models that are stoichiometrically explicit, microbes are treated as catalysts in chemical reactions in order to simplify the potential for differential partitioning of reactants into products. For example, classical equations for the conversion of $NO_3$ to $N_2$ via denitrification calculate a C:N uptake ratio of 4:5 without accounting for the respiratory costs of obtaining bioavailable organic carbon for catabolism. These simplifications work for certain scenarios, yet differences or shifts in the partitioning of energy or carbon on the cellular level can affect the position of the stoichiometric thresholds as we highlight in this study.

Another factor that can influence organic C:N-$NO_3^-$ ratios stems from the capacity of bacteria to shift intracellular stoichiometry in response to changes in resource C:N values. While often viewed as stoichiometrically constrained relative to plant communities, bacterial communities display considerable range in their tissue C:N quotients (Sterner and Elser 2002, Cleveland *et al.* 2007, Sterner *et al.* 2008). Though the C:N of marine bacterioplankton appears largely constrained between 4-7 (Goldman *et al.*

1987), when viewed across all systems, bacterial C:N ratios can range from 3 to 24, with greater variation seen in inland systems (Sterner and Elser 2002, Lancelto *et al.* 1985), particularly soils (Cleveland *et al.* 2007). This observed flexibility suggests that bacteria have the capacity to shift tissue C:N values in response to varying resources in the environment. The specific mechanisms are debated, but could reflect an advantage in shifting biomass stoichiometry to match resource composition in order to reduce energy expenditures associated with metabolic waste excretion. Results of Tezuka *et al.* (1990) may support this possibility; bacterial and resource C:N were strongly correlated when organic C bioavailability remained relatively unchanged relative to energy richness across a resource C:N gradient extending from 6 to 30. However, it is more likely that the strong correlation is consequent of broader gradients in C:N composition where energy richness relative to N abundance moderates plasticity independent of bioavailability *per se*. That is, trophic conditions of lower C:N substrate probably facilitate greater bacterial productivity (Anderson *et al.* 2005, Apple *et al.* 2007, *et al.* 1999, Lancelot *et al.* 1985), as well as BGE (Anderson *et al.* 2005, Apple *et al.* 2007, *et al.* 1999, Lancelot *et al.* 1985), which requires a proportional shift away from structural tissue generation and energy storage in lipids and carbohydrates (high C:N ratios) to greater protein (average C:N ~ 3.1; Sterner and Elser 2002) and nucleic acid (average C:N ~ 2.3; Sterner and Elser 2002) synthesis to construct biomass. In fact, a closer inspection of the substrate versus bacterial C:N plot observed by Tezuka et al. (1990) reveals a saturation function, where the discrepancy between substrate and bacterial C:N enlarges at high resource ratios, which could indicate that greater resource C:N ratios require bacteria to respire more C for every N atom gained for metabolic demands,

thereby lowering BGE. Goldman and Dennett (1987) proposed the same mechanism based on observed rapid increases in microbial biomass C:N with elevated substrate C:N in an incubation experiment. However, the maximal substrate C:N at 30:1 far surpassed potential bacterial biomass C:N, which increased to a high of 7.8:1. Likewise, results of Tezuka *et al.* (1990) show that across a substrate gradient of 6 to 30 microbial C:N ranged more widely, and reached a maximum of 17. Even in a broader context, the positive relationship between resource and organismal stoichiometries has been documented and discussed since Alfred Redfield's notion that resource and organismal stoichiometries come into balance through assimilation and remineralization (1963). These studies also collectively reiterate that the range of possible microbial C:N composition is stoichiometrically constrained, and only shows limited response to changes in resource stoichiometry.

However, for a system-specific analysis, the potential variability in microbial C:N ratio can be important. Even in a relatively oligotrophic pelagic system where BGE should be constrained to values around 40% , like at the Bermuda Atlantic Time Series site, microbial C:N can vary from ~ 3.5 to 8.5 on an annual basis (Gunderson *et al.* 2002). Assuming a constant BGE of 40% throughout the year, the range of the optimal stoichiometry for heterotrophic N assimilation can range from 21 to 51 based on the influence of changes in biomass C:N alone. In part, assimilated N is sequestered into microbial biomass N, which contributes to the depletion of $NO_3^-$, which can represent a large portion of ecosystem N (van der Heijden *et al.* 2008) . However, under conditions of N limitation, heterotrophic bacteria also greatly increase N use efficiency, which can maintain a low concentration $NO_3^-$ pool that turns over quickly. Yet, in reality, BGE

likely increases greatly as microbial C:N declines, thus dampening the potential absolute increase in the breakpoint stoichiometry expected on microbial C:N alone. Such shifts in BGE within a given system are documented on both spatial (Kanda *et al.* 2008) and temporal (Apple *et al.* 2007) scales; however, these studies often lack explicit connection to potentially simultaneous shifts in microbial stoichiometry.

While the interplay between stoichiometry and C bioavailability is not entirely understood and cannot be disentangled for the patterns shown here, it seems clear that for systems with greater phytoplankton/bacterial productivity, with trophic conditions low in resource C:N composition and abundant labile carbon, variation in BGE and intracellular resource allocation are likely to produce low C:N threshold ratios. A comparison of three open ocean regions — the Southern Ocean, Equatorial Pacific, and the Northeast Atlantic — which represents a gradient from nutrient-rich to oligotrophic systems, illustrates these controls on BGE. For ease of viewing, SI Figure 3 shows data from these three regions as originally shown in Figure 2. Among these ocean provinces, the Southern Ocean is generally more nutrient rich than the Northern Atlantic, while the Equatorial Pacific's trophic status rests somewhere between these systems. Here we highlight that previous documentation of BGE in these regions tracks the increases in POC:N-$NO_3^-$ ratios observed along the eutrophic-oligotrophic gradient. That is, high bacterial growth efficiencies correspond to low C:N uptake threshold values, and vice versa. Previously documented bacterial growth efficiencies and C:N uptake thresholds (reported herein) for the Southern Ocean, Eq. Pacific, and the North Atlantic provinces are approximately 42% (Bjornsen *et al.* 1991) and 5, 30% (Sorokin *et al.* 1980) and 10, and 15% (Suttle *et al* 1991) and 15, respectively. Hence, applying these BGE values to the observed POC:N-

$NO_3^-$ breakpoints in SI Figure 3, microbial biomass C:N is roughly 2.1, 3.0 and 2.3 for the Southern Ocean, Eq. Pacific and the North Atlantic. While these back-calculated bacterial biomass ratios are very low for tissue C:N ratios, they support the theoretical predictions described above that tissue C:N quotients should be low, and BGE values high, at the breakpoints of the organic C:$NO_3^-$ relationships.

Evidence for relatively constrained microbial C:N biomass ratios between 4 to 7 in marine systems suggests that BGE may be the primary source of variability that underlies shifts in threshold C:$NO_3$ ratios. For example, very low BGE could explain the relatively high stoichiometric threshold in the ultra-oligotrophic Sargasso Sea (SI Figure 6F), where bacterial BGE is commonly reported to be around 10% (Kirchman *et al.* 1991). That is, if the bacterial biomass C:N is assumed to be 5, the expected threshold C:$NO_3^-$ ratio is approximately 45, which roughly matches the observed breakpoint. The average oceanic threshold ratio for bacterial heterotrophy may be close to 10, based on an average biomass C:N of 5 (Goldman *et al.* 11987) and BGE of 50% (Apple *et al.* 2006) for oceanic bacteria. However, for systems that exhibit greater ranges in bacterial biomass C:N (such as soils [Anderson *et al.* 2005]), both compositional plasticity and BGE variation are likely to play a significant role in determining the breakpoints. We view additional research into the patterns and controls over both microbial C:N values and BGE to be a key need.

The stoichiometry of denitrification is comparatively more constrained for two reasons. First, stoichiometric plasticity is not a factor in this catabolic reaction. Second, the theoretical threshold ratio of ~1:1 C:$NO_3$ dampens the effect of variable BGE by preventing a wide range of potential C:$NO_3$ threshold ratios due to changes in carbon and

energy allocation. For instance, a 100% change in BGE for denitrifiers could increase the optimal stoichiometry to 2:1, whereas a similar change in heterotrophic microbial N assimilation, with a C:N stoichiometry of 6, would shift the breakpoint stoichiometry to 12, assuming no change in microbial stoichiometry in response to resource stoichiometry. Based on this example, it becomes evident that the combined influence of BGE and compositional stoichiometry on heterotrophic N assimilation has potentially greater influence than denitrification on the overall position of organic C:$NO_3^-$ breakpoint. Also, the combined influence of these two factors on heterotrophic N assimilation makes it difficult to identify a well-defined range of optimal resource stoichiometry that stimulates N assimilation across systems. Indeed, such variation may be reflected in the site-to-site variation observed in SI Figure 6. Yet, it is noteworthy that despite the possible variation in the breakpoint imparted by heterotrophic N assimilation, the global DOC:$NO_3^-$ breakpoint is well constrained between 2.19 and 5.22 (Table 2.1). This may imply that despite between-system variation (Fig. 1.6 and Table 2.6), denitrification strongly acts to lower the threshold ratio at the global scale. We believe resolving the underlying interaction of denitrification, nitrification and N assimilation and stoichiometry across the scales is an important research need, as these relationships will influence critical thresholds in $NO_3^-$ accumulation.

*2.4.2 Heterotrophic microbial influence on organic carbon – nitrate patterns*

In aquatic systems, photoautotrophs play a large role in regulating N availability. While this is true, heterotrophic bacterial production is often highly related to primary production because soluble, bioavailable organic compounds derived from phytoplankton

fuel heterotrophic growth (Sarmiento and Gruber 2006) is possible to discern between these processes, which both use $NO_3^-$ readily, using separate dark and light bottle incubations; however, such data are collected infrequently. Using data from three ocean basins (the Equatorial Pacific, Southern Ocean and North Atlantic) that represents a gradient of nutrient rich to oligotrophic conditions, we explored whether trends in $^{15}N$-$NO_3^-$ uptake are correlated with autotrophic and/or heterotrophic activity.

In aquatic systems, bulk POC measurements encompass myriad carbon compounds, ranging from phytoplankton biomass, to phytoplanktonic derivatives and exopolymers, and highly processed organic matter that is recalcitrant in nature. This reality of bulk POC analysis complicates our analysis because it becomes difficult to discern concentration-dependent N uptake by either autotrophs or heterotrophs. For example, in SI Figure 5B the positive relationships between POC and N uptake could reflect the coupling of enhanced N uptake and autotrophic biomass production or carbon limitation on heterotrophic N uptake. Because autotrophy and heterotrophy are often highly correlated in aquatic systems, the positive relationship probably reflects both metabolic processes in action. This is illustrated in data (not shown here) from the three ocean provinces used in Figs. 3 and 4, where primary production is moderately correlated with POC ($r = 0.48$, $p < 0.001$), as is heterotrophic production and biomass ($r = 0.65$, $p < 0.001$). Thus, primary and heterotrophic production is highly correlated ($r = 0.57$, $p < 0.001$). This tight coupling of autotrophic and heterotrophic production is not surprising, as the microbial loop has been long identified, but does either process act as an ultimate constraint on $NO_3^-$ uptake and accumulation?

Greater insight into the role of autotrophs and heterotrophs in $NO_3^-$ uptake patterns emerges from our analysis of autotrophic versus heterotrophic uptake across shifts in resource POC:N-$NO_3^-$ ratios. In accordance with the conceptual model (Figure 2.1 1), Figure 2.3 shows strong and nonlinear heterotrophic production at distinct ratios which correspond with critical threshold ratios underlying $NO_3^-$ uptake. Although our understanding of the role of heterotrophs in oceanic $NO_3^-$ uptake has only recently been appreciated (reviewed by Mulholland *et al.* 2008) our analysis suggests that over scales in which $NO_3^-$ uptake data are collected, that heterotrophs likely determine the ultimate accumulation of $NO_3^-$ by responding to discrete shifts in resource composition. Of course resource ratios are linked to autotrophic activity, as phytoplankton are by far the predominant source of organic C (by fixing $CO_2$) in these systems; the reliance of resource ratios on autotrophic production should be explored further in future studies.

Further evidence comes from a variety of studies documenting lower than expected POC:N-$NO_3^-$ ratios relative to the stoichiometric demands of autotrophs. Conceivably, autotrophs can simultaneously drawdown dissolved inorganic carbon and $NO_3^-$ for metabolic purposes. This process could produce an inverse relationship between POC and $NO_3^-$ as phytoplankton concurrently convert $CO_2$ gas into POC and use N-$NO_3^-$ to build cellular machinery. To the best of our knowledge, inverse POC:N-$NO_3^-$ relationships have not been interpreted as imprints of autotrophy, but given the hypothetical possibility, we consider several potential impacts of this mechanism on the relationships observed in Figure 2.3 and Figure 2.4, 2.5. While the Redfield C:N ratio suggests that autotrophs should build biomass at C:N ratios approximately twice the microbial C:N ratio of biomass (~6.125), when maintenance respiratory processes are

accounted for, recent studies suggest autotrophic C:N uptake occurs at ratios up to 18:1 C:N (e.g. Mari *et al.* 2007). Among the few studies (Banse *et al.* 1994, Dauchez *et al.* 1995, Bode *et al.* 2004) that report C:N uptake ratios, the C:N ratios fall strongly within the range of uptake ratios that would be expected for heterotrophs, for reasons outlined above. For example, Dauchez *et al.* (1995) found that C:N uptake ratios along the coastal waters of Nova Scotia were largely well-below Redfield ratio, Also, Bode et al. (2004) found that C:N uptake ratio plummeted with depth to ratios near to 3 in the Rio de Ferrol (Spain), which suggests a role for heterotrophs in $NO_3^-$ uptake when resource ratios come into balance with microbial C:N demand. Furthermore, Banse (1994) documents POC:N-$NO_3^-$ uptake ratios below the expected C:N uptake ratios for phytoplankton, and suggests that low uptake ratios imply a likely role for heterotrophs. Together, these studies support an emerging view that phytoplankton actual "over consume" carbon relative to N needs (Toggweiler 1993) to meet higher C:N stoichiometries characteristic of non-biomass production, such as transparent exopolymers (Toggweiler 1993, Biddanda and benner 1997, Keplay *et al.* 1997). To reconcile high C:N uptake ratios with the Redfield C:N ratio of ~6.6125, these studies have suggested that preferential removal of C relative to N by heterotrophic bacteria effectively lower organic C:N ratios as phytoplankton-derived carbon compounds are degraded. That is, bacteria bring the organic C:N ratio back to Redfield ratio by metabolizing "excess" C at C:N uptake ratios lower than the Redfield ratio of 6.6125. Hence, heterotrophs must exhibit lower C:N uptake ratios to produce global observed Redfield ratios if autotrophs build organic tissues at ratios much higher than Redfield ratio, as the above studies strongly document.

*2.4.3. Controls on heterotrophic N assimilation, nitrification and denitrification*

Figure 2 and SI Figure 5 consist of data from stream-based studies of denitrification and nitrification, and oceanic, coastal margins, estuarine, lacustrine and riverine $^{15}N\text{-}NO_3^-$ uptake measurements to explore C and N controls over denitrification, N assimilation and nitrification. The lack of data on denitrification, heterotrophic N assimilation and nitrification from one type of ecosystem prevented us from assessing these dynamics exclusively in streams or oceans. Stream denitrification rates were assessed using denitrification enzyme activity, acetylene-block technique, open-system $N_2$/Ar methods, and primarily $^{15}N\text{-}NO_3^-$ isotope or enrichment-style nutrient additions using nutrient spiraling methods. Stream nitrification rates were assessed using $^{15}N$ additions to streams using the same techniques as applied for denitrification, or the nitrapyrin inhibition method. Streams varied greatly in local conditions and intensity of land-use; however patterns emerged despite potentially confounding variation. Oceanic, coastal, estuarine, lacustrine and riverine N uptake was measured by quantifying $^{15}N$ uptake to particulate organic matter in the Equatorial Pacific, Southern Ocean, North Atlantic, English Channel, Scheldt Estuary, Rio de Ferrol, and Lake Superior. Our meta-analysis was used, in part, to test predictions that high rates of denitrification and heterotrophic $NO_3^-$ assimilation, and low rates of nitrification, are associated with high DOC and low $NO_3^-$ concentrations. We found partial empirical support for these predictions in data from streams (Figure 2.6) and oceans (Figure 2.6), except that denitrification rate exhibited positive relationships with $NO_3^-$ and DOC, suggesting that both constituents could limit activity. This finding fits with other recent analyses (Arango *et al.* 2008) for a dual role of DOC and $NO_3^-$ in limiting activity.

$^{15}N$ uptake data for well-oxygenated (no denitrification) surface (0-120m) waters from the North Atlantic Bloom Experiment Atlantis II, R/R Kiwi 7 and Equatorial Pacific tt008 cruises made no empirical separation between autotrophic and heterotrophic $NO_3^-$ assimilation. Separating the data into euphotic and non-euphotic zone values left data too scant to explore patterns since most studies focus on euphotic surface waters. However, with the caveat of not being sure whether $^{15}N$-$NO_3$ uptake rates directly reveal heterotrophic bacterial N assimilation, patterns in marine N cycling probably reflect close coupling of organismal uptake and regeneration which is ultimately mediated by heterotrophic microbes recycling bioavailable N forms via remineralization.

*2.4.4. System-specific analysis of $NO_3^-$ accumulation*

While the global DOC-$NO_3^-$ relationships show remarkable coherence, we acknowledge that the unexplained variation in global DOC-$NO_3^-$ concentrations remains substantial. Thus, while we believe the development of a predictive model of nitrate accumulation across multiple systems to be well beyond the scope of this particular manuscript, we inspected multiple system-specific scenarios to explore the potential for even simple regression-based models to be used at scales most relevant to management concerns. In Figure 2.7 and Table 2.5, we provide six site-specific examples for DOC-$NO_3^-$ patterns that are directly comparable to the six global-scale panels of Figure 1 in the main text. At this regional scale, DOC concentration explains substantially much more variation in $NO_3^-$ concentrations in every environment, ranging from soils to the sea. Absent other available approaches, such relationships may have utility as a predictive

framework, especially for identifying the conditions under which $NO_3^-$ accumulation is most likely.

However, despite this consistency of DOC—$NO_3^-$ relationships across systems, where possible, we do not advocate for a simple stoichiometric approach at the expense of other known controls. Rather, we stress that better incorporation of stoichiometric principles into frameworks that already have well-developed approaches for addressing kinetic and thermodynamic controls is likely the most desirable path forward. For example, we expect that adding a stoichiometric perspective to a range of widely-used mass-balance models (Caraco and Cole 1999, Seitzinger *et al.* 2008, Alexander *et al.* 2007) would significantly improve their predictive capacity.

As emphasized previously, understanding the mechanistic underpinnings of shifts in stoichiometric breakpoints may be the largest challenge for predicting when $NO_3^-$ will rise to detrimental concentrations. Better resolution on this front will require careful consideration of system-specific differences in bacterial stoichiometric plasticity and BGE. The flexibility in both of the bacterial properties presents challenges, likely requiring a combination of both *in situ* surveys and manipulative experiments to provide better resolution. Certainly global inverse DOC—$NO_3^-$ patterns reflect the simultaneous influence of denitrification, nitrification and heterotrophic N assimilation on the fate of $NO_3^-$, yet site to site variation in the organic C:$NO_3^-$ breakpoint, below which $NO_3^-$ accumulates, likely reflects the combined influence of BGE and microbial stoichiometric plasticity. Once these properties are known for a given system or region, more explicit parameterization of stoichiometric controls would be possible within model frameworks, and DOC—$NO_3^-$ trends could then potentially be used to quantify the relative roles of

denitrification, nitrification, and heterotrophic N assimilation in causing sharp changes in $NO_3$ concentrations.

## CHAPTER 3: HIGH RAINFALL DRIVES MAXIMUM $CO_2$ EXCHANGE AND STORAGE IN LOWLAND TROPICAL FORESTS

### 3.1 Abstract

A common paradigm in terrestrial – climate coupling holds that plant net primary productivity (NPP) and decomposition decline as rainfall exceeds about 2 m/yr. With the help of meta-analysis, we demonstrate opposite trends for lowland tropical forest NPP, litter decomposition and biomass above this climate threshold. Unlike cooler montane systems, high temperature combines with rainfall to accelerate nutrient turnover that fuels maximum $CO_2$ exchange and storage in wet lowland regions. Empirical models derived from our database show high pantropical NPP and biomass values of $14.4 \pm 4.4$ Pg C $y^{-1}$ and $342.6 \pm 140.5$ Pg C, respectively. At a regional scale, high precipitation, carbon allocation to wood growth and relatively low tree mortality make Southeast Asian forests notable carbon hotspots. Finally, we estimate recent deforestation losses of 1.1 Pg C $y^{1}$, with potentially escalating losses as deforestation intensifies in wet, carbon-rich lowland forests.

### 3.2 Introduction

Tropical forests play a critical role in Earth's C cycle and climate system (Field *et al.* 1998), and recent estimates (Pan *et al.* 2011) suggest that primary and re-growing tropical forests now provide the largest terrestrial sink for anthropogenic $CO_2$. In large part, this reflects high rates of NPP and substantial C stocks in forest biomass (Malhi *et al.* 2004, 2006; Lewis *et al.* 2009). The ability of tropical forests to sequester atmospheric $CO_2$ strongly depends on how climate (Brando *et al.* 2008, Malhi *et al.* 2009) and other factors (Quesada *et al.* 2009, Cleveland *et al.* 2011, Korner 2009) regulate the tropical carbon (C) cycle. As such, human-driven changes to key environmental controls can

cause globally significant changes in atmospheric $CO_2$ levels (Sitch *et al.* 2008, Phillips *et al.* 2009, Lewis *et al*. 2011). Recent observations of drought – driven forest mortality (Phillips *et al.* 2009, 2011) have focused research efforts on the interactions between seasonal water stress (Brando *et al.* 2008, Lola da Costa *et al.* 2010), fire (DeFries *et al.* 2008, Aragao and Shimabukuro 2010), rainforest retreat (Malhi *et al.* 2008) and regional C balance (Phillips *et al.* 2009, Lewis *et al.* 2011). Here we describe how long term mean levels of rainfall configure patterns of rainforest $CO_2$ exchange and storage, a lesser-known but potentially critical link between the climate system and the tropical carbon cycle.

Net primary productivity (NPP) is the fixation of $CO_2$ as biomass and is the first step of carbon sequestration within an ecosystem. It's commonly thought that NPP and decomposition in terrestrial ecosystems increase with mean annual precipitation (MAP) up to roughly 2 m per year, after which both decline sharply (Schuur 2003). This conclusion is based largely on detailed mechanistic studies along a rainfall gradient in Hawaii (Schuur and Matson 2001, Schuur *et al.* 2001, Holtgrieve *et al.* 2006), followed by a global synthesis of aboveground NPP (ANPP) data (Schuur 2003). The notion that high rainfall will reduce $CO_2$ exchange in tropical regions has influenced recent climate-carbon model assessments (del Grosso et al. 2008, Randerson *et al.* 2009). However, the initial empirical studies that informed this conclusion are biased by cooler montane systems in high rainfall regions (Clark *et al.* 2001), while data from lowland forests – which account for roughly 95% of tropical land area – are virtually absent. This discrepancy does not reflect a deliberate bias in past studies, but rather a historical legacy

of research in montane and relatively dry lowland systems, coupled with a general absence of available data from wet lowland forests until very recently.

Here, we assembled a database of tropical forest aboveground net primary production (ANPP), leaf litter decomposition, and aboveground biomass (AGB) to revisit of the relationship between rainfall and $CO_2$ exchange and storage. The past decade has seen enormous investment in tropical research, notably in the funding and coordination of plot – based research networks, including the LBA-ECO (http://www.lbaeco.org), RAINFOR (http://www.geog.leeds.ac.uk/projects/rainfor), AfriTRON (http://www.geog.leeds.ac.uk/projects/afritron), and Smithsonian's CTFS (http://www.ctfs.si.edu/group/Carbon). We combined these network data with local studies to assemble a database comprised of 944 sites from 42 tropical countries (Figure 3.1), which includes 785 lowland sites and 159 montane sites. Delineation between lowland and montane classifications was categorically determined using a mean annual temperature (MAT) cut-off of 18 $^{o}$C (Holdridge 1947), except when site – specific information defined otherwise.

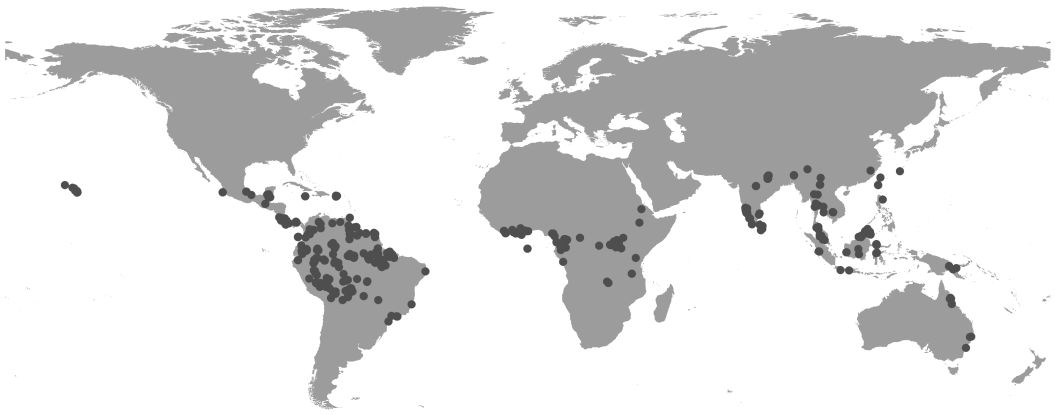

Figure 3.1 | Locations of fields sites in the TROPICS database.

ANPP was calculated as the sum of fine litterfall (i.e. leaf growth) and stem growth, which are the dominant components of ANPP in tropical ecosystems (Aragao et al. 2009). We made no corrections for frequently unmeasured above or belowground components, unless stated. For sites where only one component of ANPP was available, or only biomass values were available, allometric relationships were used to estimate ANPP akin to previous studies (Clark *et al.* 2001, Malhi *et al.* 2004). Data on AGB stocks, leaf litter decomposition rates, soil type, and forest demographics were collected to examine the climate sensitivity of plant – soil feedbacks and scaling between productivity and C storage. The database and metadata are available at www.carbonbalance.org/TROPICS.

**3.3 Results and Discussion**

Our analysis shows clear differences in the effects of increasing rainfall on ANPP and decomposition between lowland and montane (Fig. 3.2A,B). In both systems, ANPP and decomposition increase up to an MAP of 2 m $y^{-1}$, which reflects the dependency of plants on water for growth. Yet, where montane forests show a decline in productivity and decomposition with increasing rainfall, both metrics continue to increase in lowland forests. However, the ultimate mechanism behind the rainfall-C relationships may be similar in both forest systems, and consistent with those first proposed by Schuur and others (Schuur *et al.* 2001, Schuur 2003).

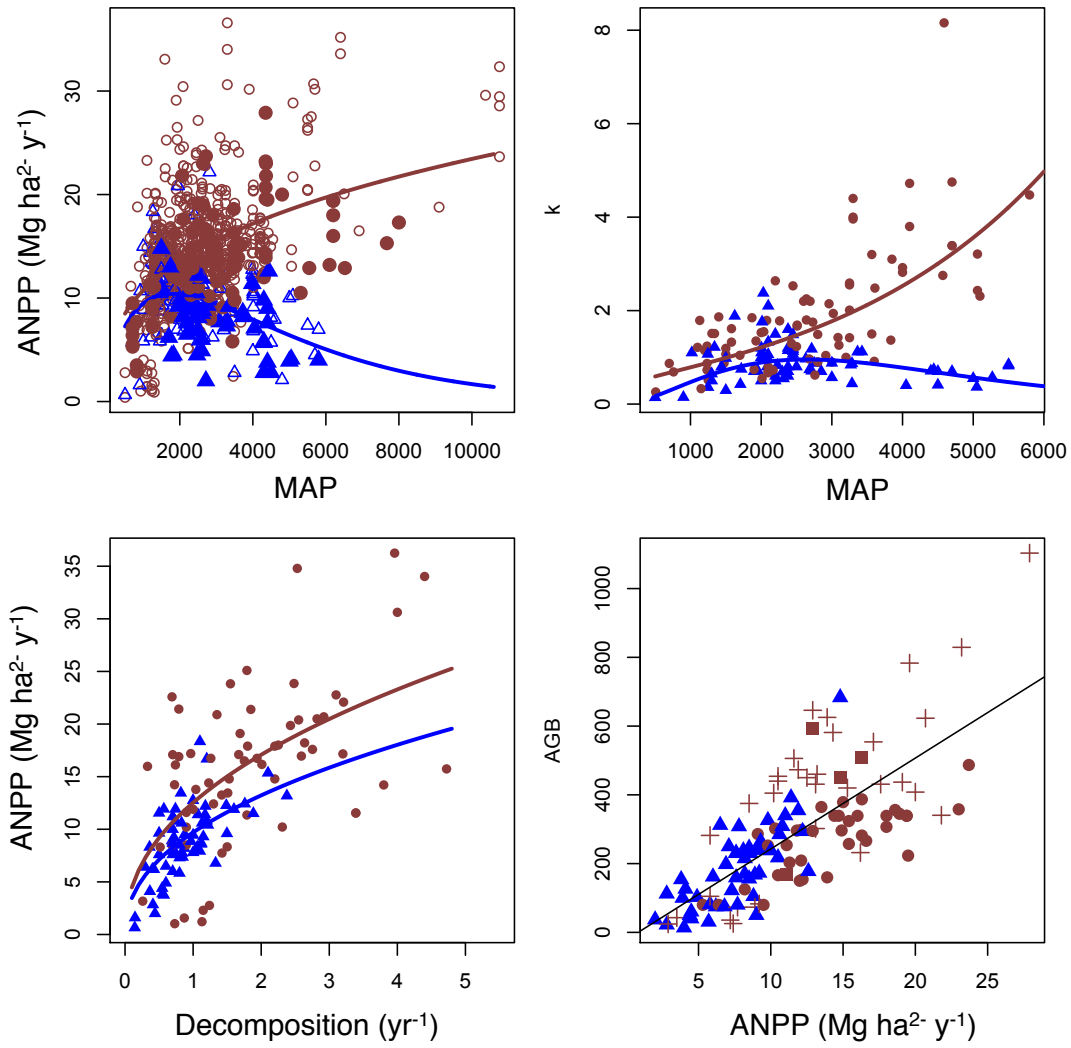


Figure 3.2 | Climate control of tropical ANPP, decomposition, plant – soil feedbacks and scaling between ANPP and AGB. Intact lowland (circles) and montane (triangles) tropical forest (A) ANPP and (B) decomposition ($k$ – decay constant) as a function of annual rainfall. (C) ANPP versus $k$ for lowland and montane forests. (D) Aboveground biomass as a function of ANPP in montane (traingles), American (circles), African (squares) and SE Asian (crosses) rainforests. Closed symbols represent sites where ANPP was measured as the sum of total litterfall and biomass increment, whereas open symbols represent sites where ANPP was estimated based on a predictive relationship between litterfall, biomass increment or biomass (Full details in SOM). Non-linear curve-fitting techniques were used to generate best-fit empirical equations, which were compared using Akaike's Information criterion.

In both montane and lowland forests, ANPP is strongly related to rates of leaf litter decomposition (Fig. 3.2C), suggesting a tight coupling between rates of nutrient mineralization from organic matter decomposition and realized forest productivity. The decline in both ANPP and decomposition in the cooler montane forests is consistent with past work (Schuur *et al.* 2001). The hypothesized mechanism behind the decline in $CO_2$ exchange is associated with declining soil $O_2$ levels reducing root and microbial metabolism under increasingly wet conditions. When high rainfall causes lower soil redox conditions, decomposition is inhibited, thereby reducing the delivery of nutrients that are essential for plant growth (Schuur and Matson date). Over time the formation of water – absorbing organic soil horizons, which are a common feature of cooler rainforests (Proctor *et al.* 1988, Salinas *et al.* 2010, Wolf *et al.* 2011), further slows nutrient turnover (Schimel *et al.* 1995, Salinas *et al.* 2010, Wolf *et al.* 2011). Lower nutrient flow throughout the ecosystem, in turn, can drive the evolutionary development of growth forms that maximize nutrient use efficiency (Vitousek *et al.* 1982). Those traits come with a trade-off against growth (Reich *et al.* 1999, Wright *et al.* 2004); for example, sclerophyllous leaves are long-lived and serve well for nutrient retention (Vitousek 1982, Reich *et al.* 1997), but their smaller size and thickness reduces photosynthetic potential (Reich *et al.* 1999. Wright *et al.* 2004).

The trajectory of lowland forest ANPP diverges from montane systems at high rainfall. Temperature is the prime difference as lowland and montane forests are defined, and its affect on plant – microbial function underlies the simultaneous and positive response of ANPP and *k* to high rainfall. Ample radiant energy promotes high evapotranspiration in lowland forests (Fisher *et al.* 2009), and water rarely accumulates in

soil to levels to restrict oxygen diffusion to roots and microbes (Silver *et al*. 1999, Schuur and Matson 2001, Wieder *et al.* 2011). Macropore flow via soil piping is common in lowland ecosystems and also improves water drainage (Chappell 2011), potentially enhancing aeration of the soil atmosphere. When warm temperatures that favor high heterotrophic decomposition (Davidson and Janssens 2006, Salinas *et al.* 2010) combine with high rainfall (Powers *et al.* 2009, Wieder *et al.* 2010), rapid soil organic matter turnover accelerates nutrient recycling (Fig. 2B). Higher recirculation of nutrients throughout the ecosystem leads to foliage with greater nutrient contents and lower recalcitrant structural tissue (Aerts and Chapin 2000). In combination with lower nutrient resorption (Vitousek *et al.* 1982, Kobe *et al.* 2005, Yuan and Chen 2009), senescent foliage creates nutrient – rich litterfall that facilitates high rates of decomposition (Schuur *et al.* 2001, Aerts and Chapin 2000) reinforcing the plant – soil feedback.

Climate (and its connected mechanisms) is only one of many factors that regulate tropical $CO_2$ exchange, as evident by the scatter in Fig. 2. Variation in cloud cover and radiation, as well as local and regional differences in evolutionary history and species composition (Baker et al. 2004, Quesada *et al.* 2009) also combines to regulate ANPP in tropical forests. Indeed, such forests display substantial biogeochemical heterogeneity at all scales, challenging generalizations about controlling mechanisms for any major ecosystem process (Porder et al. 2005, Townsend 2008). However, using site – specific information, we find further evidence for the importance of interactions between climate and nutrient availability. An analysis of residuals in Fig. 2A shows that rainforest ANPP is higher on more fertile soil orders (i.e. Alfisols, Inceptisols, Ultisols) than generally less fertility soils (i.e. Spodosols, Entisols, Oxisols; Fig. 3), which has been shown on local

(Paoli *et al.* 2007) to basin-wide scales (Mercado *et al.* 2011, Malhi *et al.* 2004, Chave *et al.* 2009). This aligns with global evidence that plant traits that favor growth over nutrient conservation strategies are associated with higher soil fertility (Ordonez *et al.* 2009). Such soil orders also vary in texture and mineralogy, and the community composition with associated physiological characteristics (i.e. wood density) of tropical forests often changes markedly with soil type (Baker *et al.* 2003, 2009). Thus, much of the variability seen in Fig. 3.2A may result from climate-nutrient interactions that play out differently across major soil orders, and are a product not only of the local soil conditions, but of the differences in species assembly such soil conditions can drive.

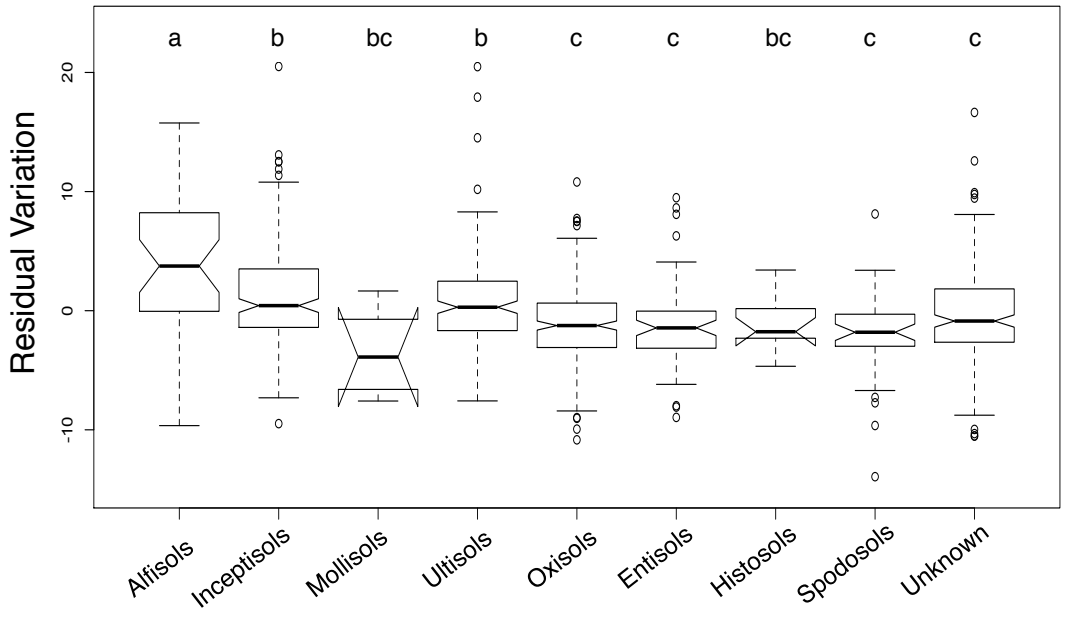


Figure 3.3 | ANPP residual variation from Fig. 3.2A categorized by soil taxonomy.

Beyond these climate-C relationships, we also find a positive, linear relationship between ANPP and AGB, indicating that places of high productivity have higher

aboveground C storage (Fig. 3.2D). While this relationship may seem intuitive, disturbance regime and stand demographics can cause differential scaling between growth and biomass among Earth's forests (Keeling and Phillips 2007). For example, redwood trees in Northern California reach tremendous stature not by growing fast, but by living for a very long time (Busing and Fujimori, 2005). For tropical systems previous work shows that Amazonia AGB saturates with respect to ANPP (Keeling and Phillips 2007), yet we find no such plateau for SE Asian forests (Fig. 3.2D).

The most C-rich tropical forests are found in SE Asia (Fig. 3.2D), a regional distinction that reflects a synergy of at least two broad life history trends. First, SE Asian lowland forests allocate more C to wood over leaf growth (Fig. 3.4). This biogeographic pattern likely reflects phylogenetic make up of the Old World tropics, which include the prevalent Dipterocarp forests (van Welzen and Slik 2009) renowned for their stature (Slik *et al.* 2011, Paoli *et al.* 2007). Second, forests in SE Asia tend to have lower mortality rates than Mesoamerican forests (Fig. 3.5), allowing more time for biomass accrual. These regional differences in forest turnover and allocation suggest that intact forests in SE Asia may have greater potential as a long term C sink than forests in the New World.

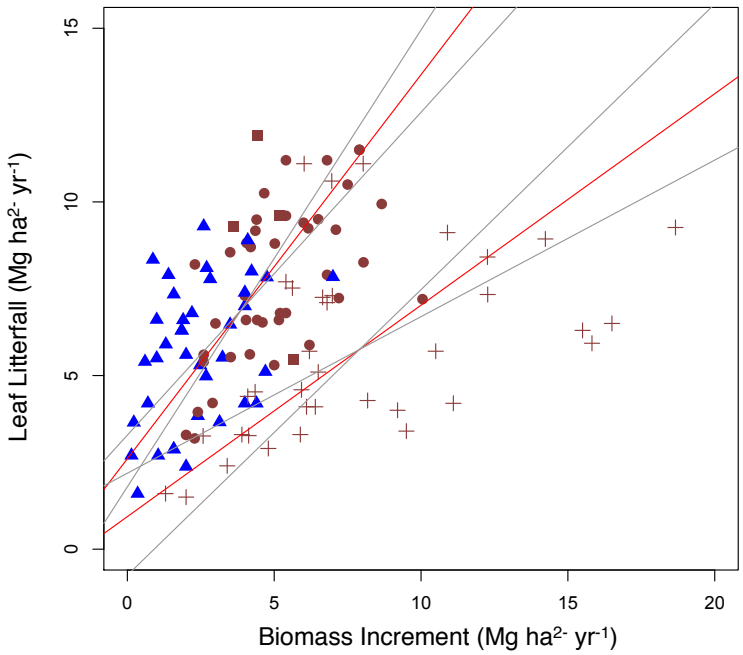


Figure 3.4 | Observed litterfall versus biomass increment growth for tropical rainforests. SE Asian lowland rainforest (crosses) carbon allocation segregates from all montane (triangles), Mesoamerican (circles) and African (squares) lowland rainforests. Monodominant rainforests, comprised mainly of Hawaiian sites, were excluded from this analysis, and are not shown. See Table 1 for statistical analysis and empirical equations.

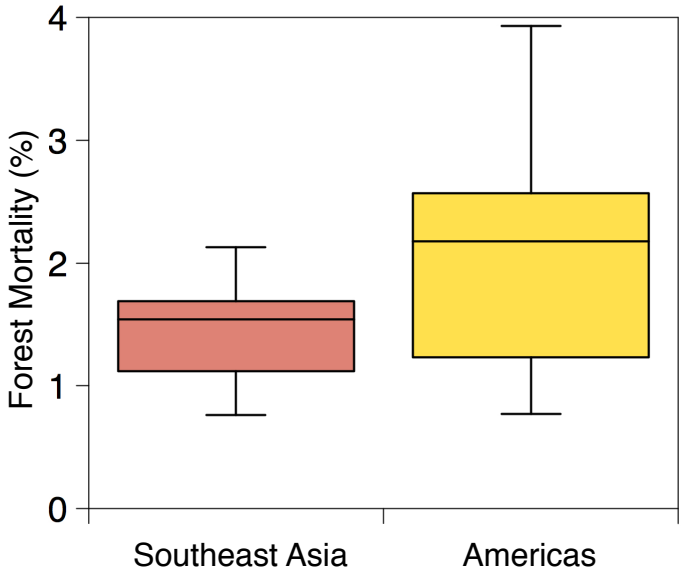


Figure 3.5 | Comparison of forest mortality rates between SE Asian and Mesoamerican rainforests. One-way ANOVA, $p = 0.034$

Table 3.1 | Empirical equations for estimation of ANPP and ANPP components based on litterfall, biomass increment and AGB.

| Predictor Variable | Estimated Variable | Region* | Estimation Parameters ‡ | |
|---|---|---|---|---|
| | | | a | b |
| Litterfall | Biomass Increment | NWL, MONT, AFR | 0.904 | -2.354 |
| Litterfall | Biomass Increment | SEA | 1.642 | -1.540 |
| Biomass Increment | Litterfall | NWL, MONT, AFR | 1.106 | 2.604 |
| Biomass Increment | Litterfall | SEA | 0.609 | 0.938 |
| Aboveground Biomass | ANPP | Lowland | 1.480 | 0.386 |
| Aboveground Biomass | ANPP | Montane | 1.087 | 0.386 |

*Regional abbreviations: NWL, new world lowland forests; MONT, all montane forests; AFR, African forests; SEA, Southeast Asia forests.
‡ Reduced Major Axis regression was used to find best-fit linear models for litterfall by biomass increment and vice versa: (y = a*[Predictor Variable] + b). A power function was used from AGB by ANPP: (y = a*[Predictor Variable] ^ b). When litterfall was used to predict biomass increment, y-intercept values were negative at low litterfall values, yielding negative biomass increment. Given this impossibility, we assumed that biomass increment was functionally zero for several sites.
¶ All models significant at $p < 0.001$.

Next, we used the climate – ANPP equations shown in Fig. 3.2A to map the potential distribution and magnitude of ANPP throughout the tropical forest biome. This empirical approach reproduced observational values with 23% relative error, at a 95% confidence interval (Fig. 3.6, 3.7; Table 2). Taking into account the additional errors associated with each step in up-scaling (Table 2), tropical ANPP averages 9.2 ± 2.9 Pg C/yr (Table 3.1). Total NPP rises to ~ 14.0 Pg C/yr when correction factors were applied to include unmeasured components (Table 3.1). Regional hotspots of C uptake are those that have high rainfall, such as northwest Amazonia, southern Central America and most of Oceania (Fig. 3.8). These regions also exhibit high carbon density because of the strong relationship between AGB and ANPP (Fig. 3.2D), and the regional differences

discussed above cause the wettest of SE Asian forests to display the highest values of ANPP and C storage.

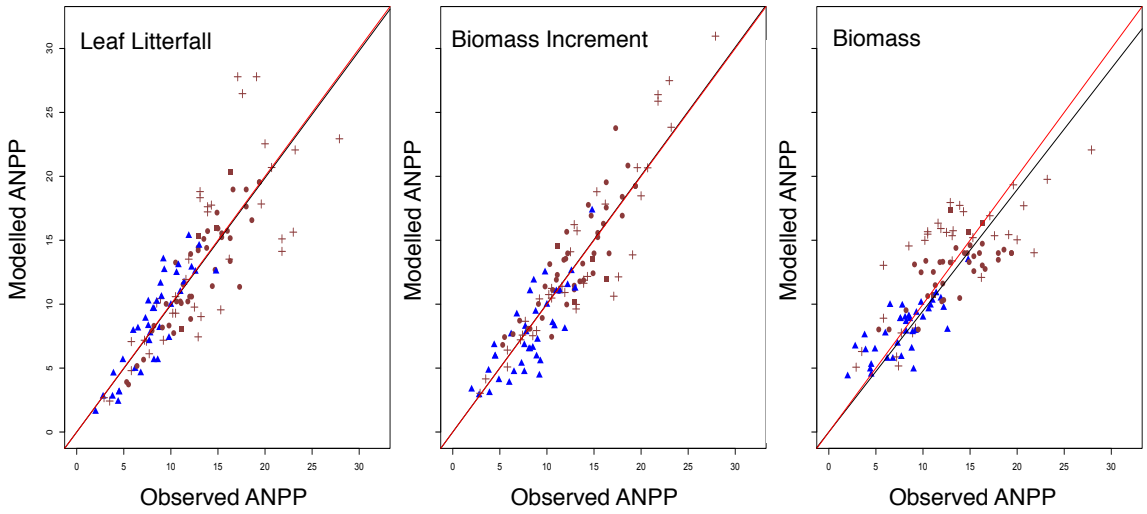


Figure 3.6 | Predicted versus observed ANPP based on the estimation of ANPP components. (A) ANPP with biomass increment estimated, (B) ANPP with litterfall estimated, and (C) ANPP estimated from forest AGB using the equation in Figure 1D. Statistical results shown in Table 3.2.

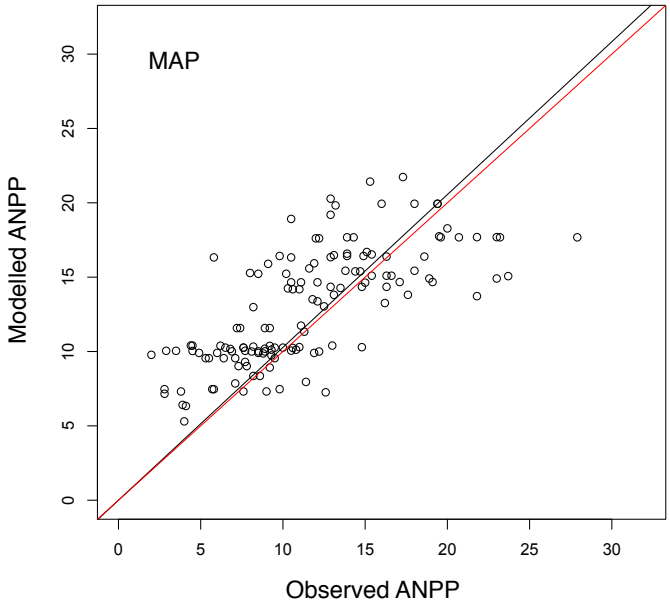


Figure 3.7 | Predicted versus observed ANPP based on the empirical modeling of ANPP using mean annual rainfall. Statistical results shown in Table 3.2.

Table 3.2 | Uncertainty estimation for up scaling ANPP and AGB at the global scale.

| Source | Reference | Estimation Error | | |
|---|---|---|---|---|
| **Measurement Precision*** | | **RMSE** | *r* | **Relative Error (%)** |
| Allometry for Aboveground Biomass | Chave et al. 2005 | | | 6.8 |
| Litterfall | Malhi et al. *In press* | | | 5.9 |
| Biomass Increment | Malhi et al. *In press* | | | 10.9 |
| **Estimation of ANPP ‡** | | | | |
| Aboveground Biomass | This study (Fig. S5A) | 2.32 | | 6.73 |
| Litterfall | This study (Fig. S5B) | 2.87 | | 9.45 |
| Biomass Increment | This study (Fig. S5C) | 2.29 | | 2.65 |
| **Empirical Prediction¶** | | | | |
| ANPP | This study (Fig. S6) | 2.69 | | 23.39 |
| AGB | This study (Fig. S7) | | | 20.57 |
| **Upscaling (plot to 1 km pixel)** | | | | |
| ANPP | Clark et al. 2000, Chave et al. 2005, Mascaro et al. 2011 | | | 10 |
| AGB | | | | 10 |
| **Mapping Tropical Carbon** | | **Combined Error (%) §** | | |
| ANPP | | 31.45 | | |
| AGB | | 37.58 | | |

* This reflects measurement precision, not methodological bias.
‡ Uncertainty was assessed using best-fit equations between observed vs. modeled ANPP when using AGB, litterfall and biomass increment as predictor variables in Reduced Major Axis regression. Regression results shown in Table S1 and Figure S5.
¶ Tests predictive power of the empirical equations in Fig. 1A (ANPP) and Fig. 1D AGB).
§ Error propogated as $\varepsilon_{\text{productivity, biomass}} = (\varepsilon^2_{\text{measuremnt}} + \varepsilon^2_{\text{ANPP estimation}} + \varepsilon^2_{\text{prediction}} + \varepsilon^2_{\text{upscaling}})^{1/2}$


Figure 3.8 | Pantropical ANPP. Field measurements were up scaled using the empirical climate – ANPP relationships in Fig. 2A applied to montane and lowland forests separately. The mean annual precipitation predictor was obtained from the Worldclim long-term (year 1950 – 1990) dataset at 10 – minute resolution.

We compared our field-based, empirical extrapolation against values obtained using a number of other methods used to estimate the tropical forest C budget. First, we compared our estimates to a similar empirical scaling approach that employs the single 'hump-shaped' equation, as was done in prior global modeling exercises (Schuur 2003, Zaks *et al.* 2007, del Grosso 2008). Using the relationships in Fig 3.2A yields a 30% increase in ANPP over estimates based on the single equation (Table 3.3), underscoring the importance of the wet lowlands in driving pan-tropical NPP. Second, biome-wide ANPP derived from the NCAR CLM CN 4.0 model (Oleson *et al.* 2010) is 25% higher than our estimate, which probably reflects model error and uncertainties associated with carbon uptake, especially in the tropics (Beer *et al.* 2010, Bonan *et al.* 2010). Third, the MOD17 algorithm used to derive MODIS-based estimates of ANPP apply ecophysiological principles of tree growth with measures of incoming radiation, water stress, and temperature (Zhao *et al.* 2010). Our pan-tropical ANPP estimate based on extrapolation of site-level data is remarkably similar to the MODIS decadal (2000 – 2010) average. However, this correspondence should be viewed with caution, as substantial spatial discrepancies exist between the patterns shown in Fig. 3.2 and those in recent MODIS estimates (Zhao *et al.* 2010). The database we report here provides a new resource for more thorough evaluations of tropical NPP estimates from processed based models and satellite derived products.

Table 3.3 | Estimates and comparison of pantropical productivity and biomass (circa 2000).

| Study | Region | Productivity (Pg C $yr^{-1}$) | | Biomass (Pg C) | |
|---|---|---|---|---|---|
| | | ANPP | NPP* | AGB‡ | TB¶ |
| This study | Tropics | 9.20 ± 2.89 | 13.98 ± 4.40 | 274.09 ± 102.78 | 342.61 ± 140.47 |
| | Americas | 5.03 ± 1.58 | 7.65 ± 2.40 | 149.97 ± 56.24 | 187.46 ± 76.86 |
| | Amazon | 4.12 ± 1.33 | 6.40 ± 2.01 | 125.41 ± 47.03 | 156.75 ± 64.27 |
| | Africa | 1.44 ± 0.45 | 2.20 ± 0.69 | 42.91 ± 16.09 | 53.64 ± 21.99 |
| | SE Asia | 2.73 ± 0.86 | 4.15 ± 1.30 | 81.28 ± 30.48 | 101.60 ± 41.66 |
| Schuur et al. 2003 | Tropics | 6.8 | | | |
| Zhao et al. 2010 § | Tropics | 9.24 | 12.84 | | |
| Bonan et al. 2010 § | Tropics | 12.32 | | | |
| Saatchi et al. 2011 § | Tropics | | | 179.36 | 224.20 |
| Reusch and Gibbs 2008 § | Tropics | | | 70.94 | 97.19 |
| Pan et al. 2011 ∞ | Tropics | | | 177.16 | 256.76 |
| Malhi et al. 2006 ∞ | Amazon | | | 95 | 129 |
| Lewis et al. 2009 ∞ | Africa | | | 52.9 | 65.8 |

Mean productivity and biomass estimates and 95% confidence intervals. ANPP extrapolation derived using the empirical equations (Fig. 1A, SOM) using rainfall at ~1-km spatial resolution (Worldclim.org) with lowland and montane forests climate responses modeled separately. AGB was predicted from modeled ANPP (Fig. 1D). Dry weight was converted to carbon units using a factor of 0.5. Uncertainties associated with each step of the estimation were propagated as: $\varepsilon_{\text{productivity, biomass}} = (\varepsilon^2_{\text{measuremnt}} + \varepsilon^2_{\text{ANPP estimation}} + \varepsilon^2_{\text{prediction}} + \varepsilon^2_{\text{upscaling}})^{1/2}$. Full details on uncertainty analysis and NPP/TB estimation in SOM.

*Includes a correction factor of 1.52 to ANPP to account for herbivory, volatile organic compounds emissions, branch fall and root production.

‡ Includes a correction factors for unmeasured components dead wood (10%) and small trees and lianas (9.9%).

¶ Includes a correction factor for root biomass (21%).

§ For comparison, spatial data were trimmed to the World Wildlife Fund's humid tropical forest extent for areas with ≥ 25% canopy cover derived from Moderate-resolution Imaging Spectroradiometer (MODIS) Vegetation Continuous Fields 250 metre pixels aggregated to in 1-km spatial resolution for year 2000, yielding an area of ~ 1,342 Mha similar to the extent considered in the FRA 2010.

∞ For comparison, biomass values were fractionally adjusted to account for differences in land area used in each study: Malhi *et al.* 2006 (+2.9%), Lewis *et al.* 2009 (-5.4%), Pan *et al.* 2011 (-3.5%).

We also mapped AGB as a function of ANPP to create a provisional estimate of intact rainforest C stocks in tree biomass. After applying a correction factor to include roots (Table 3.3), we estimate a biome-wide value of 343 ± 140 Pg C. This estimate (and its uncertainty) is higher than some recent estimates (Pan *et al.* 2011, Baccini *et al.* 2012, Quere *et al.* 2009), yet not unrealistic as our basin wide estimates are ~18% above and below recent values derived from long-term monitoring plot networks in Amazonia (Mahli *et al.* 2006) and Africa (Lewis *et al.* 2009), respectively. Recent advances in satellite-derived measures have made important advances in our ability to estimate biomass C storage (Saatchi *et al.* 2011), but yield consistently lower intact rainforest C stocks compared to the values we report here. More worrisome is the substantial discrepancy between all of these approaches and those based on the IPCC Tier-1 GPG for reporting national greenhouse gas inventories (Reusch and Gibbs 2008). Major new economic incentive structures aimed at curbing $CO_2$ emissions, such as Reduced Emissions from Deforestation and Degradation (REDD+), rely on accurate quantification of forest C stocks (Asner et al. 2010, Saatchi et al. 2011, Baccini et al. 2012). If our provisional estimates are accurate, the adoption of current IPCC Tier 1 methods for international policy mechanisms would severely undervalue C storage in tropical forests, especially in the wet, C-rich lowlands.

Finally, we used the new database and its derived empirical relationships to analyze the C consequences of tropical land use change in a new way. We multiplied estimates of forest loss from 2000 to 2005 by our provisional map of AGB to assess patterns in forest C lost to deforestation and forest degradation. Using this approach we estimate reductions in above ground C stocks in the Americas, SE Asia and Africa of

3.36 (± 1.35), 1.71 (± 0.70) and 0.28 (± 0.11) Pg C, respectively (Fig. 3.9); for a combined rate of 1.08 Pg C $y^{-1}$. This rate equates to 15% of $CO_2$ emissions from fossil fuel and cement production over that time period (Le Quere *et al.* 2009). This estimate is on the low end of prior assessments (van der Werf *et al.* 2009, Pan *et al.* 2010, Baccini et al. 2012), which partly reflects the exclusion of woodlands and savannas as our database was focused on rainforests alone.


Figure 3.9 | Cumulative aboveground biomass loss from year 2000 – 2005. The map is the product of AGB, estimated from ANPP (Fig. 3.2), and fractional forest cover loss at 18.5 km grid cells determined by Hansen *et al.* 2008. The same boundary constraints apply as in Fig. 3.8.

Our analysis suggests an opportunity for combined strategies that promote biodiversity conservation and the protection of high value C reserves: the wet lowlands that show the highest rates of CO2 exchange and biomass C storage are also among the most species rich forests of the tropics (Gentry 1988, Clinebell 1995, Myers *et al*. 2000). To date, these regions have generally been subjected to lower rates of deforestation than drier portions of the biome (Hansen *et al.* 2008). However, this trend may not last. For example, our analysis suggests that the recent surge in oil palm agroforestry is likely to drive notably high per hectare rates of forest C loss and reduced C storage potential in SE Asia, concurrent with documented biodiversity consequences (Sodhi *et al.* 2004, 2010;

Gibson *et al.* 2011). In general, our analyses imply that emerging pressures on wet, C- and species-rich lowland tropical forests such as SE Asia, the western Amazon, and portions of Africa and Central America (Hansen *et al.* 2010) would be particularly damaging to both C sequestration and conservation goals.

# CHAPTER 4: ORGANIC FORMS DOMINATE HYDROLOGIC NITROGEN LOSS FROM A LOWLAND TROPICAL WATERSHED

## 4.1 Abstract

Observations of plant – available nitrogen (N) loss in stream water have reinforced the notion that lowland, primary tropical rainforests cycle N in relative excess of plant and soil uptake. Here we challenge this generalization by showing ultra-low bioavailable N loss from a lowland rainforest on the Osa Peninsula, Costa Rica. For 48 of 52 consecutive weeks, dissolved organic nitrogen (DON) comprised on average 85% of dissolved N loss, except for a one month period in the dry season when low flows and upslope nitrification concentrated nitrate ($NO_3^-$) in stream water. Altogether, dissolved N export accounted for ~ 13% of the combined inputs from free – living N fixation and atmospheric N deposition. Notably, the largest form of N export was as particulate organic nitrogen (PON): we estimated losses of 14.6 kg N $ha^{-2}$ $yr^{-1}$, driven by episodes of high flow that appear to trigger riparian slope failure in the late wet season. Relative to N inputs, PON loss during landscape erosion may be large enough to constrain ecosystem level N stocks over longer timescales. Here we amend the DON leak hypothesis to include PON loss that also occurs independent of biotic demand, albeit by different mechanisms. High PON losses may be most common in very wet regions with complex terrain – such as my study site – but many tropical regions have similar state factor combinations to those found in the Osa region. Thus, PON loss may play an important role in shaping the tropical N cycle across a significant fraction of the biome.

## 4.2 Introduction

A widely held model in ecosystem ecology holds that tropical forests growing on highly weathered soils exhibit conservative P cycling and cycle N in excess of biological demand (*e.g.* Vitousek and Sanford 1986, Hedin *et al.* 2009). Multiple forms of evidence from plants, soils and streams have been used to support this paradigm. These include: high rates of net nitrogen processing (*e.g.* Vitousek and Matson 1988, Davidson *et al.* 2003) that elevate soil $NO_3^-$ pools (*e.g.* Davidson *et al.* 2007, Sotta *et al*. 2008), high foliar N:P ratios (McGroddy *et al.* 2004, Townsend *et al.* 2007, Fyllas *et al.* 2011) and lower foliar N resorption (Vitousek 1982). Furthermore, comparatively high $^{15}N$ values in foliage and soil of lowland imply high rates of nitrogen loss via fractionating pathways ( Martinelli *et al.* 1999; Amundson *et al.* 2003, Bai and Houlton 2009), a pattern that fits with reports of high levels of bioavailable N in streams (Bruijzneel *et al.* 1991, McDowell and Asbury 1994, Newbold *et al.* 1995, Schrumpf *et al.* 2004, Deschert *et al.* 2005, Brookshire *et al.* 2012).

These observations have shaped general paradigms of tropical forest organization and function (Davidson *et al.* 2003, Menge *et al.* 2009, Quesada *et al*. 2009, Hedin *et al.* 2009, Cleveland *et al.* 2011, Brooskhire *et al.* 2012). However, the majority of past studies have been focused in cooler montane systems (*e.g.* Bruijzneel *et al.* 1991, Marrs *et al.* 1998, Tanner *et al.* 1998) that are not likely to represent the lowlands, or lowland forests that, in general, represent drier portions of the tropical forest biome that also feature the most highly weathered soil types (*e.g.* Neill *et al.* 2001, Anaya *et al.* 2007). Yet, tropical landscapes have a myriad of state factor (climate, organisms, topography, parent material and time; Jenny 1941) combinations not fully captured in past studies (Townsend *et al.* 2008). One such understudied space in the state factor spectrum are

lowland regions with high rainfall and comparatively more fertile soils, such as the Andean arc of the Amazon, much of Southeast Asia and localities throughout Central America and the Antilles. This legacy has motivated research in a primary rainforest on the Osa Peninsula, Costa Rica, where a different picture of tropical N cycling has been emerging over the past decade.

Despite high inputs of N from deposition and biological fixation (Reed *et al.* 2007), bioavailable N rarely accumulates and is often at detection limits (Wieder et al. *In prep*). The soil N cycle is a classic example of a small pool – fast turnover system (Davdison *et al.* 1991, Stark *et al.* 1997, Perakis *et al.* 2005); i.e. net mineralization is 3 orders of magnitude lower than the gross N flux, and the entire surface soil nitrate pool turns over in a mere 2.4 hours (Wieder *et al. In prep*). Signals of "conservative" N cycling are seen throughout the ecosystem. Foliar N:P ratios vary substantially across species, but bracket the Redfield ratio of 16 (Townsend *et al.* 2007), a value that is lower than many lowland forests in drier regions (Townsend *et al.* 2007), and one that suggests the potential for N constraints to productivity (Reich and Oleskyn 2004). Likewise, foliar $^{15}N$ values bracket zero (Unpublished Data), a pattern consistent with a steady decline in isotopic values with increasing rainfall across Amazonia (Nardoto *et al.* 2008). Finally, past experimental work showed that soil respiration and root biomass increased by ~50% in response to N fertilization (Cleveland *et al.* 2006).

Conceptual models of hydrologic N loss (*e.g.* Brookshire *et al.* 2012) have been shaped by the generalization that tropical rainforests are naturally replete with N. However, the patterns summarized above for my field sites suggest that biological demand for N in this ecosystem is high, leading to low potential for exogenous losses.

The patterns also suggest that the common "N-rich, P-poor" generalization for lowland forests on highly weathered soils (such as those present in my sites) may not hold everywhere. Here, I report on a study designed to quantify N inputs and losses using a watershed approach, a method that has been used successfully for over 4 decades to understand biogeochemical cycling at the ecosystem scale.

## 4.3 Methods

### *4.3.1 Study Site*

The field site is located in the Golfo Dulce Forest Reserve in southwest Costa Rica on the Osa Peninsula ($8^{o}43'$ N, $83^{o}37'$ W). The forest is a highly diverse, old-growth forest with no known history of substantial human disturbance, at least in modern times. Mean annual rainfall is ~5000 mm and mean annual temperature is 26.5 $^{o}$C. The region has a pronounced dry season between December and February. Rainfall usually begins in March and intensifies through October and November. My research was focused on a 9.35-hectare watershed drained by Quebrada Mariposa, which is located near the village of Progresso. The underlying bedrock is basalt originating as Cretaceous/Paleocene magmatites referred to as the Osa mélange because of occasional breccia composed primarily of limestone (Berrange *et al*. 1988). Soils are predominantly ultisols with localized areas of inceptisols on the steep slopes and mollisols in the bottomlands. There is no recent volcanic activity in the region and the nature of landscape evolution restricts inter-basin water transfer. Therefore, assumptions of closed basin water dynamics apply, which allowed us to close the hydrologic portions of the ecosystem N budget.

### *4.3.2 Water Budget*

Precipitation was measured using a tipping bucket positioned in a clearing adjacent to the watershed. Runoff in Quebrada Mariposa was measured using a pressure transducer placed in gauging well. The well was dug by hand and never dried during the course of monitoring. Stage height was related to discharge using a rating curve. Instantaneous flow was determined 27 times across the year at this remote site using a salt slug injection technique, including an additional 11 times during large discharge events. A times-series of discharge at one-hour intervals was derived using the rating curve from June 1, 2009 to May 31, 2010.

*4.3.3 Sample Collection, Chemical Analyses and Calculations*

Precipitation chemistry was collected in acid-washed HDPE bottles connected to a telescopic funnel elevated two meters from ground level. The stream was sampled for chemistry using an ISCO 6200 autosampler for 52 consecutive weeks. We were unable to set up flow-triggered event sampling because of frequent instrument malfunction and rapid shifts in baseflow, so we established a sampling window of 3 days at 4-hour collection intervals. Each sample was filtered through an ashed, pre-weighed Whatman GFF 0.7 um filter. Particulate samples were immediately filtered, then frozen along with the filtrate that was used for dissolved C and N analysis. At the University of Colorado, filters were dried at 105 $^{0}$C, then pulverized with a mortar and pedestal and analyzed on CHN analyzer. POM concentrations were calculated as the percent C or N of total suspended solids per unit volume. Dissolved organic carbon and total dissolved nitrogen (TDN) was analyzed on a Shimadzu TOC/TN. Dissolved inorganic nitrogen (DIN), including $NH_4^+$ and $NO_3^-$, were analyzed colorimeterically on a Alpkem flow injection analyzer and microplater reader, respectively. DON was calculated as the difference

between TDN and DIN. Precipitation inputs of N were calculated as volume weighted mean concentrations of N in rainfall samples. Export fluxes were calculated using flow-weighted mean concentrations For POM, which scaled strongly with flow (see below), concentrations used in export calculations were derived from log – log concentration – discharge relationship.

In addition to C and N input – output measurements, we analyzed several biogeochemical parameters in upslope soils. These included net nitrogen processing, litterfall and soil solution chemistry, which are important predictors of C and N export patterns in other studies. Total litterfall (including leaves, twigs < 2mm, reproductive structures and unidentified material) was measured bi-weekly in 0.25 $m^2$ litterfall traps positioned within 10 monitoring plots throughout the watershed. Litter was collected at 2 –week intervals then dried within my field station, and subsequently dried at 60 $^oC$ for moisture correction. For net N processing, we adapted a field method similar to Ross *et al.* (2008), where four soil cores 9 (0 – 10 cm depth) were collected and composited inside 10 plots. An initial KCl-extractable N sample was taken within 1 hour of harvest at 1:10 W/V ratio, and the rest of the soil was placed in a polyethylene bag *in situ* and extruded 5 days later for final N extraction. Net transformation rates were assessed every 4 weeks for one year; and, calculated as final minus initial N concentrations expressed as ug N mg $soil^{-1}$ $d^{-1}$. Soil solution C and N chemistry was collected in 10 monitoring plots, each instrumented with a zero-tension surface lysimeters below the leaf litter layer (described in Wieder *et al.* 2009) and tension lysimeters placed at 15 and 50 cm depth. Tension lysimeters were installed using an auger to hand-dig holes, were placed within a silica slurry to improve soil – lysimeter connectivity, and given 2 months to equilibrate

within the soil matrix. Soil water was pulled at 0.3 MPa, collected bi-weekly and analyzed for the same constituents as surface water using the same analytical methods aforementioned.

## 4.4 Results

### *4.4.1 Hydrology*

Over 52 weeks it rained 3220 mm, which is substantially lower than the long-term average of ~ 5,000 mm. Runoff during this period was 1111 mm, suggesting that evapotranspiration was ~ 2,109 mm assuming no change in ecosystem water storage. Quebrada Mariposa is flashy; the runoff response to rain was short lived and grew as rainfall intensified with the progression of the wet season. Baseflow varied from < 0.5 to > 7 L/s across the year and was overlain by sharp spikes in flow coincident with high rainfall events (Figure 4.1).

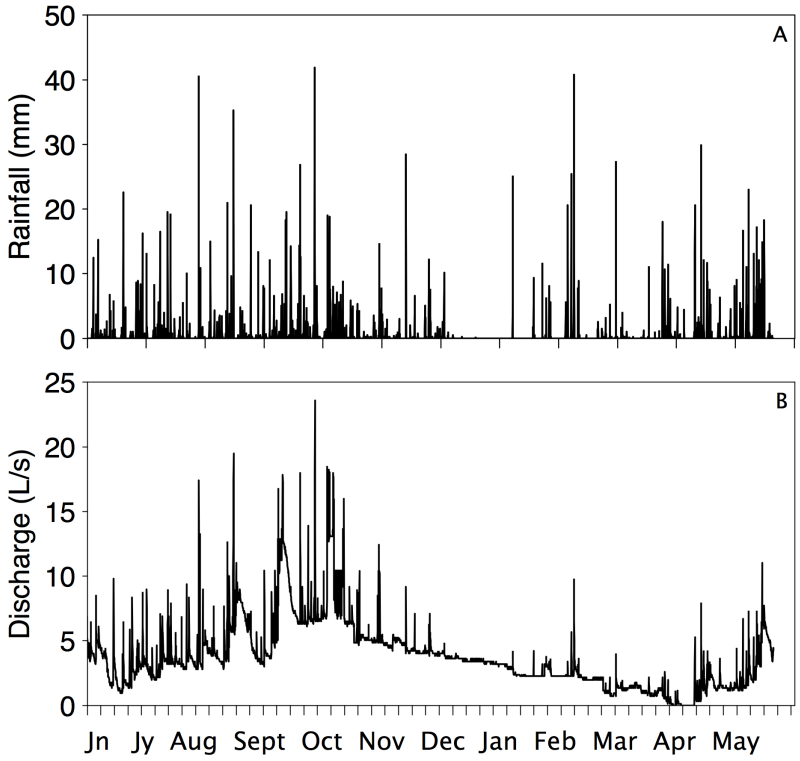


Figure 4.1. 52-week time series of (A) rainfall and (B) discharge at Quebrada Mariposa on the Osa Peninusla, Costa Rica.

*4.4.2 Terrestrial Processes and Soil Solution Chemistry*

Total litterfall was 11.6 Mg DW $ha^{-2}$ $y^{-1}$ and varied seasonally: rates are typically highest in the dry season and early wet season, and then declined throughout the remainder of the rainy portions of the year (Figure 4.2A). Net mineralization and nitrification averaged 0.30 and 0.20 ug N mg $soil^{-1}$ $d^{-1}$, respectively, whereas $NO_3^-$ and $NH_4^+$ averaged 2.40 and 1.48 ug N mg $soil^{-1}$. Soil solution chemistry also varied seasonal. Soluble DOC collected beneath leaf litter was highest after the onset of rainfall (28.5 mg/L) and declined to a low during the dry season (3.1 mg/L). This seasonal pattern was mirrored in soil solution collected in tension lysimeters, however DOC concentrations declined on average by 93% between 0 and 15 cm depth and 98% between 0 and 50 cm depth on average. DON

followed the same overall pattern as DOC and DON were closely correlated in each portion of the soil profile (data not shown).

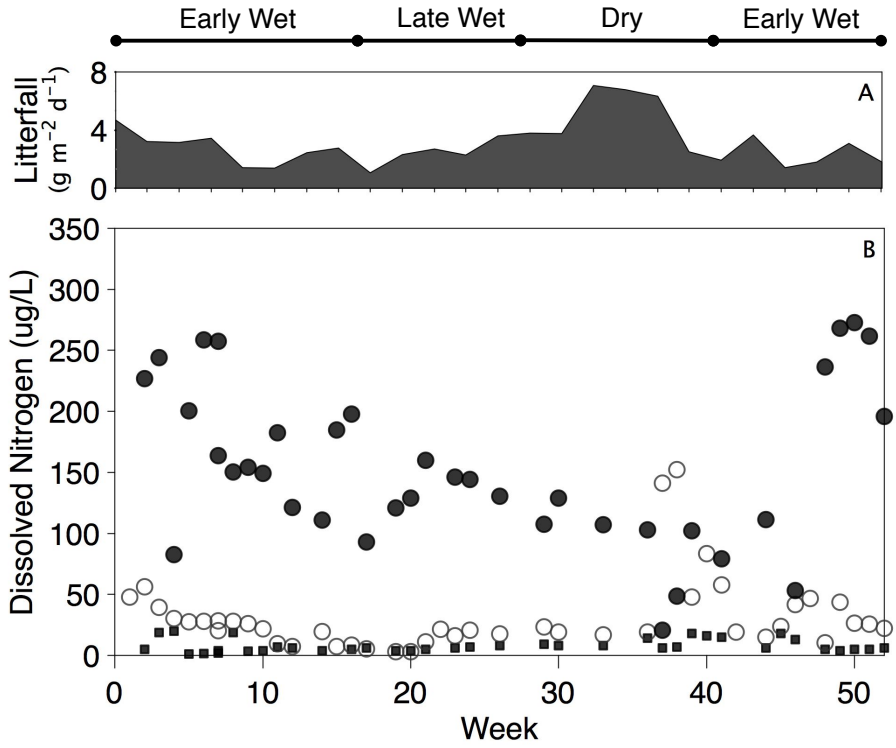


Figure 4.2. 52 weeks of (A) litterfall and (B) dissolved nitrogen concentrations in hydrologic export in Quebrada Mariposa. Labels: DON (solid circles), N-$NO_3$ (open circles), N-$NH_4$ (squares).

*4.4.3 Dissolved Carbon and Nitrogen Concentrations and Losses*

Organic nitrogen dominated dissolved N losses (Figure 2B), averaging 85% of TDN across the year. Concentrations of DON and DOC were tightly correlated (Figure 3). Hydrology exerted strong control on DOM and $NO_3^-$ concentration (Figure 4). DOM displayed a "boomerang" effect in response to rising flow (Figure 4B), which was weakly exhibited by $NO_3^-$ (Figure 4A). Antecedent litterfall rate was a moderately strong predictor of stream water DOC (DOC [mg/L] = 0.25[X] + 0.21, $R^2 = 0.56$, $p < 0.001$) and

DON (DON [ug/L] = 23.61[X] + 71.26, $R^2$ = 0.41, $p$ = 0.018) concentrations, as well as DOC and DON concentrations collected in surface, 15 and 50 cm depth lysimeters (data not shown). DOC in stream water scaled 1-to-1 with DOC collected at 15 cm depth, whereas DOC collected at 50 cm averaged half of stream concentrations (Fig. 4.5); the same was true for DON (data not shown). DOC:DON ratios showed little variation (7.94 ± 3.36) across the year (Fig. 4.3).

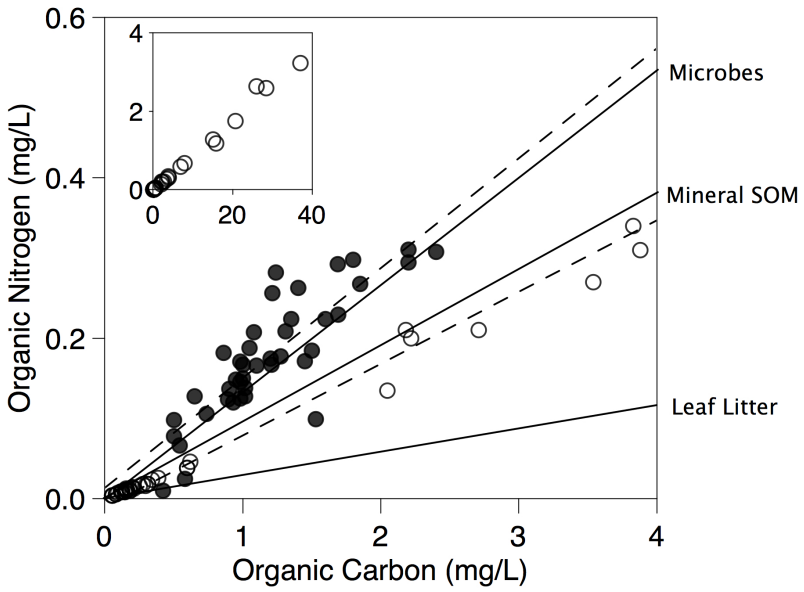


Figure 4.3. Scaling between dissolved and particulate organic carbon and nitrogen. Inset shows full scaling between POC and PON. Average stoichiometry of potential organic matter sources are shown as solid lines and labeled to the right of Figure 4.3.

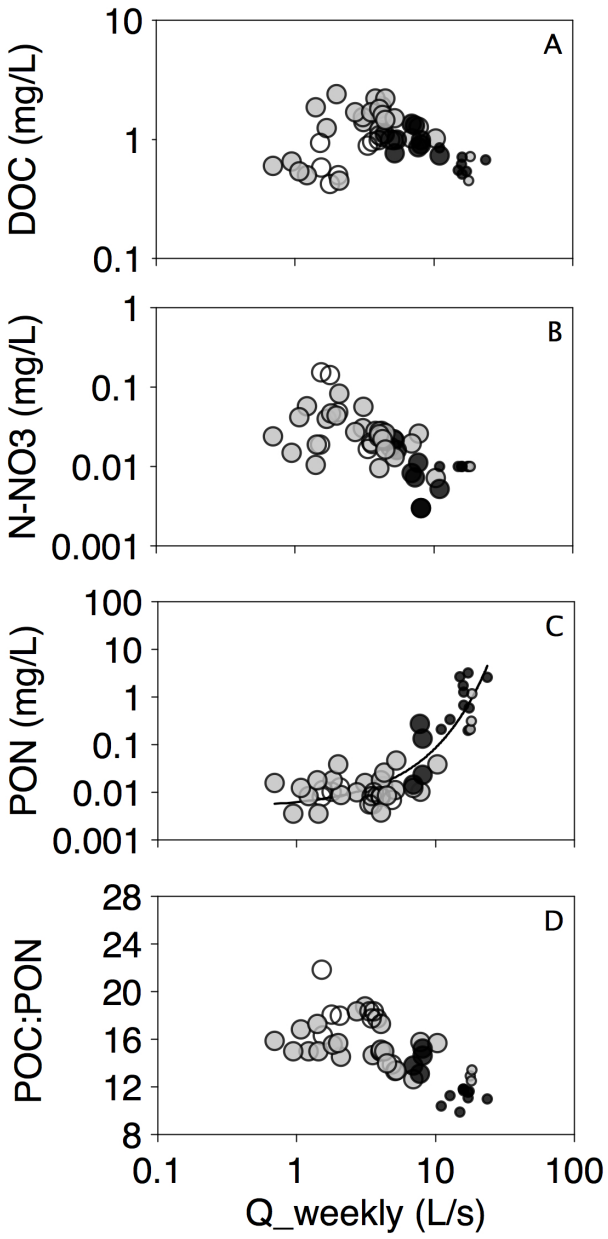


Figure 4.4. Concentration – discharge relations for (A) DOC, (B) NO3, (C) PON and (D) POC:PON. (C) The exponential equation y = 0.00564exp(X * 0.3511) was used to calculate flow-weighted mean PON concentrations.

DIN was low throughout the year, except for a brief period when $NO_3^-$ concentrations spiked during the height of the dry season when flows were very low (Fig. 2). $NO_3^-$ concentrations showed correspondence with antecedent nitrification sampled surface soils 2 months prior (y = 228.10 * [X] - 9.50, $r^2$ = 0.396199). Stream water weakly reflected $NO_3^-$ in 15 cm depth lysimeters and displayed no relationship with chemistry at 50 cm depth (Fig. 5). However, $NO_3^-$ inversely related to DOC concentration in the stream (y = 31.18 – 29.16*ln[X], $r^2$ = 0.42) and soil solution (Fig. 4.6). N-$NH_4$, N-$NO_3$ and DON fluxes in export were 0.06, 0.26 and 1.37 kg N $ha^{-1}$ $yr^{-1}$, respectively.

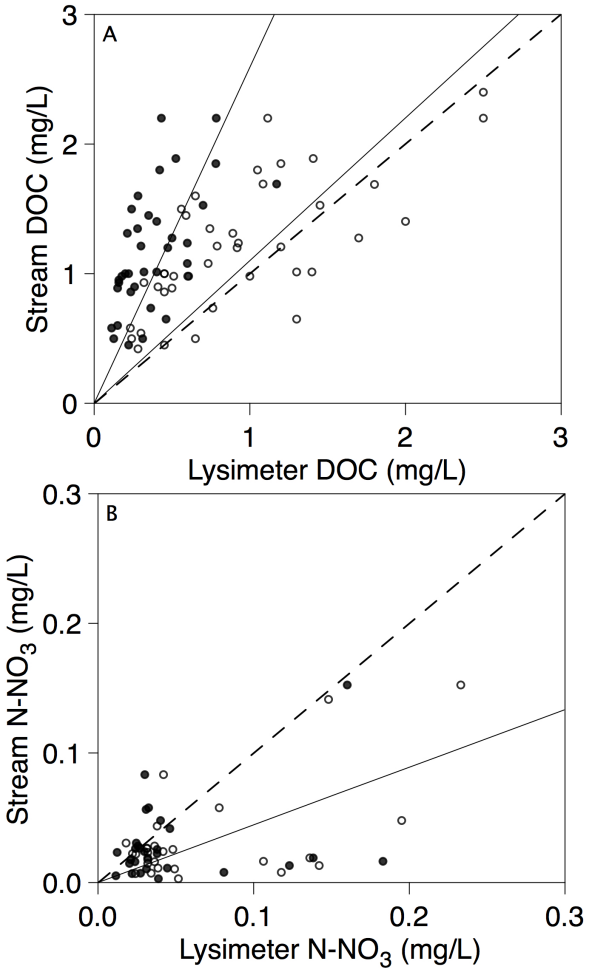


Figure 4.5. Scaling between lysimeters and stream water dissolved organic carbon (A) and nitrate (B). Open and closed circles represent chemistry from lysimeters installed at 15 and 50 cm depth, respectively. Dashed line is 1:1 ratio.

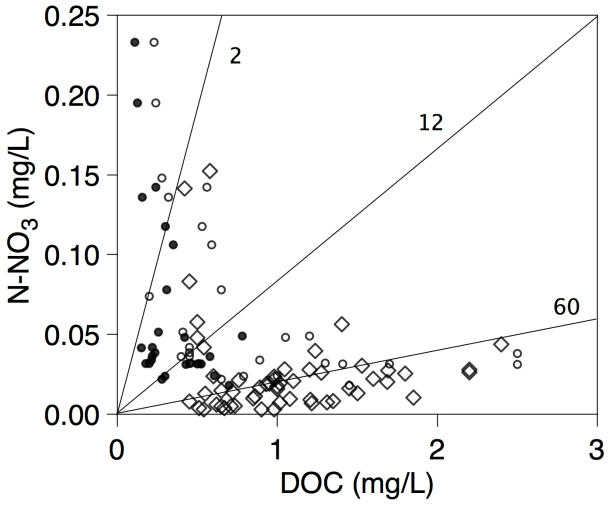


Figure 4.6. Nitrate as a function of dissolved organic carbon in shallow (open circles) and deep (closed circles) soil solution as well as stream water (diamonds). The solid lines represent ratios of DOC:N-$NO_3$.

*4.4.4 Suspended Sediment, POC and PON Concentrations and Losses*

Log – log concentration – discharge scaling shows that TSS concentrations increase exponentially with discharge. Both POC (0.00827(X) + 0.26, $r$ = 0.99) and PON (0.00075(X) + 0.01, $r$ = 0.99) increased strongly with TSS concentration. POM carbon and nitrogen concentrations were higher in the dry and early wet season, averaging 2.5 and 0.16%, respectively, and sharply declined into the wet season at high flows (%C, 0.88; %N, 0.07). The POC:PON ratio varied from 10 to 22, and declined into the wet season (Fig. 4.4D). Sediment yield was 5.10 Mg $ha^{-2}$ $y^{-1}$. Annual PON loss was higher than dissolved losses at 14.6 kg N $ha^{-2}$. Event – driven losses of PON overwhelmed baseflow export. At the highest flows exceeding 13.5 L/s, which only occurred for 51 hours during the year, the watershed lost 7.6 kg of N as PON.

## 4.5. Discussion

Under the classical notion that old-growth tropical rainforests are N-rich, inorganic N is expected to overwhelm organic N losses (*e.g.* Hedin *et al.* 2003, Brookshire *et al.* 2011, 2012). We found the opposite pattern in the watershed investigated here, which aligns with multiple indicators of conservative N cycling in the plants, soils and microbes of this rainforest. We hypothesized that the high rates of net primary productivity in this system create high biotic N demand, which in turn restricts the accumulation and loss of soluble N. In addition, substantial, episodic losses of PON that exceed measured N inputs likely prevent the accumulation of N excesses in this system, leading to higher documented indices of internal N use efficiency within the plant – soil – microbial system.

### *4.5.1 Dissolved Mineral N Loss*

In N rich systems, inorganic N loss is dominated by $NO_3^-$ (Neill *et al.* 1995, Bruijnzeel *et al.* 1991, Brookshire *et al.* 2012). $NH_4^+$ is typically favored over nitrate for biological uptake and has a greater binding affinity to the negatively charged soil matrix (Schimel and Bennett 2004). These qualities restrict $NH_4^+$ leaching, even in the most P limited systems (Hedin *et al.* 2003). The primary mechanism of hydrologic loss is through nitrification of $NH_4^+$ to $NO_3^-$ (Hedin *et al.* 2003, Lohse *et al*. 2005, Corre *et al.* 2010), which in turn can leach from soil to the stream when in excess of biotic demand (Neill *et al.* 2001; Brookshire *et al.* 2011, 2012). Early studies of several lowland forests show one-to-one scaling between the net $NH_4^+$ and $NO_3^-$ production (Vitousek and Matson 1988), and net nitrification in surface soil has been shown to be an effective predictor of $NO_3^-$ loss (Hedin *et al.* 2003).

In Quebrada Mariposa, $NH_4^+$ loss was uniformly low and $NO_3^-$ increased to appreciable levels for one-month in the dry season. Both net nitrification and soil $NO_3^-$ levels were extremely low throughout the year, except for the transition between late wet to early dry season preceding the stream water $NO_3^-$ spike. $NO_3^-$ concentrations were related to antecedent net nitrification (i.e. two – month offset) as well as shallow soil water $NO_3^-$ concentrations, suggesting a lag time between production in upslope soils and stream water chemistry due to hydrologic transit. The dry season is also a time when soil moisture and stream flows are low, factors that also concentrate surface water $NO_3^-$ (Fig. 4.4A).

Elevated net nitrification is frequently observed in other rainforest soils during the dry season (Vernimmen *et al.* 2007, Anaya *et al.* 2007, Kiese *et al.* 2008, Sotta *et al*. 2008, Owen *et al.* 2010). During this period a shortage of soluble, bioavailable organic compounds creates C limitation for heterotrophic microbes, whom lower competition for bioavailable nitrogen (Schimel and Bennett 2004). The subsequent rise in $NH_4^+$ availability at low DOC concentrations stimulates net nitrification (Verhagen 1992, Yavitt *et al.* 2004, Anaya *et al.* 2007). That is, for most of the year, $NO_3^-$ is low when soluble C levels are high enough (i.e. above microbial C:N composition) to keep heterotrophic microbes in a state of N limitation. This microbial dynamic underlies the inverse, nonlinear relationship between $NO_3^-$ and DOC in soil lysimeters and stream water (Fig. 4.6), a pattern that emerges globally (Taylor and Townsend 2010; **Chapter 2**).

Denitrification might also contribute to low stream $NO_3^-$; yet, limited surface soil production likely constrains the process for much of the year. However, during the late

wet – dry season transition, the availability of DOC and $NO_3^-$ might converge with optimal redox conditions to theoretically increase denitrification. Taylor and Townsend (2010; see **Chapter 2**) found that denitrification rates increases when DOC:$NO_3^-$ ratios are close to 1, which occur throughout the watershed for about a one-month period in the seasonal transition. Wieder *et al.* 2011 found that $N_2O$ fluxes are highest during this period, when soil oxygen was at its nadir. Though $N_2O$ fluxes were low (< 1 kg N $ha^{-2}$ $yr^{-1}$) compared to N inputs (Fig. 4.8), suggesting relatively low denitrification, the high levels of rainfall may shift gaseous N species toward $N_2$ predominance (Davidson *et al.* 2003; Houlton *et al.* 2006), which is notoriously difficult to quantify (Groffman *et al.* 2006).

There are two notable examples where physical factors are likely to override biological control. In montane systems with thick O – horizons that absorb substantial amounts of water, prolonged interaction with water can desorb and enrich shallow soil water with $NH_4^+$ (Bruijzneel *et al.* 2001, Saunders *et al.* 2006, Goller *et al.* 2005). High rainfall rates can exceed infiltration capacity of the underlying mineral soil and transfer $NH_4^+$ to streams by generating lateral flow through organic-rich soil horizons (Goller *et al.* 2005, 2006; Boy *et al.* 2009). Secondly, in soils characterized by variable charge clays, such as many of the Ultisols and Oxisols that occur throughout the lowland tropics (Sanchez 1975), anion exchange capacity can reduce $NO_3^-$ mobility through non-specific sorption (Sollins *et al.* 1988, Lohse *et al.* 2005). In a watershed near the Quebrada Mariposa, with parent material of the same origin, soil mineralogy was mainly comprised of chlorite, smectite and kaolinite with only trace levels of iron and aluminum oxide minerals such as gibbsite and goethite (Scheucher *et al.* 2008). The dominance of early to

intermediate stage weathering products suggests limited anion sorption capacity. However kaolinite can be positively charged, but often at a zero point charge well below the pH of my soils (Bolland *et al.* 1980), which averages 4.85 (Cleveland *et al.* 2006).

Overall, the export of $NO_3^-$ (0.32 kg $ha^{-2}$ $y^{-1}$) was very low compared to internal N fluxes: gross rates of ammonification and nitrification at our site are some of the highest measured in the world (Wieder et al. *in prep*), yet net accumulation of $NH_4^+$ and $NO_3^-$ are at the detection limit most of the year (Fig. 4.8). The low residence time of soil $NO_3^-$ (~2.4 hrs) is far less than the 2-day average found in N-limited forests found Oregon (Stark and Hart 1997) and Chile (Perakis and Hedin 2005). Comparison of surface to shallow soil solution shows that < 2% of $NO_3^-$ production in the litter layer leaches to 15 cm depth in this zone of invigorated plant – microbial activity. The ultra low levels of inorganic N loss relative to DON highlight the lack of bioavailable N accrual and loss.

*4.4.2 Dissolved organic matter loss*

Biology and hydrology also interact seasonally to control patterns of DOM loss. Concentrations of DON are highly correlated with DOC throughout the year (Fig. 4.3), and both vary strongly with antecedent leaf litterfall, a large source of potentially soluble organic matter. Litterfall generally declines into the wet season until a sharp increase in the dry season (Figure 4.2A), a typical pattern of many tropical forests that experience pronounced rainfall seasonality (Proctor *et al.* 1983). As a result, substantial litter stocks build up on the forest floor, which undergo microbial decomposition (Cleveland *et al.* 2006, Leff *et al*. *submitted*) and physical dissolution (Wieder *et al.* 2009) at the onset of the rainy season. The increase in DOC with baseflow in the early wet season suggests

flushing of the forest floor when soluble C fluxes are high (*e.g.* Bucker *et al*. 2011, Shanley *et al.* 2011), with subsequent depletion and dilution as the wet season progresses.

From my sampling it was not possible to identify the specific flow paths of DOM, yet the one-to-one scaling between stream water and 15 cm depth suggests hydrologic coupling between shallow surface soils and stream water, as DOM concentrations at 50 cm depth are half that of the stream. One possibility is subsurface macropore transport from shallow soil solution to the stream. How macroporosity maps across the landscape is unknown, yet a recent pantropical synthesis (Chappell *et al.* 2011) shows that soil pipes are very common, particularly in ultisols. Indeed, soil pipes are commonly found along the stream channel of Quebrada Mariposa. Since there is no known deep source of soluble C, soil pipes might be transporting DOM from relatively solute rich surface horizons that bypass deeper zones of biogeochemical processing (Negishi *et al.* 2007, Chappell and Shurlock 2007, Shanley *et al.* 2010).

Still though, the DOC transported from this region is 9-fold lower to that found beneath the litter layer, implying that soil pipes emerge at depths above which DOM has undergone significant microbial processing before export. This is reflected in stream water DOC:DON ratios that are close to microbial C:N stoichiometry (Cleveland *et al.* 2007) and consistently low throughout the year (Fig. 4.3). This uniform stoichiometry despite strong seasonal variation in biological activity and rainfall indicates consistently high, and limiting hydrologic bypassing, of microbial metabolism of organic matter. Compound – specific information using pyrolysis GC-MS reveals that the vast majority of soil organic matter displays chemical signatures of microbial degradation (Grandy *et al.* unpublished data). A small fraction of DOM does however escape retention, probably

because of its relative recalcitrance to decay; the implications of DON loss are discussed below.

*4.5.3 Particulate Organic Matter Loss*

The naturally high sediment yield (510 Mg $km^{-2}$ $y^{-1}$) reflects the erosive forces operating on the Osa Peninsula. The region is undergoing rapid uplift of ~ 5 m/kyr, and a climate conducive to high rates of weathering accelerates denudation of the landscape into the nearby ocean (Berrange and Thorpe 1988). The annual sediment load is on par with other tropical regions undergoing tectonic activity (reviewed in Douglas and Guyot 2005). There have been a tremendous number of hydrologic studies on how storms affect runoff, flow paths and sediment yield in the tropics. However, PON loss is rarely measured in tandem; only a few published studies (McDowell and Asbury 1994, Townsend-Small *et al.* 2006, Neill *et al.* 2001) provide context for my results. Nonetheless, the strong correlation between PON and SS due to the mineralogical linkage of sediment and mineral soil organic matter provides insight into the landscape mechanisms that drive high PON loss.

PON remained low for most of the year under baseflow conditions until intense rainfall events (> 20 mm $h^{-1}$) generated a sharp, nonlinear rise in suspended sediment load (Fig. 4.4D). The high nonlinearity in the discharge – PON concentration relationship suggests that waves of PON loss arise from threshold-driven geomorphological changes in the watershed (*e.g.* Douglas *et al.* 1999, Shanley *et al.* 2011). Over half of PON loss occurred during 51 separate hours of high flow (0.6% of the year) when rainfall rates exceeded 20 mm $h^{-1}$. Previous studies have reported that large sediment losses coincide with episodic landslips and breaks in in-stream debris dams (*e.g.* Douglas *et al.* 1999,

Townsend-Small *et al.* 2006, Shanley *et al.* 2011). The sharp increase in erosion during the late wet season is visually evidenced by riparian bank sloughing into the stream channel. Fig. 4.7 shows the accumulation of sediment that has settled around the gauging station before and after the wet season, which illustrates the bed load and sediment transport within Quebrada Mariposa.


Figure 4.7. Photographic comparison of the geomorphological changes to Quebrada Mariposa at the (A) beginning and (B) end of the wet season. (B) The white line highlights the gauging station for visual purposes. (Photo Credit: P. Taylor)

Slope failure is a stochastic process that likely depends on the interaction of many variables: chiefly slope angle, degree of water saturation, soil physical properties and the role of plants in soil cohesion by rooting and water balance via evapotranspiration. Though a more sophisticated approach is needed to deduce mechanisms driving soil detachment and associated PON transport, the composition of POM and its change over seasons supports the notion that heavy late season rainfall events trigger landslips into the channel. The two end members for POM sourcing are fresh leaf litter and mineral soil

organic matter; C:N ratios for these end members average 42 and 10, respectively (Fig. 3). During the dry and early wet season the POC:PON ratio is 18, which likely reflects a mix of detritus (possibly originating within stream) and mineral soil organic matter. As the wet season progresses with more frequent and intense rainfall events, the C:N ratio drops to ~ 11 (Fig. 4.3) and strongly reflects the C:N composition of mineral soil. Weintraub *et al.* (*In prep*) investigated the depth stratification of soil organic matter in a nearby field site, and found that percent C declines from 3.2 to 0.74% from surface levels to 1 meter, respectively. Percent C and N of POM reflects that of surface soil (0 – 20 cm) during the dry and early wet season, but matches deeper mineral soil (80 – 100 cm) composition in the late wet season. Such erosional processes are common in tectonically active regions (Douglas and Guyot 2005) such as the Osa Peninsula, and probably underlie the surges of PON loss.

*4.5.4. N loss in a systems perspective*

The role of N loss from ecosystems over longer timescales is best understood in relation to N inputs into the ecosystem. In this system, DON loss appears to play a minor role in balancing N deposition and fixation, as found in pristine temperate ecosystems (Hedin *et al.* 1995, 2003; Perakis *et al.* 2002). However, PON export exceeds measured N inputs (Fig. 4.8) and is a pathway of N loss that is independent of biotic demand. This phenomenon is complimentary to the DON leak concept (Hedin *et al.* 1995, Neff *et al.* 2003), which states that recalcitrant DON compounds can leach from ecosystems, despite high biotic N demand, at levels large enough to constrain N accumulation.

PON leakage differs from DON in two fundamental ways. First, PON loss is almost exclusively controlled by hydrologic regime, whereas DON loss depends on the

formation and transport of recalcitrant DON compounds. That is, the loss of DON relies on the inability of the plant – microbial system to retain all soluble DON compounds before delivery to downstream ecosystems (Hedin *et al.* 1995, Neff *et al.* 2003). Erosive PON loss bypasses N retention regardless of lability, though much of the PON appears to be affiliated with mineral soil sourced below the active rooting zone. Second, PON loss is highly episodic, whereas DON loss is typically much more consistent in space and time. Yet, the magnitude of PON export observed in my watershed suggests that short bursts of N loss could still have lasting, system level effects on N accumulation, and partiallycontribute to the metrics of conservative N cycling throughout the system.

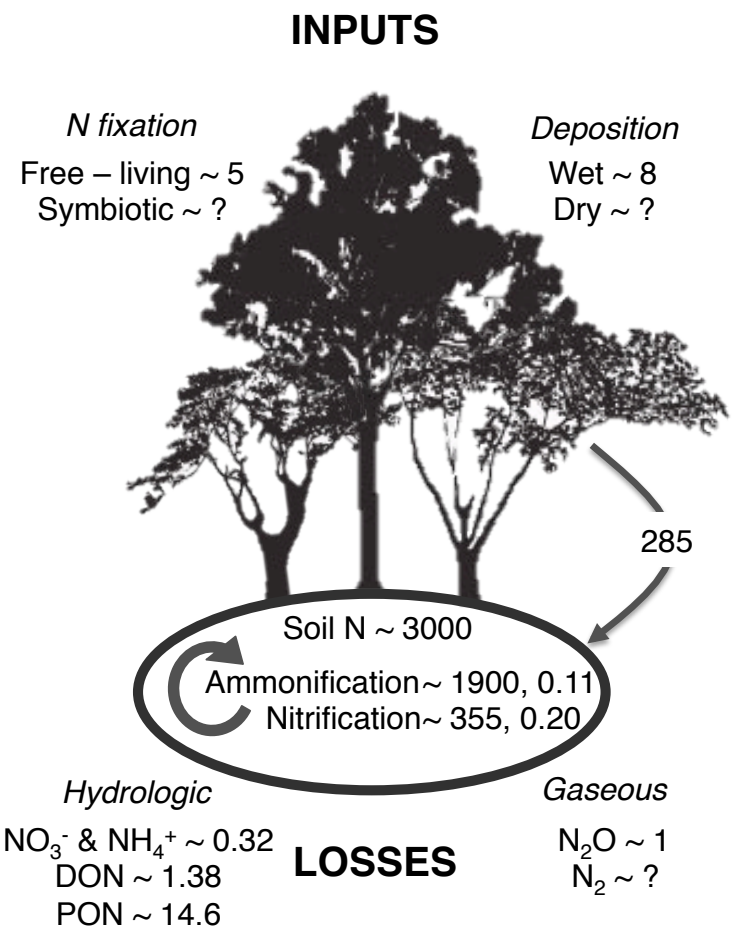

Figure 4.8. Simplified input – output budget of the watershed N cycle with emphasis on N stocks and key internal fluxes (gross and net rates, respectively) in the top 10 cm of soil. Fixation from Reed et al. 2008, soil N from Cleveland et al. 2003, gross N fluxes from Wieder et al. *In prep*, $N_2O$ fluxes from Wieder et al. 2011, net nitrogen processing, N deposition and hydrologic losses from this study. Litterfall N calculated as the product of litterfall (this study) and average fresh litter C:N ratio (Wieder et al. 2009). Symbiotic N fixation, dry N deposition and $N_2$ flux remain unmeasured. Units in kg N $ha^{-1}$ $y^{-1}$.

**4.6 Conclusions**

Here we showed that patterns of hydrologic N loss break from classical expectations of tropical N cycling. Very low concentrations and export of $NH_4^+$ and $NO_3^-$ support previous and ongoing findings of efficient N retention within this rainforest ecosystem. The dominance of DON in N losses suggests a small leak in the N cycle, potentially due to recalcitrant compounds that escape uptake and recycling before hydrologic loss. However, PON export is 8.5 fold larger than dissolved N and is regulated by different mechanisms. The magnitude of PON loss came as a surprise, and would have gone unnoticed if we'd not intensively sampled high runoff events. A focus on dissolved N alone would have led to dramatic underestimation of hydrologic N loss, and a misleading picture about how such loss may regulate long-term N accumulation in upland systems. In addition, this finding raises concern about the efficacy of the "grab-sample" campaign approach commonly employed in remote regions to characterize N loss.

PON flux measurements from small watersheds are very rare in the tropics. However, sediment yield, which is commonly measured, may be an adequate proxy for PON export in erosive systems since they are mineralogically linked; though not optimal, extrapolations based on sediment export may provide a possible proxy for examining the importance of PON loss to terrestrial ecosystem N budgets pantropically. A fuller

appreciation of the role of PON loss in the tropical N cycle will require a better understanding of how erosional processes, which are often episodic, interact with biological function in space and time. The high fluxes reported here suggest that over longer timescales PON loss in erosive regions of the world is large enough to constrain N accumulation and cause upland systems on complex terrain to depart from classic paradigms about nutrient limitation in tropical forests.

**REFERENCES**

Aerts R. & Chapin F.S. (2000) The mineral nutrition of wild plants revisited: A re-evaluation of processes and patterns. Advances in Ecological Research, Vol 30, 30, 1-67

Alexander RB, Boyer EW, Smith RA, Schwarz GE, Moore RB (2007) The role of headwater streams in downstream water quality. Journal of the American Water Resources Association 43: 41-59.

Allen A.P. & Gillooly J.F. (2009) Towards an integration of ecological stoichiometry and the metabolic theory of ecology to better understand nutrient cycling. Ecology Letters, 12, 369-384

Amundson R., Austin A.T., Schuur E.A.G., Yoo K., Matzek V., Kendall C., Uebersax A., Brenner D. & Baisden W.T. (2003) Global patterns of the isotopic composition of soil and plant nitrogen. Global Biogeochemical Cycles, 17

Anaya C.A., Garcia-Oliva F. & Jaramillo V.J. (2007) Rainfall and labile carbon availability control litter nitrogen dynamics in a tropical dry forest. Oecologia, 150, 602-610

Anderson L.O., Malhi Y., Ladle R.J., Aragao L.E.O.C., Shimabukuro Y., Phillips O.L., Baker T., Costa A.C.L., Espejo J.S., Higuchi N., Laurance W.F., Lopez-Gonzalez G., Monteagudo A., Nunez-Vargas P., Peacock J., Quesada C.A. & Almeida S. (2009) Influence of landscape heterogeneity on spatial patterns of wood productivity, wood specific density and above ground biomass in Amazonia. Biogeosciences, 6, 1883-1902.

Andersson P, Berggren D Amino acids, total organic and inorganic nitrogen in forest floor soil solution at low and high nitrogen input. Water Air and Soil Pollution 162: 369-384 (2005).

Anderson T.R., Hessen D.O., Elser J.J. & Urabe J. (2005) Metabolic stoichiometry and the fate of excess carbon and nutrients in consumers. American Naturalist, 165, 1-15.

Apple J.K., del Giorgi P.A. & Kemp W.M. (2006) Temperature regulation of bacterial production, respiration, and growth efficiency in a temperate salt-marsh estuary. Aquatic Microbial Ecology, 43, 243-254

Apple, J.K. and del Giorgio, P.A. (2007) Organic substrate quality as the link between bacterioplankton carbon demand and growth efficiency in a temperate salt-marsh estuary. ISME **1**: 729-742.

Aragao L.E.O.C., Malhi Y., Metcalfe D.B., Silva-Espejo J.E., Jimenez E., Navarrete D., Almeida S., Costa A.C.L., Salinas N., Phillips O.L., Anderson L.O., Alvarez E., Baker T.R., Goncalvez P.H., Huaman-Ovalle J., Mamani-Solorzano M., Meir P., Monteagudo A., Patino S., Penuela M.C., Prieto A., Quesada C.A., Rozas-Davila A., Rudas A., Silva

J.A. & Vasquez R. (2009) Above- and below-ground net primary productivity across ten Amazonian forests on contrasting soils. Biogeosciences, 6, 2759-2778

Arango C.P. & Tank J.L. (2008) Land use influences the spatiotemporal controls on nitrification and denitrification in headwater streams. Journal of the North American Benthological Society, 27, 90-107

Asano, Y., Compton, J. E. & Church, M. R. (2006) Hydrologic flowpaths influence inorganic and organic nutrient leaching in a forest soil. Biogeochem. **81**, 191-204.

Ashton P.S. & Hall P. (1992) Comparisons of Structure among Mixed Dipterocarp Forests of North-Western Borneo. Journal of Ecology, 80, 459-481

Asner G.P., Powell G.V.N., Mascaro J., Knapp D.E., Clark J.K., Jacobson J., Kennedy-Bowdoin T., Balaji A., Paez-Acosta G., Victoria E., Secada L., Valqui M. & Hughes R.F. (2010) High-resolution forest carbon stocks and emissions in the Amazon. Proceedings of the National Academy of Sciences of the United States of America, 107, 16738-16742

Bai E. & Houlton B.Z. (2009) Coupled isotopic and process-based modeling of gaseous nitrogen losses from tropical rain forests. Global Biogeochemical Cycles, 23: 1 – 23.

Baker T.R., Phillips O.L., Laurance W.F., Pitman N.C.A., Almeida S., Arroyo L., DiFiore A., Erwin T., Higuchi N., Killeen T.J., Laurance S.G., Nascimento H., Monteagudo A., Neill D.A., Silva J.N.M., Malhi Y., Gonzalez G.L., Peacock J., Quesada C.A., Lewis S.L. & Lloyd J. (2009) Do species traits determine patterns of wood production in Amazonian forests? Biogeosciences, 6, 297-307

Baker T.R., Phillips O.L., Malhi Y., Almeida S., Arroyo L., Di Fiore A., Erwin T., Killeen T.J., Laurance S.G., Laurance W.F., Lewis S.L., Lloyd J., Monteagudo A., Neill D.A., Patino S., Pitman N.C.A., Silva J.N.M. & Martinez R.V. (2004) Variation in wood density determines spatial patterns in Amazonian forest biomass. Global Change Biology, 10, 545-562

Balestrini, R., Arese, C. & Delconte, C. (2008) Lacustrine wetland in an agricultural catchment: nitrogen removal and related biogeochemical processes. Hydro. and Ear. Syst. Sci. 12, 539-550.

Banse K (1994) Uptake of inorganic carbon and nitrate by marine plankton and the redfield ratio. Global Biogeochemical Cycles 8: 81-84

Barnes R.T. & Raymond P.a. (2010) Land-use controls on sources and processing of nitrate in small watersheds: insights from dual isotopic analysis. Ecological Applications, 20, 1961-1978

Beer C., Reichstein M., Tomelleri E., Ciais P., Jung M., Carvalhais N., Rodenbeck C., Arain M.A., Baldocchi D., Bonan G.B., Bondeau A., Cescatti A., Lasslop G., Lindroth

A., Lomas M., Luyssaert S., Margolis H., Oleson K.W., Roupsard O., Veenendaal E., Viovy N., Williams C., Woodward F.I. & Papale D. (2010) Terrestrial Gross Carbon Dioxide Uptake: Global Distribution and Covariation with Climate. Science, 329, 834-838

Bernhardt, E. S., Hall, R. O. & Likens, G. E. (2002) Whole-system estimates of nitrification and nitrate uptake in streams of the Hubbard Brook Experimental Forest. Ecosystems 5, 419-430.

Berrange J.P. & Thorpe R.S. (1988) The Geology, Geochemistry and Emplacement of the Cretaceous Tertiary Ophiolitic Nicoya Complex of the Osa Peninsula, Southern Costa-Rica. Tectonophysics, 147, 193-&

Biddanda B, Ogdahl M, Cotner J (2001) Dominance of bacterial metabolism in oligotrophic relative to eutrophic waters. Limnology and Oceanography 46: 730-739

Biddanda B, Benner R (1997) Carbon, nitrogen and carbohydrate fluxes during the production of particulate and dissolved organic matter by marine phytoplankton Limnol. Oceanogr. 42: 506-518.

Bjornsen PK, Kuparinen J (1991) Determination of bacterioplankton biomass, net production and growth efficiency in the southern-ocean. Marine Ecology-Progress Series 71: 185-194.

Bode A, Varela, MM, Teira E, Fernandez E, Gonzalez N, Varela M. Planktonic carbon and nitrogen cycling off northwest spain: Variations in production of particulate and dissolved organic pools. Aquatic Microbial Ecology 37: 95-107 (2004).

Bohlke J.K., Antweiler R.C., Harvey J.W., Laursen A.E., Smith L.K., Smith R.L. & Voytek M.A. (2009) Multi-scale measurements and modeling of denitrification in streams with varying flow and nitrate concentration in the upper Mississippi River basin, USA. Biogeochemistry, 93, 117-141

Bohlke, J. K., Harvey, J. W. & Voytek, M. A. (2004) Reach-scale isotope tracer experiment to quantify denitrification and related processes in a nitrate-rich stream, midcontinent United States. Limno. and Oceano. 49, 821-838.

Bolland M.D.a., Posner a.M. & Quirk J.P. (1980) Ph-Independent and Ph-Dependent Surface-Charges on Kaolinite. Clays and Clay Minerals, 28, 412-41
Bonan G.B. & Levis S. (2010) Quantifying carbon-nitrogen feedbacks in the Community Land Model (CLM4). Geophysical Research Letters, 37

Bonell M., Purandara B.K., Venkatesh B., Krishnaswamy J., Acharya H.A.K., Singh U.V., Jayakumar R. & Chappell N. (2010) The impact of forest use and reforestation on soil hydraulic conductivity in the Western Ghats of India: Implications for surface and sub-surface hydrology. Journal of Hydrology, 391, 49-64

Boy J., Valarezo C. & Wilcke W. (2008) Water flow paths in soil control element exports in an Andean tropical montane forest. European Journal of Soil Science, 59, 1209-1227

Brookshire E.N.J., Gerber S., Menge D.N.L. & Hedin L.O. (2012a) Large losses of inorganic nitrogen from tropical rainforests suggest a lack of nitrogen limitation. Ecology Letters, 15, 9-16

Brookshire E.N.J., Hedin L.O., Newbold J.D., Sigman D.M. & Jackson J.K. (2012b) Sustained losses of bioavailable nitrogen from montane tropical forests. Nature Geoscience, 5, 123-126

Bruijnzeel L.a. (1991) Nutrient Input Output Budgets of Tropical Forest Ecosystems - a Review. Journal of Tropical Ecology, 7, 1-24

Bucker a., Crespo P., Frede H.G. & Breuer L. (2011) Solute behaviour and export rates in neotropical montane catchments under different land-uses. Journal of Tropical Ecology, 27, 305-317

Busing R.T. & Fujimori T. (2005) Biomass, production and woody detritus in an old coast redwood (Sequoia sempervirens) forest. Plant Ecology, 177, 177-188

Caraco NF, Cole JJ (1999) Human impact on nitrate export: An analysis using major world rivers. Ambio 28: 167-170

Carlson Ca, Ducklow HW (1996) Growth of bacterioplankton and consumption of dissolved organic carbon in the sargasso sea. Aquatic Microbial Ecology 10: 69-85101.

Carlson Ca, Bates NR, Ducklow HW, Hansell DA (1999) Estimation of bacterial respiration and growth efficiency in the Ross Sea, Antarctica. Aquatic Microbial Ecology 19: 229-244

Cebrian J. (1999) Patterns in the fate of production in plant communities. American Naturalist, 154, 449-468

Chappell N.A. (2010) Soil pipe distribution and hydrological functioning within the humid tropics: a synthesis. Hydrological Processes, 24, 1567-1581

Chappell N.A. & Sherlock M.D. (2005) Contrasting flow pathways within tropical forest slopes of Ultisol soils. Earth Surface Processes and Landforms, 30, 735-753

Chave J., Navarrete D., Almeida S., Alvarez E., Aragao L.E.O.C., Bonal D., Chatelet P., Silva-Espejo J.E., Goret J.Y., von Hildebrand P., Jimenez E., Patino S., Penuela M.C., Phillips O.L., Stevenson P. & Malhi Y. (2010) Regional and seasonal patterns of litterfall in tropical South America. Biogeosciences, 7, 43-55

Cherrier J, Bauer JE, Druffel ERM (1996) Utilization and turnover of labile dissolved organic matter by bacterial heterotrophs in eastern north pacific surface waters. Marine Ecology-Progress Series 139: 267-279

Christensen, L., Riley, W. J. & Ortiz-Monasterio, L. (2006) Nitrogen cycling in an irrigated wheat system in Sonora, Mexico: measurements and modeling. Nutr. Cycl. in Agroeco. 75, 175-186.

Christensen, P. B., Nielsen, L. P., Sorensen, J. & Revsbech, N. P. (1990) Denitrification in Nitrate-Rich Streams - Diurnal and Seasonal-Variation Related to Benthic Oxygen-Metabolism. Limno. and Oceano. 35, 640-651.

Clark D.A., Brown S., Kicklighter D.W., Chambers J.Q., Thomlinson J.R. & Ni J. (2001a) Measuring net primary production in forests: Concepts and field methods. Ecological Applications, 11, 356-370

Clark D.A., Brown S., Kicklighter D.W., Chambers J.Q., Thomlinson J.R., Ni J. & Holland E.A. (2001b) Net primary production in tropical forests: An evaluation and synthesis of existing field data. Ecological Applications, 11, 371-384

Cleveland C.C. & Liptzin D. (2007) C: N: P stoichiometry in soil: is there a "Redfield ratio" for the microbial biomass? Biogeochemistry, 85, 235-252

Cleveland C.C., Reed S.C. & Townsend A.R. (2006) Nutrient regulation of organic matter decomposition in a tropical rain forest. Ecology, 87, 492-503

Cleveland C.C. & Townsend A.R. (2006) Nutrient additions to a tropical rain forest drive substantial soil carbon dioxide losses to the atmosphere. Proceedings of the National Academy of Sciences of the United States of America, 103, 10316-10321

Cleveland C.C., Townsend A.R., Taylor P., Alvarez-Clare S., Bustamante M.M.C., Chuyong G., Dobrowski S.Z., Grierson P., Harms K.E., Houlton B.Z., Marklein A., Parton W., Porder S., Reed S.C., Sierra C.A., Silver W.L., Tanner E.V.J. & Wieder W.R. (2011) Relationships among net primary productivity, nutrients and climate in tropical rain forest: a pan-tropical analysis (vol 14, pg 939, 2011). Ecology Letters, 14, 1313-1317

Clinebell R.R., Phillips O.L., Gentry a.H., Stark N. & Zuuring H. (1995) Prediction of Neotropical Tree and Liana Species Richness from Soil and Climatic Data. Biodiversity and Conservation, 4, 56-90

Cole JJ, Findlay S, Pace ML (1988) Bacterial production in fresh and saltwater ecosystems - a cross-system overview. Marine Ecology-Progress Series 43: 1-10

Cole JJ, Pace ML (1995) Bacterial secondary production in oxic and anoxic fresh-waters. Limnology and Oceanography 40: 1019-102798.

Corre M.D., Veldkamp E., Arnold J. & Wright S.J. (2010) Impact of elevated N input on soil N cycling and losses in old-growth lowland and montane forests in Panama. Ecology, 91, 1715-1729

Cronan, C. S. and Aiken, G. R. (1985) Chemistry and transport of soluble humic substances in forestsed watersheds of the Adirondack Park, New York. Gechem. et Cosmo. Acta, 49, 1697-1705.

Cross WF, Benstead JP, Frost PC, Thomas SA (2005) Ecological stoichiometry in freshwater benthic systems: Recent progress and perspectives. Freshwater Biology 50: 1895-1912.

Currie, W. S., Aber, J. D., McDowell, W. H., Boone, R. D. & Magill, A. H. (1996) Vertical transport of dissolved organic C and N under long-term N amendments in pine and hardwood forests. Biogeochem. 35, 471-505.

da Costa A.C.L., Galbraith D., Almeida S., Portela B.T.T., da Costa M., Silva J.D., Braga A.P., de Goncalves P.H.L., de Oliveira A.A.R., Fisher R., Phillips O.L., Metcalfe D.B., Levy P. & Meir P. (2010) Effect of 7 yr of experimental drought on vegetation dynamics and biomass storage of an eastern Amazonian rainforest. New Phytologist, 187, 579-591

Dauchez S, Legendre L, Fortier L (1995) Assessment of simultaneous uptake of nitrogenous nutrients (n-15) and inorganic carbon (c-13) by natural phytoplankton populations. Marine Biology 123: 651-666

Davidson E.A., de Carvalho C.J.R., Figueira A.M., Ishida F.Y., Ometto J.P.H.B., Nardoto G.B., Saba R.T., Hayashi S.N., Leal E.C., Vieira I.C.G. & Martinelli L.A. (2007) Recuperation of nitrogen cycling in Amazonian forests following agricultural abandonment. Nature, 447, 995-U6

Davidson E.a., Hart S.C., Shanks C.a. & Firestone M.K. (1991) Measuring Gross Nitrogen Mineralization, Immobilization, and Nitrification by N-15 Isotopic Pool Dilution in Intact Soil Cores. Journal of Soil Science, 42, 335-349

Davidson E.A. & Janssens I.A. (2006) Temperature sensitivity of soil carbon decomposition and feedbacks to climate change. Nature, 440, 165-173

Davidson E.A., Keller M., Erickson H.E., Verchot L.V. & Veldkamp E. (2000) Testing a conceptual model of soil emissions of nitrous and nitric oxides. Bioscience, 50, 667-680

Defries R.S., Morton D.C., van der Werf G.R., Giglio L., Collatz G.J., Randerson J.T., Houghton R.A., Kasibhatla P.K. & Shimabukuro Y. (2008) Fire-related carbon emissions from land use transitions in southern Amazonia. Geophysical Research Letters, 35

del Giorgio P.A. & Cole J.J. (1998) Bacterial growth efficiency in natural aquatic systems. Annual Review of Ecology and Systematics, 29, 503-541

Del Grosso S. (2008) Global potential net primary production predicted from vegetation class, precipitation, and temperature (vol 89, pg 2117, 2008). Ecology, 89, 2971-2971

Dittman, J. a., Driscoll, C. T., Groffman, P. M. & Fahey, T. J. (2007) Dynamics of nitrogen and dissolved organic carbon at the Hubbard Brook Experimental Forest. Ecology 88, 1153-1166.

Douglas I., Bidin K., Balamurugan G., Chappell N.A., Walsh R.P.D., Greer T. & Sinun W. (1999) The role of extreme events in the impacts of selective tropical forestry on erosion during harvesting and recovery phases at Danum Valley, Sabah. Philosophical Transactions of the Royal Society of London Series B-Biological Sciences, 354, 1749-1761

Duff, J. H., Pringle, C. M. & Triska, F. J. (1996) Nitrate reduction in sediments of lowland tropical streams draining swamp forest in Costa Rica: An ecosystem perspective. Biogeochem. 33, 179-196.

Duff, J. H., Triska, F. J. & Oremland, R. S. (1984) Dentrification Associated with Stream Periphyton - Chamber Estimates from Undisrupted Communities. J. of Environ. Qual. 13, 514-518.

Elser J.J. (2002) Biological stoichiometry from genes to ecosystems: ideas, plans, and realities. Integrative and Comparative Biology, 42, 1226-1226

Evans, C. D. *et al.* (2006) Evidence that soil carbon pool determines susceptibility of semi-natural ecosystems to elevated nitrogen leaching. Ecosystems 9, 453-462.

Feldpausch T.R., Banin L., Phillips O.L., Baker T.R., Lewis S.L., Quesada C.A., Affum-Baffoe K., Arets E.J.M.M., Berry N.J., Bird M., Brondizio E.S., de Camargo P., Chave J., Djagbletey G., Domingues T.F., Drescher M., Fearnside P.M., Franca M.B., Fyllas N.M., Lopez-Gonzalez G., Hladik A., Higuchi N., Hunter M.O., Iida Y., Salim K.A., Kassim A.R., Keller M., Kemp J., King D.A., Lovett J.C., Marimon B.S., Marimon B.H., Lenza E., Marshall A.R., Metcalfe D.J., Mitchard E.T.A., Moran E.F., Nelson B.W., Nilus R., Nogueira E.M., Palace M., Patino S., Peh K.S.H., Raventos M.T., Reitsma J.M., Saiz G., Schrodt F., Sonke B., Taedoumg H.E., Tan S., White L., Woll H. & Lloyd J. (2011) Height-diameter allometry of tropical forest trees. Biogeosciences, 8, 1081-1106

Fisher J.B., Malhi Y., Bonal D., Da Rocha H.R., De Araujo A.C., Gamo M., Goulden M.L., Hirano T., Huete A.R., Kondo H., Kumagai T., Loescher H.W., Miller S., Nobre A.D., Nouvellon Y., Oberbauer S.F., Panuthai S., Roupsard O., Saleska S., Tanaka K., Tanaka N., Tu K.P. & Von Randow C. (2009) The land-atmosphere water flux in the tropics. Global Change Biology, 15, 2694-2714

Fyllas N.M., Patino S., Baker T.R., Nardoto G.B., Martinelli L.A., Quesada C.A., Paiva R., Schwarz M., Horna V., Mercado L.M., Santos A., Arroyo L., Jimenez E.M., Luizao F.J., Neill D.A., Silva N., Prieto A., Rudas A., Silviera M., Vieira I.C.G., Lopez-Gonzalez G., Malhi Y., Phillips O.L. & Lloyd J. (2009) Basin-wide variations in foliar properties of Amazonian forest: phylogeny, soils and climate. Biogeosciences, 6, 2677-2708

Galloway J.N., Townsend A.R., Erisman J.W., Bekunda M., Cai Z.C., Freney J.R., Martinelli L.A., Seitzinger S.P. & Sutton M.A. (2008) Transformation of the nitrogen cycle: Recent trends, questions, and potential solutions. Science, 320, 889-892

Gentry a.H. (1988) Tree Species Richness of Upper Amazonian Forests. Proceedings of the National Academy of Sciences of the United States of America, 85, 156-159

Gibson L., Lee T.M., Koh L.P., Brook B.W., Gardner T.A., Barlow J., Peres C.A., Bradshaw C.J.A., Laurance W.F., Lovejoy T.E. & Sodhi N.S. (2011) Primary forests are irreplaceable for sustaining tropical biodiversity. Nature, 478, 378-+

Godsey S., Elsenbeer H. & Stallard R. (2004) Overland flow generation in two lithologically distinct rainforest catchments. Journal of Hydrology, 295, 276-290

Goldman JC, Dennert MR (2001) Rapid nitrogen uptake by marine bacteria. Limnology and Oceanography 46: 1195-1198.

Goldman, J.C. et al. (1987) Regulation of Gross Growth Efficiency and Ammonium regeneration in bacteria by substrate C:N ratio. Limnol. Oceanogr. 32: 1239-1252

Goller R., Wilcke W., Fleischbein K., Valarezo C. & Zech W. (2006) Dissolved nitrogen, phosphorus, and sulfur forms in the ecosystem fluxes of a montane forest in ecuador. Biogeochemistry, 77, 57-89

Goller R., Wilcke W., Leng M.J., Tobschall H.J., Wagner K., Valarezo C. & Zech W. (2005) Tracing water paths through small catchments under a tropical montane rain forest in south Ecuador by an oxygen isotope approach. Journal of Hydrology, 308, 67-80

Goodale C.L., Aber J.D., Vitousek P.M. & McDowell W.H. (2005) Long-term decreases in stream nitrate: Successional causes unlikely; Possible links to DOC? Ecosystems, 8, 334-337

Groffman P.M., Altabet M.A., Bohlke J.K., Butterbach-Bahl K., David M.B., Firestone M.K., Giblin A.E., Kana T.M., Nielsen L.P. & Voytek M.A. (2006) Methods for measuring denitrification: Diverse approaches to a difficult problem. Ecological Applications, 16, 2091-2122

Gundersen K, Heldal M, Norland S, Purdie DA, Knap AH (2002) Elemental C, N, and P cell content of individual bacteria collected at the bermuda atlantic time-series study (BATS) site. Limnology and Oceanography 47: 1525-1530.

Hamilton, S. K. et al. (2001) Nitrogen uptake and transformation in a midwestern US stream: A stable isotope enrichment study. Biogeochem. 54, 297-340.

Hansen M.C., Stehman S.V. & Potapov P.V. (2010) Quantification of global gross forest cover loss. Proceedings of the National Academy of Sciences of the United States of America, 107, 8650-8655

Hansen M.C., Stehman S.V., Potapov P.V., Loveland T.R., Townshend J.R.G., DeFries R.S., Pittman K.W., Arunarwati B., Stolle F., Steininger M.K., Carroll M. & DiMiceli C. (2008) Humid tropical forest clearing from 2000 to 2005 quantified by using multitemporal and multiresolution remotely sensed data. Proceedings of the National Academy of Sciences of the United States of America, 105, 9439-9444

Hedin L.O., Armesto J.J. & Johnson a.H. (1995) Patterns of Nutrient Loss from Unpolluted, Old-Growth Temperate Forests - Evaluation of Biogeochemical Theory. Ecology, 76, 493-509

Harrison, J. & Matson, P. (2003) Patterns and controls of nitrous oxide emissions from waters draining a subtropical agricultural valley. Glob. Biogeochemi. Cycles 17, 56 - 72

Hedin L.O., Brookshire E.N.J., Menge D.N.L. & Barron A.R. (2009) The Nitrogen Paradox in Tropical Forest Ecosystems. Annual Review of Ecology Evolution and Systematics, 40, 613-635

Hedin L.O., Vitousek P.M. & Matson P.A. (2003) Nutrient losses over four million years of tropical forest development. Ecology, 84, 2231-2255

Hedin L.O., von Fischer J.C., Ostrom N.E., Kennedy B.P., Brown M.G. & Robertson G.P. (1998) Thermodynamic constraints on nitrogen transformations and other biogeochemical processes at soil-stream interfaces. Ecology, 79, 684-703

Hidaka a. & Kitayama K. (2009) Divergent patterns of photosynthetic phosphorus-use efficiency versus nitrogen-use efficiency of tree leaves along nutrient-availability gradients. Journal of Ecology, 97, 984-991

Hill a.R., Devito K.J., Campagnolo S. & Sanmugadas K. (2000) Subsurface denitrification in a forest riparian zone: Interactions between hydrology and supplies of nitrate and organic carbon. Biogeochemistry, 51, 193-223

Hill, A. R. (1979) Denitrification in the Nitrogen Budget of a River Ecosystem. Nature 281, 291-292.

Holdridge L.R. (1947) Determination of World Plant Formations from Simple Climatic Data. Science, 105, 367-368

Holmes, R. M., Jones, J. B., Fisher, S. G. & Grimm, N. B. (1996) Denitrification in a nitrogen-limited stream ecosystem. Biogeochem. 33, 125-146.

Holtgrieve G.W., Jewett P.K. & Matson P.A. (2006) Variations in soil N cycling and trace gas emissions in wet tropical forests. Oecologia, 146, 584-594

Hood, E. & Scott, D. (2008) Riverine organic matter and nutrients in southeast Alaska affected by glacial coverage. Nature Geo. 1, 583-587.

Inwood, S. E., Tank, J. L. & Bernot, M. J. (2005) Patterns of denitrification associated with land use in 9 midwestern headwater streams. J. of the North Am. Benth. Soc. 24, 227-245.

Jahnke R.a. & Craven D.B. (1995) Quantifying the Role of Heterotrophic Bacteria in the Carbon-Cycle - a Need for Respiration Rate Measurements. Limnology and Oceanography, 40, 436-441

Johnson M.S., Lehmann J., Couto E.G., Novaes J.P. & Riha S.J. (2006) DOC and DIC in flowpaths of Amazonian headwater catchments with hydrologically contrasting soils. Biogeochemistry, 81, 45-57

Johnson, M. S. et al. (2006) Organic carbon fluxes within and streamwater exports from headwater catchments in the southern Amazon. Hydro. Pro. 20, 2599-2614.

Kanda, J. (2008) Vertical profiles of nitrate uptake obtained from in situ N-15 incubation experiments in the western North Pacific. J. of Mar. Syst. 71, 63-78.

Keeling H.C. & Phillips O.L. (2007) The global relationship between forest productivity and biomass. Global Ecology and Biogeography, 16, 618-631

Kemp, M. J. & Dodds, W. K. (2001) Spatial and temporal patterns of nitrogen concentrations in pristine and agriculturally-influenced prairie streams. Biogeochem. 53, 125-141

Kemp, M. J. & Dodds, W. K. (2002) Comparisons of nitrification and denitrification in prairie and agriculturally influenced streams. Ecol. Apps. 12, 998-1009

Kepkay PE *et al.* (1997) Respiration and the carbon-to-nitrogen ratio of a phytoplankton bloom. *Mar. Ecol. Prog. Ser.* 150: 249-261

Kiese R., Hewett B. & Butterbach-Bahl K. (2008) Seasonal dynamic of gross nitrification and N(2)O emission at two tropical rainforest sites in Queensland, Australia. Plant and Soil, 309, 105-117

Kirchman DL, Suzuki Y, Garside C, Ducklow HW (1991) High turnover rates of dissolved organic-carbon during a spring phytoplankton bloom. Nature 352: 612-614

Kirchman, D. L., Ducklow, H. W., Mccarthy, J. J. & Garside, C. (1994) Biomass and Nitrogen Uptake by Heterotrophic Bacteria during the Spring Phytoplankton Bloom in the North-Atlantic Ocean. Deep-Sea Res. Part I-Oceano. Res. P. 41, 879-895

Kobe R.K., Lepczyk C.A. & Iyer M. (2005) Resorption efficiency decreases with increasing green leaf nutrients in a global data set. Ecology, 86, 2780-2792

Konohira, E. & Yoshioka, T. (2005) Dissolved organic carbon and nitrate concentrations in streams: a useful index indicating carbon and nitrogen availability in catchments. Ecolo. Res. 20, 359-365

Kumar S, Sterner RW, Finlay JC (2008) Nitrogen and carbon uptake dynamics in lake superior. Journal of Geophysical Research-Biogeosciences 113: 1-15.

Lancelot C, Billen G. (1985) Carbon-nitrogen relationships in nutrient metabolism of coastal marine ecosystems. Aquat. Microbiol. 3: 263-321.

Le Quere C., Raupach M.R., Canadell J.G., Marland G., Bopp L., Ciais P., Conway T.J., Doney S.C., Feely R.A., Foster P., Friedlingstein P., Gurney K., Houghton R.A., House J.I., Huntingford C., Levy P.E., Lomas M.R., Majkut J., Metzl N., Ometto J.P., Peter

G.P., Prentice I.C., Randerson J.T., Running S.W., Sarmiento J.L., Schuster U., Sitch S., Takahashi T., Viovy N., van der Werf G.R. & Woodward F.I. (2009) Trends in the sources and sinks of carbon dioxide. Nature Geoscience, 2, 831-836

Lewis S.L., Brando P.M., Phillips O.L., van der Heijden G.M.F. & Nepstad D. (2011) The 2010 Amazon Drought. Science, 331, 554-554

Lewis S.L., Lopez-Gonzalez G., Sonke B., Affum-Baffoe K., Baker T.R., Ojo L.O., Phillips O.L., Reitsma J.M., White L., Comiskey J.A., Djuikouo M.N., Ewango C.E.N., Feldpausch T.R., Hamilton A.C., Gloor M., Hart T., Hladik A., Lloyd J., Lovett J.C., Makana J.R., Malhi Y., Mbago F.M., Ndangalasi H.J., Peacock J., Peh K.S.H., Sheil D., Sunderland T., Swaine M.D., Taplin J., Taylor D., Thomas S.C., Votere R. & Woll H. (2009) Increasing carbon storage in intact African tropical forests. Nature, 457, 1003-U3

Lohse K.A. & Matson P. (2005) Consequences of nitrogen additions for soil processes and solution losses from wet tropical forests (vol 15, pg 629, 2005). Ecological Applications, 15, 2209-2209

Lopez-Urrutia A, Moran XA. (2007) Resource limitation of bacterial production distorts the temperature dependence of oceanic carbon cycling. Ecology 88: 817-822.

Malhi Y., Aragao L.E.O.C., Metcalfe D.B., Paiva R., Quesada C.A., Almeida S., Anderson L., Brando P., Chambers J.Q., da Costa A.C.L., Hutyra L.R., Oliveira P., Patino S., Pyle E.H., Robertson A.L. & Teixeira L.M. (2009) Comprehensive assessment of carbon productivity, allocation and storage in three Amazonian forests. Global Change Biology, 15, 1255-1274

Malhi Y., Baker T.R., Phillips O.L., Almeida S., Alvarez E., Arroyo L., Chave J., Czimczik C.I., Di Fiore A., Higuchi N., Killeen T.J., Laurance S.G., Laurance W.F., Lewis S.L., Montoya L.M.M., Monteagudo A., Neill D.A., Vargas P.N., Patino S., Pitman N.C.A., Quesada C.A., Salomao R., Silva J.N.M., Lezama A.T., Martinez R.V., Terborgh J., Vinceti B. & Lloyd J. (2004) The above-ground coarse wood productivity of 104 Neotropical forest plots. Global Change Biology, 10, 563-591

Malhi Y., Wood D., Baker T.R., Wright J., Phillips O.L., Cochrane T., Meir P., Chave J., Almeida S., Arroyo L., Higuchi N., Killeen T.J., Laurance S.G., Laurance W.F., Lewis S.L., Monteagudo A., Neill D.A., Vargas P.N., Pitman N.C.A., Quesada C.A., Salomao R., Silva J.N.M., Lezama A.T., Terborgh J., Martinez R.V. & Vinceti B. (2006) The regional variation of aboveground live biomass in old-growth Amazonian forests. Global Change Biology, 12, 1107-1138

Malhi Y., Aragao L.E.O.C., Galbraith D., Huntingford C., Fisher R., Zelazowski P., Sitch S., McSweeney C. & Meir P. (2009) Exploring the likelihood and mechanism of a climate-change-induced dieback of the Amazon rainforest. Proceedings of the National Academy of Sciences of the United States of America, 106, 20610-20615x

Manzoni S, Jackson RB, Trofymow JA, Porporato A (2008) The global stoichiometry of litter nitrogen mineralization. Science 321: 684-686.

Manzoni S., Trofymow J.A., Jackson R.B. & Porporato A. (2010) Stoichiometric controls on carbon, nitrogen, and phosphorus dynamics in decomposing litter. Ecological Monographs, 80, 89-106

Marrs R.H., Proctor J., Heaney a. & Mountford M.D. (1988) Changes in Soil Nitrogen-Mineralization and Nitrification Along an Altitudinal Transect in Tropical Rain-Forest in Costa-Rica. Journal of Ecology, 76, 466-482

Mari et al. (2001) Non-Redfield C:N ratio of transparent exopolymeric particles in the northwestern Mediterranean Sea. Limnol. Oceanogr. 46: 1831-1836.

Martinelli L.A., Piccolo M.C., Townsend A.R., Vitousek P.M., Cuevas E., McDowell W., Robertson G.P., Santos O.C. & Treseder K. (1999) Nitrogen stable isotopic composition of leaves and soil: Tropical versus temperate forests. Biogeochemistry, 46, 45-65

McCutchan, J.H. and Lewis, W.M. (2008) Spatial and temporal patterns of denitrification in an effluent-dominated plains river. Verh. Internat. Verein. Limnol. 30, 323-328

Mcdowell W.H. & Asbury C.E. (1994) Export of Carbon, Nitrogen, and Major Ions from 3 Tropical Montane Watersheds. Limnology and Oceanography, 39, 111-125

Mcdowell W.H., Lugo a.E. & James a. (1995) Export of Nutrients and Major Ions from Caribbean Catchments. Journal of the North American Benthological Society, 14, 12-20

McDowell, W. H. Internal nutrient fluxes in a Puerto Rican rain forest. J. of Trop. Ecol. 14, 521-536 (1998).

McGroddy M.E., Daufresne T. & Hedin L.O. (2004) Scaling of C: N: P stoichiometry in forests worldwide: Implications of terrestrial redfield-type ratios. Ecology, 85, 2390-2401

McSwiney, C.P., Mcdowell, W.H., Keller, M. (2001) Distribution of nitrous oxide and regulators of its production across a tropical rainforest catena in the Luquillo Experimental Forest, Puerto Rico. Biogeochem. 56, 265-286

Menge D.N.L., Pacala S.W. & Hedin L.O. (2009) Emergence and Maintenance of Nutrient Limitation over Multiple Timescales in Terrestrial Ecosystems. American Naturalist, 173, 164-175

Mercado L.M., Patino S., Domingues T.F., Fyllas N.M., Weedon G.P., Sitch S., Quesada C.A., Phillips O.L., Aragao L.E.O.C., Malhi Y., Dolman A.J., Restrepo-Coupe N., Saleska S.R., Baker T.R., Almeida S., Higuchi N. & Lloyd J. (2011) Variations in Amazon forest productivity correlated with foliar nutrients and modelled rates of photosynthetic carbon supply. Philosophical Transactions of the Royal Society B-Biological Sciences, 366, 3316-3329

Merriam, J. L. et al. (2002) Characterizing nitrogen dynamics, retention and transport in a tropical rainforest stream using an in situ N-15 addition. Fresh. Biol. 47, 143-160

Moller, a., Kaiser, K. & Guggenberger, G. (2005) Dissolved organic carbon and nitrogen in precipitation, throughfall, soil solution, and stream water of the tropical highlands in northern Thailand. J. of Pl. Nutrit. and Soil Sci. 168, 649-659

Monteith D.T., Stoddard J.L., Evans C.D., de Wit H.A., Forsius M., Hogasen T., Wilander A., Skjelkvale B.L., Jeffries D.S., Vuorenmaa J., Keller B., Kopacek J. & Vesely J. (2007) Dissolved organic carbon trends resulting from changes in atmospheric deposition chemistry. Nature, 450, 537-U9

Mulholland P.J., Helton A.M., Poole G.C., Hall R.O., Hamilton S.K., Peterson B.J., Tank J.L., Ashkenas L.R., Cooper L.W., Dahm C.N., Dodds W.K., Findlay S.E.G., Gregory S.V., Grimm N.B., Johnson S.L., McDowell W.H., Meyer J.L., Valett H.M., Webster J.R., Arango C.P., Beaulieu J.J., Bernot M.J., Burgin A.J., Crenshaw C.L., Johnson L.T.,

Niederlehner B.R., O'Brien J.M., Potter J.D., Sheibley R.W., Sobota D.J. & Thomas S.M. (2008) Stream denitrification across biomes and its response to anthropogenic nitrate loading. Nature, 452, 202-206

Murrell MC (2003) Bacterioplankton dynamics in a subtropical estuary: Evidence for substrate limitation. Aquatic Microbial Ecology $^{32}$: 239-250.

Myers N., Mittermeier R.A., Mittermeier C.G., da Fonseca G.A.B. & Kent J. (2000) Biodiversity hotspots for conservation priorities. Nature, 403, 853-858

Nardoto G.B., Ometto J.P.H.B., Ehleringer J.R., Higuchi N., Bustamante M.M.D. & Martinelli L.A. (2008) Understanding the Influences of Spatial Patterns on N Availability Within the Brazilian Amazon Forest. Ecosystems, 11, 1234-1246

Neill C., Deegan L.A., Thomas S.M. & Cerri C.C. (2001) Deforestation for pasture alters nitrogen and phosphorus in small Amazonian Streams. Ecological Applications, 11, 1817-1828

Neill C., Piccolo M.C., Steudler P.a., Melillo J.M., Feigl B.J. & Cerri C.C. (1995) Nitrogen Dynamics in Soils of Forests and Active Pastures in the Western Brazilian Amazon Basin. Soil Biology & Biochemistry, 27, 1167-1175

Newbold J.D., Sweeney B.W., Jackson J.K. & Kaplan L.a. (1995) Concentrations and Export of Solutes from 6 Mountain Streams in Northwestern Costa-Rica. Journal of the North American Benthological Society, 14, 21-37

Owen J.S., King H.B., Wang M.K. & Sun H.L. (2010) Net nitrogen mineralization and nitrification rates in forest soil in northeastern Taiwan. Soil Science and Plant Nutrition, 56, 177-185

Pan Y.D., Birdsey R.A., Fang J.Y., Houghton R., Kauppi P.E., Kurz W.A., Phillips O.L., Shvidenko A., Lewis S.L., Canadell J.G., Ciais P., Jackson R.B., Pacala S.W., McGuire A.D., Piao S.L., Rautiainen A., Sitch S. & Hayes D. (2011) A Large and Persistent Carbon Sink in the World's Forests. Science, 333, 988-993

Paoli G.D. & Curran L.M. (2007) Soil nutrients limit fine litter production and tree growth in mature lowland forest of Southwestern Borneo. Ecosystems, 10, 503-518

Paoli G.D., Curran L.M. & Zak D.R. (2005) Phosphorus efficiency of Bornean rain forest productivity: Evidence against the unimodal efficiency hypothesis. Ecology, 86, 1548-1561

Perakis S.S., Compton J.E. & Hedin L.O. (2005) Nitrogen retention across a gradient of N-15 additions to an unpolluted temperate forest soil in Chile. Ecology, 86, 96-105

Perakis S.S. & Hedin L.O. (2002) Nitrogen loss from unpolluted South American forests mainly via dissolved organic compounds (vol 415, pg 416, 2002). Nature, 418, 665-665

Pett-Ridge J., Silver W.L. & Firestone M.K. (2006) Redox fluctuations frame microbial community impacts on N-cycling rates in a humid tropical forest soil. Biogeochemistry, 81, 95-110

Phillips O.L., Aragao L.E.O.C., Lewis S.L., Fisher J.B., Lloyd J., Lopez-Gonzalez G., Malhi Y., Monteagudo A., Peacock J., Quesada C.A., van der Heijden G., Almeida S., Amaral I., Arroyo L., Aymard G., Baker T.R., Banki O., Blanc L., Bonal D., Brando P., Chave J., de Oliveira A.C.A., Cardozo N.D., Czimczik C.I., Feldpausch T.R., Freitas M.A., Gloor E., Higuchi N., Jimenez E., Lloyd G., Meir P., Mendoza C., Morel A., Neill D.A., Nepstad D., Patino S., Penuela M.C., Prieto A., Ramirez F., Schwarz M., Silva J., Silveira M., Thomas A.S., ter Steege H., Stropp J., Vasquez R., Zelazowski P., Davila E.A., Andelman S., Andrade A., Chao K.J., Erwin T., Di Fiore A., Honorio E., Keeling H., Killeen T.J., Laurance W.F., Cruz A.P., Pitman N.C.A., Vargas P.N., Ramirez-Angulo H., Rudas A., Salamao R., Silva N., Terborgh J. & Torres-Lezama A. (2009) Drought Sensitivity of the Amazon Rainforest. Science, 323, 1344-1347

Phillips O.L., van der Heijden G., Lewis S.L., Lopez-Gonzalez G., Aragao L.E.O.C., Lloyd J., Malhi Y., Monteagudo A., Almeida S., Davila E.A., Amaral I., Andelman S., Andrade A., Arroyo L., Aymard G., Baker T.R., Blanc L., Bonal D., de Oliveira A.C.A., Chao K.J., Cardozo N.D., da Costa L., Feldpausch T.R., Fisher J.B., Fyllas N.M., Freitas M.A., Galbraith D., Gloor E., Higuchi N., Honorio E., Jimenez E., Keeling H., Killeen T.J., Lovett J.C., Meir P., Mendoza C., Morel A., Vargas P.N., Patino S., Peh K.S.H., Cruz A.P., Prieto A., Quesada C.A., Ramirez F., Ramirez H., Rudas A., Salamao R., Schwarz M., Silva J., Silveira M., Slik J.W.F., Sonke B., Thomas A.S., Stropp J., Taplin J.R.D., Vasquez R. & Vilanova E. (2010) Drought-mortality relationships for tropical forests. New Phytologist, 187, 631-646

Porder S., Asner G.P. & Vitousek P.M. (2005) Ground-based and remotely sensed nutrient availability across a tropical landscape. Proceedings of the National Academy of Sciences of the United States of America, 102, 10909-10912

Powers J.S., Montgomery R.A., Adair E.C., Brearley F.Q., DeWalt S.J., Castanho C.T., Chave J., Deinert E., Ganzhorn J.U., Gilbert M.E., Gonzalez-Iturbe J.A., Bunyavejchewin S., Grau H.R., Harms K.E., Hiremath A., Iriarte-Vivar S., Manzane E., de Oliveira A.A., Poorter L., Ramanamanjato J.B., Salk C., Varela A., Weiblen G.D. & Lerdau M.T. (2009b) Decomposition in tropical forests: a pan-tropical study of the effects of litter type, litter placement and mesofaunal exclusion across a precipitation gradient. Journal of Ecology, 97, 801-811

Proctor J., Lee Y.F., Langley a.M., Munro W.R.C. & Nelson T. (1988) Ecological-Studies on Gunung Silam, a Small Ultrabasic Mountain in Sabah, Malaysia.1. Environment, Forest Structure and Floristics. Journal of Ecology, 76, 320-340

Qualls, R. G. & Haines, B. L. (1992) Biodegradability of Dissolved Organic-Matter in Forest Throughfall, Soil Solution, and Stream Water. Soil Sci. Soc. of Am. J. 56, 578-586

Raich J.W., Russell A.E., Crews T.E., Farrington H. & Vitousek P.M. (1996) Both nitrogen and phosphorus limit plant production on young Hawaiian lava flows. Biogeochemistry, 32, 1-14

Raich J.W., Russell A.E. & Vitousek P.M. (1997) Primary productivity and ecosystem development along an elevational gradient on Mauna Loa, Hawai'i. Ecology, 78, 707-721

Ram ASP, Nair S, Chandramohan D (2003) Bacterial growth efficiency in the tropical estuarine and coastal waters of Goa, southwest coast of India. Microbial Ecology 45: 88-96.

Randerson J.T., Hoffman F.M., Thornton P.E., Mahowald N.M., Lindsay K., Lee Y.H., Nevison C.D., Doney S.C., Bonan G., Stockli R., Covey C., Running S.W. & Fung I.Y. (2009) Systematic assessment of terrestrial biogeochemistry in coupled climate-carbon models. Global Change Biology, 15, 2462-2484

Raymond P.a. & Bauer J.E. (2001) Use of (14)C and (13)C natural abundances for evaluating riverine, estuarine, and coastal DOC and POC sources and cycling: a review and synthesis. Organic Geochemistry, 32, 469-485

Redfield A.C. (1958) The Biological Control of Chemical Factors in the Environment. American Scientist, 46, 205-221

Redfield, A., Ketchum, B., Richards, F. in *The Sea* (ed. Hill, M.) The influence of organisms on the composition of sea-water. 26-77 (Interscience, 1963).

Reed S.C., Cleveland C.C. & Townsend A.R. (2007) Controls over leaf litter and soil nitrogen fixation in two lowland tropical rain forests. Biotropica, 39, 585-592

Reich P.B. & Oleksyn J. (2004) Global patterns of plant leaf N and P in relation to temperature and latitude. Proceedings of the National Academy of Sciences of the United States of America, 101, 11001-11006

Richardson, W.B., Strauss, E. A., Bartsch, L. A., Monroe, E. M., Cavanaugh, J.C. *et al.* (2004) Denitrification in the Upper Mississippi River: rates, controls, and contribution to nitrate flux. Can. J. Fish. Aquatic. Sci. 61, 1102-1112

Richey, J.E., R.L. Victoria, J.I. Hedges, T. Dunne, L.A. Martinelli, L. Mertes, and J. Adams. 2008. Pre-LBA Carbon in the Amazon River Experiment (CAMREX) Data. Data set. Available on-line [http:/daac.ornl.gov] from Oak Ridge National Laboratory Distributed Active Archive Center, Oak Ridge, Tennessee, U.S.A. doi:10.3334/ORNLDAAC/904

Roman MR, Ducklow HW, Fuhrman JA, Garside C, Glibert PM, Malone TC, Mcmanus GB (1988) Production, consumption and nutrient cycling in a laboratory mesocosm. Marine Ecology-Progress Series 42: 39-52

Ross D.S., Wemple B.C., Jamison A.E., Fredriksen G., Shanley J.B., Lawrence G.B., Bailey S.W. & Campbell J.L. (2009) A Cross-Site Comparison of Factors Influencing Soil Nitrification Rates in Northeastern USA Forested Watersheds. Ecosystems, 12, 158-178

Royer, T. V., Tank, J. L. & David, M. B. Transport and fate of nitrate in headwater agricultural streams in Illinois. J. of Environ. Qual. **33**, 1296-1304 (2004).

Saatchi S.S., Harris N.L., Brown S., Lefsky M., Mitchard E.T.A., Salas W., Zutta B.R., Buermann W., Lewis S.L., Hagen S., Petrova S., White L., Silman M. & Morel A. (2011b) Benchmark map of forest carbon stocks in tropical regions across three continents. Proceedings of the National Academy of Sciences of the United States of America, 108, 9899-9904

Salinas N., Malhi Y., Meir P., Silman M., Cuesta R.R., Huaman J., Salinas D., Huaman V., Gibaja A., Mamani M. & Farfan F. (2011) The sensitivity of tropical leaf litter decomposition to temperature: results from a large-scale leaf translocation experiment along an elevation gradient in Peruvian forests. New Phytologist, 189, 967-977

Sanchez P.a. & Buol S.W. (1975) Soils of Tropics and World Food Crisis. Science, 188, 598-603

Saunders, T. J., McClain, M. E. & Llerena, C. A. (2006) The biogeochemistry of dissolved nitrogen, phosphorus, and organic carbon along terrestrial-aquatic flowpaths of a montane headwater catchment in the Peruvian Amazon. Hydro. Proc. 20, 2549-2562

Schaller, J. L., Royer, T. V., David, M. B. & Tank, J. L. (2004) Denitrification associated with plants and sediments in an agricultural stream. J. of the North Am. Benth. Soc. 23, 667-676

Schimel D.S., Braswell B.H. & Parton W.J. (1997) Equilibration of the terrestrial water, nitrogen, and carbon cycles. Proceedings of the National Academy of Sciences of the United States of America, 94, 8280-8283

Schrumpf M., Zech W., Lehmann J. & Lyaruu H.V.C. (2006) TOC, TON, TOS and TOP in rainfall, throughfall, litter percolate and soil solution of a montane rainforest succession at Mt. Kilimanjaro, Tanzania. Biogeochemistry, 78, 361-387

Schuur E.A.G. (2003) Productivity and global climate revisited: The sensitivity of tropical forest growth to precipitation. Ecology, 84, 1165-1170

Schuur E.A.G., Chadwick O.A. & Matson P.A. (2001) Carbon cycling and soil carbon storage in mesic to wet Hawaiian montane forests. Ecology, 82, 3182-3196

Schuur E.A.G. & Matson P.A. (2001) Net primary productivity and nutrient cycling across a mesic to wet precipitation gradient in Hawaiian montane forest. Oecologia, 128, 431-442

Seastedt, T. R. et al. (2004) The landscape continuum: A model for high-elevation ecosystems. Bioscience 54, 111-121

Seitzinger, S. P. (1988). Denitrification in Fresh-Water and Coastal Marine Ecosystems - Ecological and Geochemical Significance. Limno. and Oceano. 33, 702-724

Seitzinger, S.P. and Harrison, J.A. in *Nitrogen in the Marine Envrionment* (eds. Capone , D. *et al.*) Chapter 3 (Academic Press, 2008).

Seitzinger, S. P. (1994). Linkages between Organic-Matter Mineralization and Denitrification in 8 Riparian Wetlands. Biogeochem. 25, 19-39

Shanley J.B., McDowell W.H. & Stallard R.F. (2011) Long-term patterns and short-term dynamics of stream solutes and suspended sediment in a rapidly weathering tropical watershed. Water Resources Research, 47

Silver W.L., Lugo A.E. & Keller M. (1999) Soil oxygen availability and biogeochemistry along rainfall and topographic gradients in upland wet tropical forest soils. Biogeochemistry, 44, 301-328

Slik J.W.F., Aiba S.I., Brearley F.Q., Cannon C.H., Forshed O., Kitayama K., Nagamasu H., Nilus R., Payne J., Paoli G., Poulsen A.D., Raes N., Sheil D., Sidiyasa K., Suzuki E. & van Valkenburg J.L.C.H. (2010) Environmental correlates of tree biomass, basal area, wood specific gravity and stem density gradients in Borneo's tropical forests. Global Ecology and Biogeography, 19, 50-60

Solinger, S., Kalbitz, K. & Matzner, E. (2001) Controls on the dynamics of dissolved organic carbon and nitrogen in a Central European deciduous forest. Biogeochem. 55, 327-349

Smil V. (1999) Nitrogen in crop production: An account of global flows. Global Biogeochemical Cycles, 13, 647-662

Sodhi N.S., Koh L.P., Brook B.W. & Ng P.K.L. (2004) Southeast Asian biodiversity: an impending disaster. Trends in Ecology & Evolution, 19, 654-660

Smith KL, Carlucci AF, Jahnke RA, Craven DB (1987) Organic-carbon mineralization in the santa-catalina basin - benthic boundary-layer metabolism. Deep-Sea Research Part a-Oceanographic Research Papers 34: 185-211

Sodhi N.S., Koh L.P., Clements R., Wanger T.C., Hill J.K., Hamer K.C., Clough Y., Tscharntke T., Posa M.R.C. & Lee T.M. (2010) Conserving Southeast Asian forest biodiversity in human-modified landscapes. Biological Conservation, 143, 2375-2384

Sollins P., Robertson G.P. & Uehara G. (1988) Nutrient Mobility in Variable-Charge and Permanent-Charge Soils. Biogeochemistry, 6, 181-199

Sorokin YI, Mameva TI. 1980. Rate and efficiency of the utilization of labile or-ganic matter by planktonic microflora in coastal Peruvian waters. Pol. Arch. Hy-drobiol. 27:447-56

Sotta E.D., Corre M.D. & Veldkamp E. (2008) Differing N status and N retention processes of soils under old-growth lowland forest in Eastern Amazonia, Caxiuana, Brazil. Soil Biology & Biochemistry, 40, 740-750

Stark J.M. & Hart S.C. (1997) High rates of nitrification and nitrate turnover in undisturbed coniferous forests. Nature, 385, 61-64

Sterner RW, Andersen T, Elser JJ, Hessen DO, Hood JM, McCauley E, Urabe J (2008) Scale-dependent carbon: Nitrogen: Phosphorus seston stoichiometry in marine and freshwaters. Limnology and Oceanography 53: 1169-1180.

Stutter, M. I. & Billett, M. F. (2003) Biogeochemical controls on streamwater and soil solution chemistry in a High Arctic environment. Geoderma 113, 127-146

Suttle Ca, Chan aM, Fuhrman Ja (1991) Dissolved free amino-acids in the Sargasso Sea - uptake and respiration rates, turnover times, and concentrations. Marine Ecology-Progress Series 70: 189-199

Tanner E.V.J., Vitousek P.M. & Cuevas E. (1998) Experimental investigation of nutrient limitation of forest growth on wet tropical mountains. Ecology, 79, 10-22

Taylor P.G. & Townsend A.R. (2010) Stoichiometric control of organic carbon-nitrate relationships from soils to the sea. Nature, 464, 1178-1181

Taylor P.G. & Townsend A.R. (2010) Stoichiometric control of organic carbon-nitrate relationships from soils to the sea. Nature, 464, 1178-1181

Tezuka Y. (1990) Bacterial Regeneration of Ammonium and Phosphate as Affected by the Carbon - Nitrogen - Phosphorus Ratio of Organic Substrates. Microbial Ecology, 19, 227-238

Toggweiler JR 1993. Carbon overconsumption. Nature 363:
210 –211.

Touratier F, Legendre L, Vezina A (1999) Model of bacterial growth influenced by substrate c: N ratio and concentration. Aquatic Microbial Ecology 19: 105-118.

Townsend A.R., Cleveland C.C., Asner G.P. & Bustamante M.M.C. (2007) Controls over foliar N: P ratios in tropical rain forests. Ecology, 88, 107-118

Townsend A.R., Asner G.P. & Cleveland C.C. (2008) The biogeochemical heterogeneity of tropical forests. Trends in Ecology & Evolution, 23, 424-431

Townsend-Small A., McClain M.E., Hall B., Noguera J.L., Llerena C.A. & Brandes J.A. (2008) Suspended sediments and organic matter in mountain headwaters of the Amazon River: Results from a 1-year time series study in the central Peruvian Andes. Geochimica Et Cosmochimica Acta, 72, 732-740

van der Werf G.R., Morton D.C., DeFries R.S., Olivier J.G.J., Kasibhatla P.S., Jackson R.B., Collatz G.J. & Randerson J.T. (2009) CO(2) emissions from forest loss. Nature Geoscience, 2, 737-738

Vernimmen R.R.E., Verhoet H.A., Verstraten J.M., Bruijnzeel L.A., Kiomp N.S., Zoomer H.R. & Wartenbergh P.E. (2007) Nitrogen mineralization, nitrification and denitrification potential in contrasting lowland rain forest types in Central Kalimantan, Indonesia. Soil Biology & Biochemistry, 39, 2992-3003

van der Heijden, M.G.A., Bardgett, R.D., van Straalen,. N.M. (2008) The unseen majority: soil microbes as drivers of plant diversity and productivity in terrestrial ecosystems. Ecology Letters 11: 296-310

Vitousek P. (1982) Nutrient Cycling and Nutrient Use Efficiency. American Naturalist, 119, 553-572

Vitousek P.M. (1997) Human domination of Earth's ecosystems (vol 277, pg 494, 1997). Science, 278, 21-21

Vitousek P.M., Gosz J.R., Grier C.C., Melillo J.M. & Reiners W.a. (1982) A Comparative-Analysis of Potential Nitrification and Nitrate Mobility in Forest Ecosystems. Ecological Monographs, 52, 155-177

Vitousek P.M. & Howarth R.W. (1991) Nitrogen Limitation on Land and in the Sea - How Can It Occur. Biogeochemistry, 13, 87-115

Vitousek P.M. & Matson P.a. (1988) Nitrogen Transformations in a Range of Tropical Forest Soils. Soil Biology & Biochemistry, 20, 361-367

Vitousek P.M. & Sanford R.L. (1986) Nutrient Cycling in Moist Tropical Forest. Annual Review of Ecology and Systematics, 17, 137-167

Webster, J. R. et al. (2003) Factors affecting ammonium uptake in streams - an inter-biome perspective. Fresh. Biol. 48, 1329-1352

Wafar M, L'Helguen S, Raikar V, Maguer JF, Corre PL Nitrogen uptake by size-fractionated plankton in permanently well-mixed temperate coastal waters. Journal of Plankton Research 26: 1207-1218 (2004).

Wieder W.R., Cleveland C.C. & Townsend A.R. (2009) Controls over leaf litter decomposition in wet tropical forests. Ecology, 90, 3333-3341

Wieder W.R., Cleveland C.C. & Townsend A.R. (2011) Throughfall exclusion and leaf litter addition drive higher rates of soil nitrous oxide emissions from a lowland wet tropical forest. Global Change Biology, 17, 3195-3207

Wilcke, W., Yasin, S., Valarezo, C. & Zech, W. (2001) Change in water quality during the passage through a tropical montane rain forest in Ecuador. Biogeochem. 55, 45-72

Williams PJ. (1995) Evidence for the seasonal accumulation of carbon-rich dissolved organic material, its scale in comparison with changes in particulate material and the consequential effect on net C/N assimilation ratios. Mar. Chem. 51: 17-29.

Wheeler, P.A. and Kirchman, D.L. (1986) Utilization of inorganic and organic nitrogen by bacteria in marine systems. Limno. Oceanogr. 32**,** 998-1009

Wolf K., Veldkamp E., Homeier J. & Martinson G.O. (2011) Nitrogen availability links forest productivity, soil nitrous oxide and nitric oxide fluxes of a tropical montane forest in southern Ecuador. Global Biogeochemical Cycles, 25

Yavitt J.B., Wright S.J. & Wieder R.K. (2004) Seasonal drought and dry-season irrigation influence leaf-litter nutrients and soil enzymes in a moist, lowland forest in Panama. Austral Ecology, 29, 177-188

Yuan Z.Y. & Chen H.Y.H. (2009a) Global-scale patterns of nutrient resorption associated with latitude, temperature and precipitation. Global Ecology and Biogeography, 18, 11-18

Zaks D.P.M., Ramankutty N., Barford C.C. & Foley J.A. (2007) From Miami to Madison: Investigating the relationship between climate and terrestrial net primary production. Global Biogeochemical Cycles, 21

Zhao M.S. & Running S.W. (2010) Drought-Induced Reduction in Global Terrestrial Net Primary Production from 2000 Through 2009. Science, 329, 940-943